STUDY OF HEAVY-LIGHT D AND B MESONS USING HEAVY QUARK EFFECTIVE THEORY

A THESIS

Submitted to the

FACULTY OF SCIENCE

TIET, PATIALA

for the degree of

DOCTOR OF PHILOSOPHY

by

Pallavi Gupta

THAPAR INSTITUTE
OF ENGINEERING & TECHNOLOGY
(Deemed to be University)

SCHOOL OF PHYSICS AND MATERIALS SCIENCE

THAPAR INSTITUTE OF ENGINEERING AND TECHNOLOGY

PATIALA-147004, INDIA

SEPTEMBER, 2019

Dedicated to

My Beloved Parents

CERTIFICATE

This is to certify that the thesis entitled "**STUDY OF HEAVY-LIGHT D AND B MESONS USING HEAVY QUARK EFFECTIVE THEORY**" being submitted by **Ms. Pallavi Gupta** for the fulfillment of the requirements for the award of Degree of Doctor of Philosophy in the School of Physics and Materials Science, Thapar Institute of Engineering and Technology, Patiala, is a record of the candidate's own work carried out by her under my supervision. The matter presented in this thesis has not been submitted in part or full for the award of any degree in any university or institute.

Supervisor

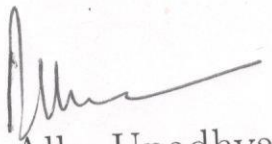

Dr. Alka Upadhyay

Associate Professor

School of Physics and Materials Science

Thapar Institute of Engineering and Technology (TIET)

Patiala- 147004

Punjab (India)

Acknowledgments

" Work becomes worship when you dedicate it to GOD and perform it with an awareness of his presence" - Rick Warren

On this moment of submission of my thesis, I would like to express my sincere gratitude and obligation to my esteemed supervisor, Dr. Alka Upadhyay, Associate Professor, School of Physics and Materials Science, Thapar Institute of Engineering and Technology, Patiala. I am very grateful for her continuous support, motivation and showing confidence towards me. Her guidance helped me in all the time of research and writing of this thesis. Thank you for believing in me and encouraging my research.

Besides my advisor, I would like to thank the rest of my thesis committee members Dr. Soumendu Jana, Dr. Debabrata Deb and Dr. Mahesh Kumar for their insightful comments and encouragement, and for the hard question which incented me to widen my research from various perspectives. I express my sincere thanks to Prof. Manoj K. Sharma for his valuable advice, excellent guidance and encouragement. His insight into the subject has always made me realize and understand the subject in a broader perspective.

I wish to express sincere and humble gratitude to Prof. O. P. Pandey, Head, School of Physics and Materials Science, and former Dean, Research and Sponsored Projects, TIET, Patiala, for providing me the necessary facilities in the department. My sincere thanks also goes to all the staff of the School for their help and kind support. My sincere thanks also goes to Prof. Rafat Siddique, present Dean, Research and Sponsored Projects, TIET, Patiala for providing the grants to attend the conferences and necessary resources to accomplish my research work.

I am happy to acknowledge the help and co-operation given to me by Dr. Meenakshi Batra and my fellow labmates Amanpreet Kaur and Kundan Kumar for the stimulating discussions and suggestions at various points of my research programme. Also I thank my friends Shivani Jain, Kanishka Sharma, Neha Grover, Amandeep Kaur, Gurjit Kaur, Ishita Sharma and Dr. Rajni who made my time at

this institution enjoyable and became a part of my life. In particular, I am grateful to my all time friend Arshpreet Kaur for all the enjoyment, moral support and being a delightful company.

Last but not the least, I would like to thank my family: my parents and to my brother for their countless blessing and supporting me spiritually throughout writing this thesis and my life in general.

I gratefully acknowledge the financial support from Thapar Institute of Engineering and Technology, Department of Science and Technology (DST) and University Grants Commission (UGC), that made my Ph.D work possible.

Patiala
Date 9/12/19

(Pallavi Gupta)

List of Publications

I. International Journals:

1. **Pallavi Gupta**, Alka Upadhyay, Placing the newly observed state $B_J(5840)$ in bottom spectra along with states $B_1(5721)$, $B_2^*(5747)$, $B_{s1}(5830)$, $B_{2s}^*(5840)$ and $B_J(5970)$, Phys. Rev. D. 99, 094043 (2019) (Impact: 4.568)..

2. **Pallavi Gupta**, Alka Upadhyay, Masses and Strong Decay properties of Radially Excited Bottom states B(2S)and B(2P) with their Strange Partners Bs(2S) and Bs(2P) Eur. Phys. J. A **54** 160 (2018)(Impact: 2.7).

3. **Pallavi Gupta**, Alka Upadhyay, Analysis of strong decays of charmed mesons $D_2^*(2460)$, $D_0(2560)$, $D_2(2740)$, $D_1(3000)$, $D_2^*(3000)$ and their spin partners $D_1^*(2680)$, $D_3^*(2760)$ and $D_0^*(3000)$, Phys. Rev. D, **97**, 014015 (2018) (Impact: 4.568).

4. **Pallavi Gupta**, Alka Upadhyay, Study of 1D stranged-charm meson family using HQET, Advances In High Energy Phys., **2016** 4957236 (2016)(Impact: 1.740).

5. Amanpreet Kaur, **Pallavi Gupta**, Alka Upadhyay, Properties of $J^P = 1/2^+$ baryon octets at low energy, Prog. Theor. Exp. Phys. **2017** 063B02 (2017) (Impact: 2.294).

6. Meenakshi Batra, Alka Upadhyay, **Pallavi Gupta**, Heavy-light charm mesons spectroscopy and decay widths, Prog. Theor. Exp. Phys **2016** 053B02 (2016)(Impact: 2.294).

7. **Pallavi Gupta**, Alka Upadhyay, Strong Decays and Coupling Constants of 1P and 1D Bottom Meson Springer Proc.Phys. 203 (2018) 885-888.

8. **Pallavi Gupta**, Alka Upadhyay, Decay width and coupling constants of charm and bottom mesons, PoS Hadron2017 (2018) 025.

II. International/National Conferences, Symposiums and Workshops:

1. **Pallavi Gupta**, Alka Upadhyay, Study of 1F doublet $(3^+, 4^+)$ for Bottom spectra using HQET, Volume 63, Page no. 854, in DAE symposium on Nuclear physics, 2018.

2. **Pallavi Gupta**, Alka Upadhyay,Mass spectra for higher excited D-wave charm meson family, in DAE symposium on High Energy Physics, 2018.

3. **Pallavi Gupta** and Alka Upadhyay, Masses and Decays of excited bottom mesons, Volume 62, Page no. 760, in DAE symposium on Nuclear physics 2017.

4. **Pallavi Gupta** and Alka Upadhyay, Masses and Decays of 2P family of charm mesons, Volume 61, Page no. 716, in DAE symposium on Nuclear physics, 2016.

5. A. Kaur, **P. Gupta**, A. Upadhyay, Charge radii of nucleons, Volume 61, Page no. 718, DAE symposium on Nuclear physics 2016.

6. **Pallavi Gupta** and Alka Upadhyay, Decay modes and coupling constants for D(2700) and D(2860), Volume 60, Page no. 654, DAE Symposium on nuclear Physics 2015.

7. A. Sharma, **P. Gupta** , K. Sharma and A.Upadhyay, Magnetic momemt of nucleons with effective mass and charge, Volume 60, Page no. 654, DAE Symposium on nuclear Physics 2014.

Contents

List of Tables

List of Figures

Abstract

In this thesis, a comprehensive study is carried out to explore the recently observed heavy light charm (D) and bottom (B) mesons. Ever since the discovery of heavy quarks c and b, study of the properties of heavy hadrons drew a special attention. Experiments at LHCb, BaBar, Belle, BESII/III, CLEO, CDF etc are producing many new charm and bottom meson states with high precision that can be relied upon. Therefore, relevant theoretical approaches should be applied to understand these mesons. Various theoretical models like heavy quark effective theory (HQET), potential model, lattice QCD, QCD sum rules etc are available for the study of these D and B mesons. In the past few years, HQET has emerged out as a successful model for studying the properties of heavy mesons. In this thesis, we intend to study the basic properties like masses, strong decays, branching ratios, splittings for the newly observed heavy -light mesons in both charm and bottom sector. By this study we will be able to complete the charm and bottom spectra up to F-wave and P-wave mesons for radial quantum numbers n=1 and n=2 respectively. This thesis is organized into six chapters, a transient outline of which is given below.

- **Chapter 1** involves the fundamental discussion about the theoretical phenomenons available for study of bound state of quarks interacting by the exchange of gluons. Here, we have classified the bound state hadrons into baryons composed of qqq structure and mesons having $q\bar{q}$ composition. To study the mesons especially the heavy-light D and B mesons which come in the low energy regime, various non-perturbative approaches like potential models, lattice QCD, effective theories, QCD sum rules used in literature are reviewed in detail. The major focus is given on the effective field theories. Contrary to the other phenomenological models, the Lagrangians in theories are constructed according to QCD symmetries and the interaction terms are organized systematically by some expansion parameter(s). The effective theories

are model-independent. We mainly emphasize on the basic concept behind the effective theories specifically for the heavy quark effective theory and heavy hadron chiral perturbation theory. Two basic symmetries of the QCD one in the infinite heavy quark limit $m_Q \to \infty$, Q = c,b and other in the chiral limit of the light quarks $m_q \to 0$, q = u,d,s are explored. Later in this chapter, the idea of spontaneous symmetry breaking of chiral symmetry and its consequences leading to the origin of light pseudoscalar mesons are reanalyzed. Finally we have shown the connection between the theoretical and experimental study that are going to brief the motivation of provided thesis.

- In **Chapter 2**, we give details of the HQET framework used in the thesis to study the heavy-light charm and bottom mesons. We start by exploring the concept of heavy quark $SU(2N_f)$ spin and flavor symmetry which serve as the origin of heavy quark effective theory. We present a general notation $nL_{S_l}J^P$ for any heavy-light state for its quantum numbers. In particular, J^P notations for the S-wave ground state and low-lying excited P-wave states are mentioned. We also define how the static nature of the heavy quark, classify the states into doublets which are represented by some covariant effective fields like H_a, S_a, T_a^μ etc. We proceed to write the effective general lagrangian for heavy-light system in the inverse powers of $1/m_Q$, by emboding the heavy quark symmetry in the QCD lagrangian. This results in the modification of the QCD Feynman rules in the $m_Q \to \infty$ limit. The leading order term of this lagrangian will preserve the heavy quark symmetries while the higher orders will break these symmetries. This chapter also provides a short introduction to the chiral perturbation theory which describes the low energy interactions between the higher excited heavy-light charm and bottom mesons and their ground state S-wave mesons by the emission of goldstone bosons π, η, K. Effective chiral lagrangians at the leading order describing the interactions among different doublets help in calculating the two-body strong decay widths. The strong

decay widths formulae dependent on the initial and final meson masses, their strong coupling constants g, pion decay constant, energy scale Λ, mass and momentum of light pseudo-scalar mesons are listed at the end of this chapter.

- In **Chapter 3**, Using the effective Lagrangian approach, we examine the recently observed non-strange charm states $D_J^*(2460)$, $D_J(2560)$, $D_J^*(2680)$, $D_J(2740)$, $D_J^*(2760)$, $D_J(3000)$ and $D_J^*(3000)$ with J^P states $1P_{\frac{3}{2}}2^+$, $2S_{\frac{1}{2}}0^-$, $2S_{\frac{1}{2}}1^-$, $1D_{\frac{5}{2}}2^-$, $1D_{\frac{5}{2}}3^-$, $2P_{\frac{1}{2}}1^+$ and $2P_{\frac{1}{2}}0^+$ respectively along with the charmed strange states $D_{sJ}(3040)$, $D_{s1}^*(2710)$, $D_{s1}^*(2860)$, $D_{s3}^*(2860)$ for J^P states $2P_{\frac{1}{2}}1^+$, $2S_{\frac{1}{2}}1^-$, $1D_{\frac{3}{2}}1^-$ and $1D_{\frac{5}{2}}3^-$ respectively. We study their two body strong decay channels, strong couplings and various branching ratios along with the emission of $J^P = 0^-$ light pseudo-scalar mesons (π, η, K). We also analyze the J^P for newly observed charm state $D_2^*(3000)$. On the basis of theoretically available masses, we suggest it to belong to either $1F(2^+)$ or $2P(2^+)$ state. We then study the branching ratio BR=$\frac{\Gamma(D_2^*(3000)\to D^*\pi)}{\Gamma(D_2^*(3000)\to D\pi)}$ by plotting a graph between this BR and the charm meson mass. The graphical analysis for this state helps us in justifying one of them to be the most favorable assignment for $D_2^*(3000)$. We study the partial and the total decay width of unobserved states $D(1^1F_3)$, $D_S(1^1F_3)$ $D_S(1^3F_2)$, $D_S(1^1D_2')$, $D_S(2^1S_0)$ and $D_S(2^3P_0)$. The branching ratios and the coupling constants g_{TH}, $\widetilde{g}_{HH}$, g_{YH}, g_{XH}, $\widetilde{g}_{SH}$ and g_{ZH} calculated in this work can be compared with various upcoming experimental data.

- In **Chapter 4**, we examine all possible two body strong decay channels, branching ratios and strong coupling constants of the highly excited bottom states $B_1(5721)$, $B_2^*(5747)$, $B_{1s}(5830)$, $B_{2s}^*(5840)$, $B_J(5960)$ and $B_J(5840)$ along the emission of light pseudo-scalar mesons (π, η, K) within the framework of HQET. We aim to search the possible J^P's for

the newly observed non-strange bottom state $B_J(5840)$ and justify one of them to be the most favorable assignment for it by studying the associated branching ratios and decay widths. For this, we examine the theoretically available masses for all bottom states and filter out six possible J^Ps $2S(1^-)_{1/2}, 2S(0^-)_{1/2}, 1D(2^-)_{3/2}, 1D(1^-)_{3/2}, 1D(3^-)_{5/2}$ and $1D(2^-)_{5/2}$ for it. Independency of coupling constants in the branching ratio $BR = \frac{\Gamma(B_J(5840)\to B\pi)}{\Gamma(B_J(5840)\to B^*\pi)}$ has helped us to choose the one among the six J values for $B_J(5840)$ state. LHCb observed $B_J(5840)$ state through $B\pi$ channel in 2015 and no other decay mode has been seen, we believe $B\pi$ decay mode to be more favorable and prominent as compared to $B^*\pi$. Hence, the probability for $B_J(5840)$ state decaying to this partial decay mode is greater than the other decay modes.

We examine the newly observed bottom states $B_J(5721)$ and $B_2^*(5747)$ and their strange partners $B_{s1}(5830)$ and $B_{2s}^*(5840)$ for their coupling constants involved. We also focus on the strong decays and coupling constant $\widetilde{g}_{HH}$ of $B_J(5970)$ for its $J^P 2S_{1/2}1^-$. The computed decay widths of experimentally missing bottom states $B(2^1S_0)$, $B_s(2^3S_1)$, $B_s(2^1S_0)$, $B(1^1D_2)$, $B_s(1^3D_1)$ and $B_s(1^1D_2)$ will provide a crucial information about upcoming experimental studies. The branching ratios and the coupling constants g_{TH}, $\widetilde{g}_{HH}$ and g_{XH} calculated in this work can shed some light on the future experimental data.

- In **Chapter 5**, we investigate the available experimental radially excited S and P wave charm states for estimating the similar spectra of the missing n=2 bottom states. Within the HQET, we examine the flavor independent parameters Δ_F and λ_F for both charm and bottom mesons, where Δ_F gives the spin averaged mass splittings between the excited states and S-wave ground state and λ_F is the mass splittings between the spin partners of the same doublets. In the limit $m_Q \to \infty$, we expect these parameters to be independent

of the heavy quark flavor i.e. $\Delta_F^{(b)} = \Delta_F^{(c)}$ and $\lambda_F^{(b)} = \lambda_F^{(c)}$. We apply this heavy quark symmetry on the experimental available data for n = 2 charm states to predict the masses of experimentally missing n=2 bottom mesons B(2S), B(2P), $B_s(2S)$ and $B_s(2P)$. We also examine these bottom masses by applying the QCD and $1/m_Q$ corrections of higher order to the leading order lagrangian, which modifies the flavor symmetry parameters like $\Delta_F^{(b)} = \Delta_F^{(c)} + \delta\Delta_F$ and $\lambda_F^{(b)} = \lambda_F^{(c)}\delta\lambda_F$. We determine strong decay widths using these calculated masses, to check the sensitivity of these corrections for these radially excited mesons. The calculated strong decay rates are in the terms of coupling constants $\widetilde{g}_{HH}$, $\widetilde{g}_{SH}$ and $\widetilde{g}_{TH}$. We conclude that, these corrections are less sensitive for n=2 masses as compared to n=1 masses. To check the validity of this framework, we also predict the masses and strong decays for other doublets like $(2^-, 3^-)_{5/2}$, $(2^+, 3^+)_{5/2}$. Branching ratios and branching fractions of these states can be helpful to search for these states experimentally.

- **Chapter 6**, summarizes the work carried out in this thesis. A brief account of results obtained and conclusion so drawn is discussed and possible extension of this work from future prospective is outlined.

Chapter 1

Introduction

Particle physics is one of the most important branch of the science as it aims in searching the most primitive, unchanging form of matter, along with the forces by which the fundamental particles interact. Basically particle physics is the journey into the heart of matter. Everything in the universe, from stars and planets, to us is made from the same basic building blocks of matter. The classification of matter started in ancient Greece, where fire, water, earth and air were considered as the basic elements from which all materials were made up of. This conception changes by famous scientist John Dalton with the discovery of several non-decomposable elements and the idea of "atom" being the smallest particle was introduced in the 1800's. However at the end of 19^{th} century, it was found that the atoms themselves were not elementary, but rather have constituents.

In 1897, a new era evoked by the discovery of electron by J. J. Thompson [1]. Soon in 1911, Rutherford revealed that atoms are no longer indivisible, but have non-uniform structure which is very dense at the center [2]. During first half of the 20^{th} century, proton, neutron and electron were considered to be the fundamental particles of atom. But again, inquest nature of human being motivated to go beyond and in 1956, the spectrum of emitted electrons during beta decay suggested that, very light (zero mass) and neutral particle called **neutrino** are also emitted in the this process [3].

At present, spin 1/2 fermions- quarks and leptons are considered as the smallest units of matter. Presence of quarks within hadrons is confirmed at lepton-hadron scattering experiment [4, 5].

From this historical remark, we can say that the study of elementary particles has changed the scenario over the course of time. Today, particle physics is considered to be the study of (i) the interactions of the elementary particles which are known till date and (ii) the identification of the new elementary constituents of the matter. The rapid progress in particle physics has made possible due to the unremitting interplay between the theoretical and experimental knowledge. The usual method of studying matter, is to "break it apart" which is held together by very strong forces. To investigate the structure of the most fundamental particle, we need to accelerate them to the huge energies. The de Broglie relation $\lambda \sim \frac{1}{p}$ suggests that, the smaller the distance one would like to analyze, the higher must be the momentum, and thus the energy of the probe. Therefore, the present technology aims in accelerating the particles at high energies. At present, 13 TeV energy can be provided to particles at the worlds most powerful particle accelerator - Large Hadron Collider (LHC). Due to this fact particle physics is also called as high energy physics. The present state of experimentation has allowed the study of physics at distance scales down to about 10^{-16} cm.

1.1 Standard Model

Steven Weinberg, Abdus Salam and Sheldom Glashow's formulated a model in 1970's to classify the fundamental particles - leptons and quarks and their interactions in terms of the three fundamental forces - strong, weak and electromagnetic interactions [6–8]. Quantum field theory assembles all the observed particles and their interactions with the help of the standard model. Both quarks and leptons are of six types, which are paired in different generations. This model contains 24 fermions, 12 vector bosons, and 4 scalars, which combine to form hundreds of other

composite particles. At present, three different generations of quarks and leptons are observed. These generations have been established over a period when these particles were detected at experiments. All the present stable matters are made from first generation particles. The heavier particles rapidly decay to the lower stable generation particles.

The standard model forms a gauge theory with $SU(3)_{strong} \times SU(2)_{weak} \times U(1)_{electromagnetic}$ group. The SU(3) group describes the strong interactions between quarks whereas $SU(2) \times U(1)$ group combines to give the electroweak interactions. Each group represents a gauge interaction, with associated gauge boson, for the above three fundamental forces. Associated gauge bosons i.e. gluons (g), photon (γ), W and Z bosons ($W^{\pm}$,Z) are vector particles having $J^P = 1^-$. Gluon mediates the strong interactions and it comes in eight different colors. In 1964, Peter Higgs predicted the higgs boson to be the main component of the standard model. Later in 2003, it got confirmed at LHC experiment by the ATLAS and CMS collaborations [9, 10]. Fundamental particles of the Standard model in particle physics are tabulated in Table 1.1.

Table 1.1: Classification of fundamental particles of standard model, where P and J are parity and total angular momentum of particles.

Fundamental Particles	Particles	J	P
leptons	$(e^-, \nu_e), (\mu^-, \nu_\mu), (\tau^-, \nu_\tau)$	1/2	-
quarks	(u, d), (c, s), (t, b)	1/2	+
gauge bosons	g, γ, $W^{\pm}$, Z^0	1	-
Higgs boson	H	0	+

The electroweak symmetry $SU(2) \times U(1)$ is spontaneously broken by the Higgs doublet which gives mass to the $W^{\pm}$ and Z^0 gauge bosons.

The standard model has made stunningly accurate predictions about certain behaviors of the fundamental particles, which are confirmed by many experimental

measurements. The theory has even predicted the existence of particles that scientists had not observed till then. The top quark, tau neutrinos and higgs boson were discovered by designing experiments based on theoretical calculations [9, 10, 98]. Despite the fact that, Standard Model accurately describes the phenomena within its domain, it is still incomplete [11]. The most familiar force i.e. gravity is not included in this model, as fitting gravity into this is a very difficult task. The general theory of relativity describing the macroscopic world and the quantum theory describing the microscopic world, are very difficult to fit into a single framework due to large difference in their couplings. Many other issues like low mass of the higgs particle, mass of the neutrinos, matter-antimatter symmetry, nature of the dark energy are yet completely not answered. Many ideas are formulated to address the problems that require some kind of "new physics" at higher energy scales. Grand Unified Theory (GUT) is the main challenge for scientists to look into the unification of three forces. Beyond GUT, there lie Super-Symmetry and Theory of Everything.

1.2 Quark Model

Two theoreticians Gell-Mann [12] and Zweing [13, 14] suggest that hadron is a composite particle made of two or more quarks bound by strong forces. They proposed quark model which classifies various available hadrons in terms of their quantum numbers like charge(Q), strangness(S), hypercharge(Y), isospin(I), baryon number(B) etc. Quark model is based on the eightfold way scheme, which arranged these hadrons according to their charge and strangeness and fitted them into some geometrical patterns like octet and decuplet. Discovery of J/Ψ in 1974 by experiments at SLAC and BNL supports the existence of more than three quarks. Properties and quantum numbers of all six quarks up(u), down(d), strange(s), charm(c), bottom(b) and top(t) are listed in Table 1.2. Electric charge (Q) of all particles is related to their isospin(I_z), Baryon number(B), Strangeness(S), Charmness(C), Bottomness($B^{'}$) and

Topness(T) by generalized Gell-Mann-Nishijima formula [15, 16]

$$Q = I_z + Y/2, \tag{1.1}$$

where Y is the hypercharge defined as Y = B + S + C + $B^{'}$ + T.

Table 1.2: Properties of six flavors of quarks with their quantum numbers. Masses of the quarks are taken from PDG, where the u, d, and s masses are in (MeV) given in the $\overline{MS}$ scheme at a scale of $\mu \approx 2$ GeV. The charm and bottom masses are the running masses in (GeV) taken in $\overline{MS}$ scheme. The top quark mass results from CMS and ATLAS experiments at CERN [17].

Property of quark	up (u)	down (d)	strange (s)	charm (c)	bottom (b)	top (t)
Mass (M)	2.20	4.70	96.00	1.27	4.18	173.21
Electric charge (e)	2/3	-1/3	-1/3	2/3	-1/3	2/3
Strangeness (S)	0	0	-1	0	0	0
Charmness (C)	0	0	0	1	0	0
Bottomness ($B^{'}$)	0	0	0	0	-1	0
Topness (T)	0	0	0	0	0	1
Isospin (I)	1/2	1/2	0	0	0	0
Isospin z-component (I_Z)	+1/2	-1/2	0	0	0	0

Later in 1964, O.W. Greenberg observed the $\Delta^{++} = (uuu)$ hadron and introduced the concept of color charges of quarks [18]. Color quantum number explained the presence of same flavored quarks in some hadron without violating the Pauli exclusion principle. He proposed that, quark not only comes in three different flavors (u, d, and s) but also comes in three different colors: red, blue or green (antiquark comes in three anticolors: cyan, yellow and magenta). In Δ^{++}, each quark is considered to be of different color, thereby conserving Pauli exclusion principle. In addition to charge and strangeness, quarks are given three new properties labeled as redness, blueness, and greenness. A quark having red color charge has one unit of redness quantum number and zero units of greenness and blueness quantum numbers. And its antiparticle has one minus unit of redness, and so on. All the hadrons

form singlets i.e are colorless under $SU(3)_{color}$ symmetry. The word "colorless" describes that, either all quarks present in a hadron have equal amount of three colors or total amount of each quark color is zero. This explains why a single quark is not observed and why hadron cannot come in combination of two quarks qq, or four quarks qqqq. The only possible combinations which give colorless states are $q\overline{q}$ (mesons), qqq (baryons) and $\overline{qqq}$ (anti-baryons). As each quark comes in three colors, so in color space, a mesonic state is represented as:

$$\text{Color Space} \qquad 3 \otimes 3 = 1 \oplus 8,$$

here 1 represents the color singlet states. The strong force mediator gluons which carries two colors in opposite directions comes in eight flavors as $r\overline{b}$, $b\overline{r}$, $r\overline{g}$, $g\overline{r}$, $g\overline{b}$, $b\overline{g}$, $\frac{1}{\sqrt{2}}(r\overline{r} - g\overline{g})$ and $\frac{1}{\sqrt{6}}(r\overline{r} + g\overline{g} - 2b\overline{b})$.

1.3 Bound states of quarks

In accordance with color confinement, hadrons must be color singlet states [19]. The quark model has classified hadrons as fermionic baryons formed by qqq combination and as bosonic mesons formed by $q\overline{q}$ pair. Baryons have non-integral spin with Baryon number B = 1, while mesons have integral spins and zero baryon number. The Quark Model has been successfully applied to classify the observed spectra of hadrons in terms of quarks. In addition to qqq and $q\overline{q}$, there can be other combinations of q and $\overline{q}$ that can give color singlet states, for example $qqqq\overline{q}$, $qq\overline{qq}$. These are also allowed in quantum chromodynamics. Such combinations of q and $\overline{q}$ other than qqq and q$\overline{q}$ are categorized as exotic hadrons. $qqqq\overline{q}$ states are known as pentaquark and $qq\overline{qq}$ are tetra-quarks.

1.3.1 Baryons

Baryons are the massive member of the hadrons, made up of three quarks (qqq). Each baryon has its antiparticle called antibaryon, where their corresponding anti-

quarks replace quarks. Baryon number of the antibaryons is B = -1. Baryons are strongly interacting particles which participate in the strong interactions mediated by gluons. The most stable baryons are proton (uud) and neutron (udd), forming the basic components of nuclei. The conservation of baryon quantum number is very important for the study of baryon interactions. In flavor space, a hadronic state formed by combining three quarks can form the multiplet as:

$$\text{Flavor Space} \quad 3 \otimes 3 \otimes 3 = 10 \oplus 8 \oplus 8 \oplus 1$$

Thus, baryons appear as decuplets and octets. Decuplets have 10 particles with $J^P = 3/2^+$ named deltas($\Delta^{++}, \Delta^+, \Delta^0, \Delta^-$), sigmas ($\Sigma^{*+}, \Sigma^{*0}, \Sigma^{*-}$), cascades ($\Xi^{*0}, \Xi^{*-}$) and omega($\Omega^-$). Similarly octet has eight particles with $J^P = 1/2^+$ named nucleons (p,n), sigmas ($\Sigma^+, \Sigma^0, \Sigma^-$), lambda ($\Lambda$) and cascades ($\Xi^0, \Xi^-$).
In this thesis, our main focus is on mesons, so we will discuss mesons in detail in the next sub section 1.3.2 ahead.

1.3.2 Mesons

It can be seen from the Table 1.2, that there is a large difference between the masses of quarks. Thus, by using the QCD fundamental scale "Λ_{QCD}" which is of the orders of few hundreds of MeV ($\Lambda_{QCD} \sim 200MeV$) [20], quarks can be divided into two groups i.e. light quarks u, d, s and heavy quarks c, b, t. In heavy quarks, charm is not that massive relative to the bottom and top quarks. Ordinary mesons are formed by the combination of one quark and one anti-quark. Different quark anti-quark combination results in different mesonic states with different spin and parities. For example, for the lowest lying mesons with angular momentum $l = 0$, spins of quark and anti-quark can combine to give singlet state ($\uparrow\downarrow$) with $J^{PC} = 0^{-,+}$ or triplet state ($\uparrow\uparrow$) with $J^{PC} = 1^{-,-}$. The quantum numbers J, P and C are the total angular momentum, intrinsic parity and charge conjugation of a meson. For any meson, P and C are defined as $(-1)^{l+1}$ and $(-1)^{l+s}$ respectively. Also, based

on the two mass groups of quarks, ordinary mesons are further classified into three categories: light-light mesons, heavy-light mesons and heavy-heavy mesons.

(a) Light-Light Mesons

As the name suggests, light-light mesons are formed by combining any one of the three light quarks (u, d, s) with any of the three light anti-quarks ($\overline{u}, \overline{d}, \overline{s}$). The ground state of light mesons for S = 0 are represented with $J^P = 0^-$ and lower excited states for S = 1 are given as $J^P = 1^-$. The former mesons corresponding to $J^P = 0^-$ are known as light-pseudoscalar mesons and the latter ones corresponding to $J^P = 1^-$ are vector mesons. In the flavor space, three quark and three anti-quark can combine as

$$\text{Flavor Space} \quad 3 \otimes \overline{3} = 1 \oplus 8$$

combinations of light mesons. These nine states for light mesons are divided into SU(3) octet and a singlet. SU(3) octet for light pseudoscalar meson is shown diagrammatically in Figure 1.1. The diagram is plotted with isospin and strangeness taken on horizontal and vertical axis respectively. Particles along the same diagonals share the same charge Q.

The same mass of up and down quark gives an SU(2) group of isospin symmetry. With the similar understanding, π^0, π^+ and π^- establish SU(2) flavor or isospin symmetry. But due to different electric charges of these quarks, this symmetry is broken by their charge dependent electromagnetic interaction. Being the lightest hadrons, decay of pseudoscalar mesons to other hadrons is kinematically forbidden, so these mesons are long lived particles.

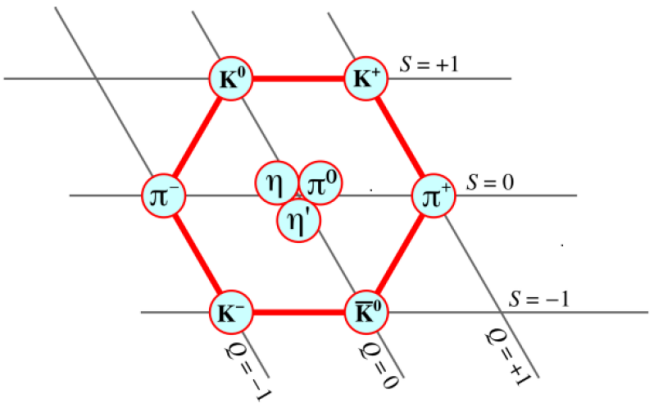

Figure 1.1: The meson nonet for light-pseudoscalar mesons with $J^P = 0^-$.

Quantum numbers for light pseudoscalar mesons defined as ${}^1S_0$ state along with their quark content are tabulated in Table 1.3. Later, in this chapter, we will study these $J^P = 0^-$ mesons as pseudoscalar Goldstone bosons resulting from the chiral symmetry breaking [21, 22].

Table 1.3: $J^P = 0^-$ Pseudoscalar meson states with their quark content and quantum numbers.

Particle	Quark contents	Quantum numbers				
		I	I_Z	Y	Mass (MeV) [17]	
π^+	$u\bar{d}$	1	1	0	139.57	
π^0	$\frac{1}{\sqrt{2}}(d\bar{d} - u\bar{u})$	1	0	0	134.97	
π^-	$d\bar{u}$	1	-1	0	139.57	
K^+	$u\bar{s}$	$\frac{1}{2}$	$+\frac{1}{2}$	1	493.67	
K^0	$d\bar{s}$	$\frac{1}{2}$	$-\frac{1}{2}$	1	497.61	*octet*
K^-	$\bar{u}s$	$\frac{1}{2}$	$-\frac{1}{2}$	-1	493.67	
$\overline{K}^0$	$\bar{d}s$	$\frac{1}{2}$	$+\frac{1}{2}$	-1	497.61	
η_8	$\frac{1}{\sqrt{6}}(d\bar{d} + u\bar{u} - 2s\bar{s})$	0	0	0	547.86	
η_0	$\frac{1}{\sqrt{3}}(d\bar{d} + u\bar{u} + s\bar{s})$	0	0	0	957.78	*singlet*

Similarly the quantum numbers for vector mesons defined as $^3S_1$ state with their quark content are tabulated in Table 1.4

Table 1.4: $J^P = 1^-$ Vector meson states with their quark content and quantum numbers.

Particle	Quark contents	Quantum numbers				
		I	I_Z	Y	Mass (MeV) [17]	
ρ^+	$u\overline{d}$	1	1	0	775.26	*octet*
ρ^0	$\frac{1}{\sqrt{2}}(u\overline{u} - d\overline{d})$	1	0	0	775.26	
ρ^-	$d\overline{u}$	1	-1	0	775.26	
K^{*+}	$u\overline{s}$	$\frac{1}{2}$	$+\frac{1}{2}$	1	891.76	
K^{*0}	$d\overline{s}$	$\frac{1}{2}$	$-\frac{1}{2}$	1	895.55	
K^{*-}	$s\overline{u}$	$\frac{1}{2}$	$-\frac{1}{2}$	-1	891.76	
$\overline{K}^{*0}$	$s\overline{d}$	$\frac{1}{2}$	$+\frac{1}{2}$	-1	895.55	
ω	$\frac{1}{\sqrt{2}}(d\overline{d} + u\overline{u})$	0	0	0	782.65	
ϕ	$s\overline{s}$	0	0	0	1019.46	*singlet*

The particles ρ and π have similar quark content but different spin angular momentum. The lighter mass of pseudoscalar meson π, illustrates the extraordinary variation of hyperfine interaction among quark and anti-quark.

(b) Heavy - Light Mesons

Heavy-light meson is composed of one of the heavy quark Q(c or b) and a light anti-quark q(u, d or s) or vice versa. Mesons formed by the coupling of charm quark are known as D mesons and the heavy-light system formed by bottom quark are known as B mesons. Due to the large mass difference between the light non-strange quarks (u and d) and the strange quark (s), these heavy light mesons are further classified as non-stranged and stranged mesons. The suggested $Q\overline{q}$ quark model assignments for D and B mesons are shown in Table 1.5.

Top quark being the most massive with mass of 173 GeV, interacts primarily by

strong interactions. Lifetime of the top quark is very small roughly of the order of $\sim 10^{-25}$ sec [17], making it very unstable particle. As a result, top quark does not form hadrons.

Table 1.5: Different quark combinations for heavy-light charm and bottom mesons.

	Quark content	Particle	Anti-Particle	S	C	B
D - mesons	$c\overline{u}$	D^0	D^0	0	1	0
	$c\overline{d}$	D^+	D^-	0	1	0
	$c\overline{s}$	D_s^+	D_s^-	-1	1	0
B - Mesons	$b\overline{u}$	B^-	B^+	0	0	1
	$b\overline{d}$	B^0	B^0	0	0	1
	$b\overline{s}$	B_s^0	B_s^0	-1	0	1

Under the isospin symmetry ($m_u = m_d$), non-strange D and B mesons transform as a SU(2) doublet, which when combined with strange mesons form SU(3) triplet ($m_u = m_d = m_s$).

The $l = 0$ ground state D and B mesons being the lightest heavy-light systems can only decay via weak interactions. Higher excited heavy-light states ($l \neq 0$) can strongly decay to the ground state mesons through the exchange of either light pseudoscalar mesons or vector mesons. And for the weak decays, the charm quark in the D meson can decay to s quark and the b quark in B mesons, can decay to c or s quark via an exchange of W particles. These D and B mesons can also decay electromagnetically by the emission of photons. As the value of the strong coupling constant is very high as compared to the weak and EM interactions, so the preferential decay modes are associated with kaon's (K) and pion's (π).

The first D meson is observed in a bubble chamber at SLAC in 1976 [23,24] and the first B meson is observed in 1983 by the CLEO Collaboration [25]. Till now, many new charmed and bottom mesons are experimentally available. The newly observed charm states like $D_2^*(2460)$, $D_0(2560)$, $D_2(2740)$, $D_J(3000)$, $D_2^*(3000)$ $D_1^*(2680)$,

$D_3^*(2760)$, $D_J^*(3000)$ etc. and bottom states like $B_1(5721)$, $B_2^*(5747)$, $B_J(5840)$, $B_J(5970)$, $B_{s1}(5830)$, $B_{2s}^*(5840)$ etc. are at the top interest of the experimentalists and theorists to study [26–45].

By examining the ground state spectra, it is observed that the mass splitting between the non-strange and strange D and B states for $J^P = 0^-, 1^-$ is consistent with the SU(3) symmetry breaking of the order of ~ 100 MeV $(m_s - m_u)$. Center of momentum of these mesons is almost same as that of the heavy quark, as a result these D and B mesons possess various symmetries. These symmetries help in formulating the properties of the heavy-light system in terms of the effective theories.

The origin of different symmetries and effective theories will be discussed later in this chapter in section 1.5 and 1.6. In this thesis, our main interest is to study the various properties like splittings, J^P assignment, decay widths, masses etc. for the heavy-light D and B mesons using heavy quark effective theory as our framework.

(c) Heavy - Heavy Mesons

Heavy-heavy mesons are composed by the coupling of both heavy quarks Q(c, b) to form states like $c\bar{b}$, $c\bar{c}$, $b\bar{b}$. Most important among these are the mesons made of same type of quark-antiquark, which are commonly known as quarkonium mesons i.e. charmonium for $c\bar{c}$ and bottomonium for $b\bar{b}$. Quantum numbers like charmness and bottomness are zero for these states. Since Compton wavelength of these systems is small, thus effective theories unlike heavy-light mesons are not required in heavy-heavy mesons. These systems behave quite similar as the hydrogen atom and thus can be approximated quantum mechanically. This approach gives so-called potential models, in which the basic form of the potential is chosen to recreate the known properties of the strong interaction [46,47]. In recent years, Non Relativistic Quantum Chromodynamics (NRQCD), has been used to study the heavy quarkonium systems [48].

Due to the low rest mass, $J/\psi = c\bar{c}$ is the most common form of charmonium, and

is discovered simultaneously by two independent experimental groups (SLAC and Brookhaven) in November 1974. Its discovery led the scientists to extend the old version of the quark model having three light flavored quarks (u, d, s) to include the first heavy flavored quark named charm. Its discovery is named as November Revolution in high energy physics. OZI rule strongly suppresses the hadronic decay modes of J/ψ, thus this particle has long lifetime of 7.2×10^{-21} sec with a very narrow decay width of 93.2 keV. The first bottomonium state named as $\Upsilon = b\bar{b}$ is first observed at Fermilab in 1977. Its narrow width of 54.02 keV and lifetime of 1.21×10^{-20}sec gives the evidence of another new heavy quark called bottom [17]. Various potential models [49, 50] have predicted the higher excited spectra for both charmonium and bottomonium system, but experimentally only few are known. Figures 1.2 and 1.3 shows the experimental available spectra for the heavy-heavy systems with the horizontal and vertical axis as J^{PC} and invariant mass (GeV) respectively of the states. The solid red color lines represent the states as listed in Particle Data Group (PDG) and the dashed red lines give the experimentally observed states seen by Belle, and the states represented by boxes are the theoretically predicted masses by Ref. [51].

1.3.3 Exotic States

In QCD, since gluons carry color charges, they not only mediate by strong interactions with quarks, but can also interact among themselves. States with $J^{PC} = 0^{--}, 0^{+-}, 1^{-+}, 2^{+-}$, with parity P = $(-)^{L+1}$ and C-parity C = $(-)^{L+S}$, which are not included in quark model are referred as exotic mesons. Even during the origin of the quark model, Gell-Mann and Zweing proposed the possibility of the existence of the multiquark states $q\bar{q}q\bar{q}$, $qqqq\bar{q}$, $\overline{q}\overline{q}qqqq$ etc [12,13,52,53]. These multiquarks were classified as tetraquarks with quark configuration $qq\overline{q}\overline{q}$, pentaquark with $qqqq\bar{q}$, baryonium as $qqq\overline{q}\overline{q}\overline{q}$, dibaryon $qqqqqq$ etc. In the last decade, experimental collaborations like BaBar, Belle, BESII/III, CDF, CLEO, LHCb, CMS,

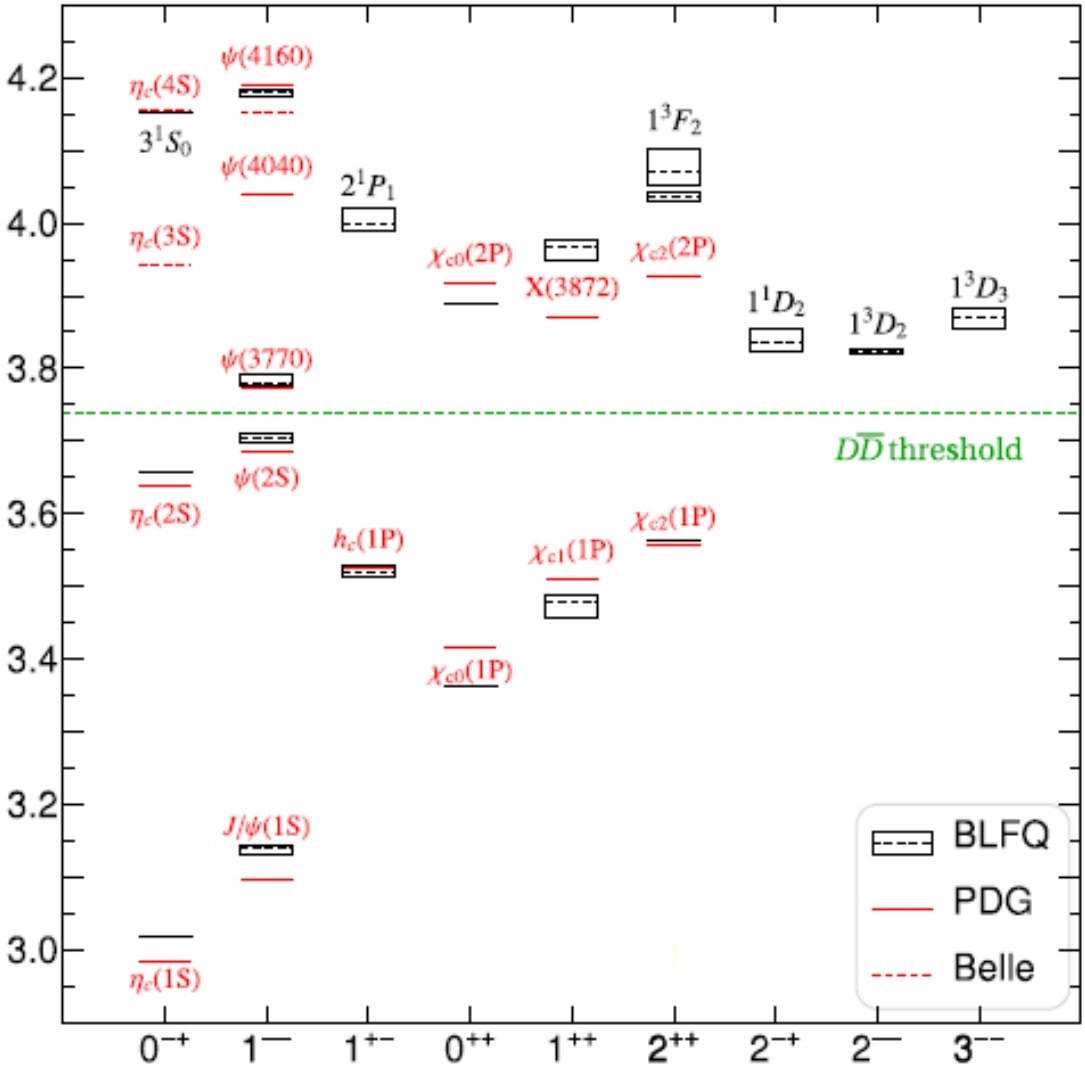

Figure 1.2: Spectra of charmonium states.

DØ [54–62, 101, 102] have detected many new charmonium and bottomonium states. Some of these states cannot be studied by the simple quark model, so are considered to be good candidates for the hidden charmed/bottom exotic states including tetraquarks, pentaquarks or di-meson molecule states etc. Especially the X, Y, Z states are classified as exotic states, e.g. The states X(3872), Y(3940) are considered as tetraquarks with $c\overline{u}\overline{c}u$ structure or as molecular state of $D\overline{D}^*$ and the state $Z_c(4248)$ as $cu\bar{c}d$. Many of the known exotic states are listed in the Particle Data Group [17], and theoretically there are various potential models [63–67] which are

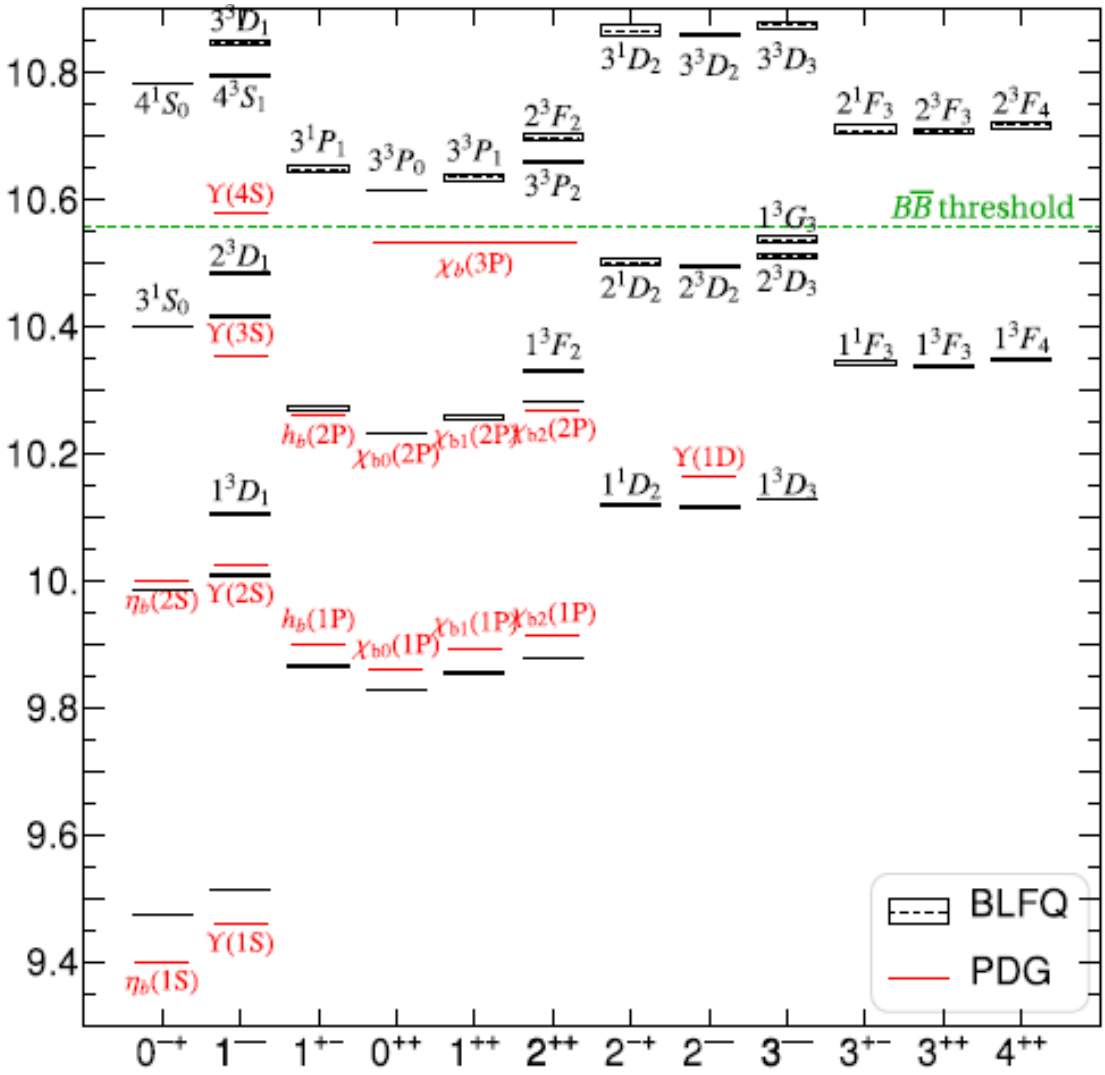

Figure 1.3: Spectra of bottomonium states.

able to find the spectra for such states.

Experimental discovery of pentaquarks was first made in 2003 at LEPS in Japan, but it got confirmed in 2015 by the LHCb prediction of two exotic states $P_c(4380)^+$ and $P_c(4450)^+$ [68]. These two states are assigned as the molecular state of $\Sigma_c(2455)\overline{D}^*$ and $\Sigma_c^*(2520)\overline{D}^*$ with $uudc\bar{c}$ structure [69].

1.4 Quantum Chromodynamics

Quantum chromodynamics (QCD) deals with the strong interactions of colored quarks and gluons. QCD is a non-Abelian $SU(3)_c$ gauge symmetry, where c stands for the color charge of the strong interaction. The massless gluons, force carriers of strong interaction, themselves carry color charges. The most general structure of the QCD lagrangian is given as

$$\mathscr{L} = \mathscr{L}_{gauge} + \mathscr{L}_{fermions}$$

where the gauge part $\mathscr{L}_{gauge}$ is

$$\mathscr{L}_{gauge} = -\frac{1}{4} G^A_{\mu\nu} G^{A\mu\nu}, \tag{1.2}$$

with

$$G^A_{\mu\nu} = \partial_\mu A^A_\nu - \partial_\nu A^A_\mu - g f^{ABC} A^B_\mu A^C_\nu \tag{1.3}$$

where $G^A_{\mu\nu}$ is the gluon field tensor describing the propagation of gluons and their self interactions. The last term in Eq.(1.3) makes it invariant under the non-abelian gauge transformation. A_μ is the gluon field with A,B,C being color indices that run from 1 to $N_C^2 - 1$, for the color group $SU(N_C)$. For SU(3) group, there are three colors, thus eight types of gluon fields are present.
And the fermionic part $\mathscr{L}_{fermions}$ is

$$\mathscr{L}_{fermions} = \sum \overline{\Psi}_i (i \not{D}_i - m_i) \Psi_i \tag{1.4}$$

Here $\overline{\Psi}_i$ describes the dirac spinors of i^{th} quark with mass m_i. The SU(3) color covariant derivative D_μ is defined as $D_\mu = \partial_\mu + i g A^A_\mu T^A$. This fermionic part represents the quark propagation and their interaction with the gluon gauge field $A_\mu = A^A_\mu T^A$.

The quantity g is the strong coupling constant. The μ and ν are the lorentz indices that identify the spatial and temporal components of the vector gauge fields. T^A are the SU(3) group generators satisfying $[T^A, T^B] = if^{ABC}T^C$, where f^{ABC} is the structure constant of SU(3) group [70–74].

QCD possess the similar structure as that of QED, except the difference that in QCD, the gauge group is non - abelian with self interacting gluons. This makes the coupling constant as running coupling constant. Coupling constant $\alpha_s(\mu)$ in QCD can be defined as the function of the momentum transfer which depicts the interaction between quarks and gluons in QCD [75]. The lowest order for the strong interaction constant is given by

$$\alpha_s(\mu) = \frac{12\pi}{(33 - 2N_q)ln(\frac{\mu^2}{\Lambda^2_{QCD}})} \tag{1.5}$$

where N_q is the number of quark flavor and μ is the energy-scale parameter known as the renormalization point. Λ_{QCD} is the QCD dynamical scale at which coupling diverges. The numerical value of Λ_{QCD} can be estimated either theoretically or experimentally. Value of the Λ_{QCD} is $\sim$ 200 MeV [20]. Dependence of coupling constant on energy shown in Eq.(1.5) depicts the underlying phenomenon of hadron physics from color confinement at large distances to asymptotic freedom at short distances. It is essential to know the behavior and magnitude of QCD coupling over the entire energy scale for describing the hadronic interactions at all energy scales. The change of coupling constant with the energy scale (distance range) is shown in Figure 1.4.

According to this figure, the two peculiar properties of QCD can be studied as:

- At high energies (short distances) the strong coupling constant α_s decreases logarithmically. When quarks are probed at large energies, they behave as free particles inside hadrons. This property of strong interactions is known as

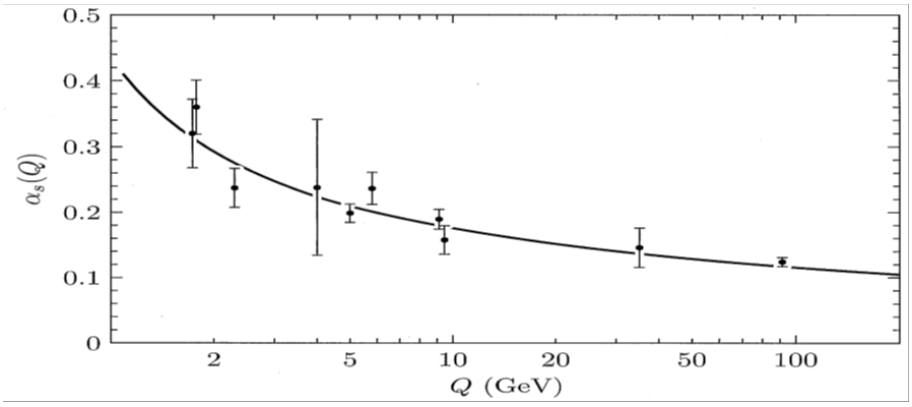

Figure 1.4: The behavior of strong coupling constant α_s as a function of the momentum transfer Q or, equivalently, the inverse of the quark separation distance.

asymptotic freedom. In this limit, a perturbative treatment is reliable where the physical observable can be expanded in terms of α_s. The perturbative (high energy) side of QCD has been confirmed in many experiments. At high energy, precise knowledge of α_s is required to test the high energy models that unify the strong and electroweak interactions.

- At low energies (large distances), coupling constant becomes strong and quarks, antiquarks, and gluons are confined. This is known as color or ***quark confinement***. Experimentally, individual quarks and gluons have not yet been observed. Instead colorless hadrons are detected. This indeed provides a strong evidence for the color - confinement hypothesis. In the case of large coupling constant, the direct solution of QCD is complicated. There are, however, various non perturbative techniques to solve the system at low energy.

There are many non-perturbative approaches to study the hadrons. Most common approach is an effective field theory (EFT) and can be somehow considered as a phenomenological theory. Effective field theories are constructed to probe and interpret the dynamics of hadrons by exploiting the symmetries of QCD.
Thus for studying the hadrons, we have two approaches in our hand. The first one is the perturbative QCD method and the other are non-perturbative phenomeno-

logical models.

In this thesis, we will utilize phenomenological field theories to investigate the properties of mesons containing a single heavy quark, in particular charm and bottom mesons.

1.5 Phenomenological Approaches

As discussed in previous section, we have two approaches to study the hadrons i.e. perturbative methods and non-perturbative methods. In field theory, a common technique for extracting information regarding the physical quantities at low energy is perturbation theory. Due to the asymptotic nature of QCD, perturbative series expansion breaks at very low energy. This means perturbative analysis can only be applied well at shorter distances i.e. $\sim$ less than 0.1 fm or momenta larger than 2 GeV. The most important QCD phenomena takes place in the infrared region (0-2 GeV momenta), so perturbation technique does not help us in understanding these phenomenons. This means that perturbative approach is not sufficient to get a complete picture of QCD. So, one has to look for the other available approaches. Non-perturbative QCD is used at low energy regime where the direct theoretical approaches are hard to apply. At small momentum transfer of around Q $\sim$ 500 MeV, the value of running coupling constant $\alpha(Q^2)$ approaches the value 1, making QCD, a non-perturbative phenomenon. There are various non-perturbative methods available in literature like sum rules, potential models, lattice QCD, effective theories etc.

1.5.1 QCD sum rules

The QCD sum rule is phenomenological approach to study non-perturbative phenomena. The QCD sum rules, were developed twenty years back by Shifman, Vainshtein and Zakharov (SVZ), and have become an interesting tool in hadron phenomenology [76]. This appears to work well for the calculation of masses of the

lowest hadronic states and effective coupling constants. The advantages of this method are well known. In this technique, hadrons are represented by their interpolating quark currents taken at large virtualities. The general representation of two-point correlation function matrix is given as:

$$\langle \Omega | T\Phi(x)\Phi(y) | \Omega \rangle$$

where $|\Omega\rangle$ represents the ground state of interacting theory and T is the time ordering symbol. By performing an operator product expansion (OPE), where the short and long-distance quark-gluon interactions are separated, a general form for the required matrix elements is derived. The former is calculated using QCD perturbation theory, whereas the latter is parameterized in terms of universal vacuum condensation or light-cone distribution amplitudes. The result of the QCD calculation is then matched, via dispersion relation, to a sum over hadronic states. The sum rule obtained in this way allows the calculation of observable for the hadronic ground states. In contrast, the parameters of QCD such as quark masses and vacuum condensate densities can be extracted from the sum rules that are experimentally known. The interactions of quark-gluon currents with QCD vacuum fields critically depend on the quantum numbers (spin, parity, flavor content) of these currents. Therefore, by using hadronic fields in terms of current, the resulting quantum numbers are not same. Numerous properties of hadrons with possible flavor combinations have been calculated by the sum rule method [77,78]. The results are encouraging and in most cases, they reveal information about the hadronic structure with remarkable agreement with experimental data. Therefore, whenever one needs to determine unknown hadronic parameters, QCD sum rule prediction is one of the reliable technique.

1.5.2 Potential Models

Another very famous category of phenomenological models involve the introduction of effective potentials in Hamiltonian formalism. Potential models use the constituent masses of quarks and incorporate interaction terms in it. Quarks within a

hadron are considered to be non-relativistic and the change in the hadronic properties due to the addition of gluonic field is represented by the effective potential. This interaction is in the form of spin dependent potentials, color Coulomb potentials, flavor dependent potentials etc. This interaction is described in terms of the Wilson coefficients and matrix elements of chromo-magnetic and electric operators. The simplest potential model derived to study the hadrons containing heavy quark includes a Coulomb like and a linear term. These are in the form of

$$V = -C_F \frac{\alpha(r)}{r} + br \tag{1.6}$$

The first term is for the short distance interactions and the other term is for the strong coupling limit. Later, models were modified and additional terms of spin-spin, spin-orbit interactions were included in this simplest form [49, 80].
All these models provide effective way to analyze various properties of the heavy mesons. But these models contain many unknown theoretical parameters which need to be fitted with the experimental data to obtain a precise information of hadrons.

1.5.3 Lattice QCD

The lattice QCD is a well known approach for the study of strong interactions between colored quarks and gluons. It is formulated on lattice or grid having space and time points. This grid has lattice spacing a between the points with L being the total length of the lattice. The quark fields exist at these lattice points with the gluons existing on the links connecting neighboring sites. Essentially, the links represent the color field which transforms under SU(3) gauge transformation [81,82]. There are many technical problems involved in the lattice QCD calculations and some of which can even introduce an unknown amount of systematic error. In the chiral limit, while studying the properties of light quarks, a very small lattice spacing a is required which results in increasing the number of lattice points on the

grid. Lattice QCD calculations for large number of lattice points is both time and money consuming. Monte Carlo methods for solving the lattice QCD calculations require the largest supercomputers. But, now quenched approximations and Dyson-Schwinger equation formalism have effectively modified this approach.

1.5.4 Effective Field Theory

Effective field theory is another non-perturbative approach to study the QCD dynamics. Effective theory is type of approximation, in which a physical phenomenon is separated at different scales, so that one can examine the required physics at a particular scale and certain degrees of freedom (DOF) at this chosen energy scale are ignored. At a chosen energy scale, one explores the symmetry limits and describes the non-perturbative effects in terms of some low energy constants which are determined from the experimental data. This works when the effects of a very heavy particle are not so important for certain low energy phenomena, and one can remove the corresponding degrees of freedom and construct an effective low energy field theory. For that purpose, one has to identify the heavy quark fields and integrate them out in the generating function. This theory simplifies the practical calculations at low energy scale of Λ_{QCD} in field theory. The basic idea behind the effective field theory is to describe dynamics of hadrons in terms of a fully consistent theory but in limited nature.

Bag models, heavy quark effective theory, heavy hadron chiral perturbation, chiral perturbation theory and many more are the examples of effective theories.

(a)Bag Models

Bag models are the effective models used to study the nucleons. Chiral bag model is a hybrid model of the MIT bag model and the skyrme model. These models were developed to explain the hadron spectrum and different properties of the particles [83]. The phenomenological assumptions of these models are based on the fact that

the quark and gluons are regarded as massless particles moving freely inside the bag of radius R. The quarks are massless inside the bag but infinitely heavy outside. Wavefunctions of these relativistic free quarks are generated to calculate hadron spectrum and other properties. The radius R is determined from the fact that the pressure on the bag walls from the outside is being balanced by the pressure resulting from the kinetic energy of the quarks inside the bag. This is done by fitting the model parameters with the experimental data like masses, magnetic moments etc.

(b)Heavy Quark Effective theory (HQET)

HQET is applicable for studying the QCD properties of heavy hadrons containing a single heavy quark Q and light degrees of freedom (DOF). It describes the interaction between the heavy and light quarks, where momentum transfer p between them is very small as compared to the mass of heavy quark m_Q. An effective lagrangian is formulated in the terms of inverse powers of heavy quark mass m_Q. Effective lagrangian of the hadronic system is formulated such that it becomes independent of the mass of the heavy quark when $m_Q \to \infty$ limit is applied [20, 75, 84]. HQET is typically applied to the hadrons containing a heavy quark c or b. Size of the hadrons containing a heavy quark is given by R_{had} ∼1 fm, and the momentum exchanged between the heavy and light constituents of hadron is of the order of Λ_{QCD}. Effectiveness of this theory comes from the fact that the compton wavelength of the heavy quark is much smaller than the size of the hadron i.e.

$$m_Q \gg \Lambda_{QCD} \tag{1.7}$$

$$\Rightarrow \lambda_Q \ll R_{had} \tag{1.8}$$

Thus the light constituent which can only resolve distances much larger than the λ_Q becomes blind to the nature of the heavy quark in the hadron. Light constituent only experiences the color field of the heavy quark irrespective of the flavor, mass and spin of heavy quark. Heavy hadron system holds certain symmetries which are

known as heavy quark spin and flavor symmetry. This symmetry is embodied in a low energy effective theory which is known as heavy quark effective field theory. This will allow us to derive Feynman rules for the heavy quarks and construct an effective lagrangian for strong interaction of the heavy hadrons.

In this thesis, we will be using heavy quark effective theory to study the various properties of the heavy-light D and B mesons. This theory is studied in detail in Chapter 2. In our current work, we restrict to charm and bottom mesons only, as top quark being very heavier than this scale has not predicted separately yet and exhibit weak decays.

(c)Heavy Hadron Chiral Perturbation Theory

Heavy hadron chiral perturbation theory (HHχPT) is a framework in which chiral and heavy quark spin symmetries are incorporated together. The mass of the light quarks u, d and s is very small as compared to the hadronic energy scale Λ_{QCD}, thus they posses a $SU(3)_L \times SU(3)_R$ flavor chiral symmetry. This symmetry is spontaneously broken which is reflected in the presence of eight Goldstone bosons $\pi^{\pm}, \pi^0, K^{\pm}, K^0, \overline{K}^0$ and η.

The mass of the heavy quarks c and b is very large as compared to $\Lambda_{QCD} \sim 200$ MeV [20], as a result the dynamics of a heavy quark in QCD becomes independent of mass and spin of heavy quark. A new flavor and spin symmetry appears for the hadrons containing single heavy quark. The heavy quark spin-flavor symmetry along with the chiral symmetry of light quarks are coupled together in this framework [85–87]. Using these symmetries, an effective lagrangian is constructed which helps in redeeming the properties of the hadrons.

1.6 Symmetries

Symmetries play significant role in quantum field theory, as they are essential tools to probe strongly interacting systems, and to examine their dynamics. For a given physical phenomenon, symmetries introduce constraints in the interactions and simplify the Lagrangian of the theory. Transformations which do not change the physics of a system are called symmetry transformations. There are mainly two types of symmetry transformations [88] i.e. local and global transformations. In local transformation, parameters are spacetime dependent, whereas in global they are spacetime independent. In general, local symmetries are followed by gauge theories, while global symmetries result in the origin of massless particles. QCD is a gauge theory having $SU(N_c)$ local symmetry group of color degrees of freedom. The QCD Lagrangian is invariant under the local gauge symmetry SU(3) in which all quark flavors experience the same strong force. The only term that distinguishes between quark flavors is the mass term. One can express this term of the Lagrangian in the following way:

$$\mathscr{L}^{m}_{QCD} = \overline{q}(i\gamma^{\mu}D_{\mu} - m_q)q + \overline{Q}(i\gamma^{\mu}D_{\mu} - m_Q)Q \tag{1.9}$$

where first term represents the light quarks q (u, d and s) whose mass $m_q \ll \Lambda_{QCD}$ and the second term reflects the heavy quarks Q (c and b) with $m_Q \gg \Lambda_{QCD}$. This lagrangian helps us to investigate some symmetries that arise due to some limits in the quark masses. At low energy, the QCD Lagrangian shows some global symmetries like chiral symmetry, heavy quark symmetry and isospin symmetry.

Chiral symmetry is the invariance of the massless Dirac fields under chiral rotations, i.e. left handed and right handed parts of the Dirac fields transform independently. Using the projection operators $P_L = \frac{1}{2}(1-\gamma_5)$ and $P_R = \frac{1}{2}(1+\gamma_5)$, the Dirac spinors for quark (anti-quark) q ($\overline{q}$) can be decomposed into its chiral left handed component

q_L and right handed component q_R [88–90] as: $q = \begin{pmatrix} q_R \\ q_L \end{pmatrix}$ ($\overline{q} = \begin{pmatrix} \overline{q}_R & \overline{q}_L \end{pmatrix}$).

These left and right handed quark components modify the QCD lagrangian as

$$\mathscr{L}_{QCD} = i\overline{q}_L \not{\partial} q_L + i\overline{q}_R \not{\partial} q_R - \overline{q}_R m q_L - \overline{q}_L m q_R \tag{1.10}$$

In the low energy limit, when light quark masses $m_q \ll \Lambda_{QCD}$ approaches to zero, this lagrangian becomes

$$\mathscr{L}_{QCD} = i\overline{q}_L \not{\partial} q_L + i\overline{q}_R \not{\partial} q_R \tag{1.11}$$

The terms in the Eq.(1.11) are now independent of each other, leading to the symmetrical group of this lagrangian. This symmetry is known as chiral symmetry that dominates at very low energy scale as compared to Λ_{QCD}.

The *heavy quark symmetry* in heavy hadron arises because the heavy quark m_Q is massive in comparison to the QCD energy scale Λ_{QCD}. So it is always a good approximation to take limit $\frac{1}{m_Q} \to 0$, ($\frac{1}{m_c} = 0.00078$ MeV^{-1}, $\frac{1}{m_b} = 0.00023$ MeV^{-1}). In this limit, the higher order lagrangian terms which contain $\frac{1}{m_Q}$ factor vanish, thus making it heavy quark flavor independent. As a result, the light quarks within a meson will experience same potential for both c and b quarks, making it blind to the flavor of heavy quark.

Since the mass of the heavy quark is finite, so this heavy quark symmetry is just an approximate symmetry and requires corrections. This symmetry is complementary to the chiral symmetry, which results in the opposite limit of massless quarks.

There is one more commonly used symmetry in the strong interactions known as *Isospin symmetry*. This symmetry results when two light quarks up and down have same mass, $m_u = m_d = m_q$. Nearly degenerate states for pions ($\pi^{\pm}, \pi^0$) and nucleons (p, n) are the consequence of the isospin symmetry. This symmetry is broken

in the presence of electromagnetic interactions.

1.7 Chiral Symmetry Breaking

Chiral symmetry is observed in the low energy limit, when mass of the quarks approaches to zero. But in reality, quarks have mass, therefore chiral symmetry can not be seen as an exact symmetry of the QCD lagrangian. When $m_q \neq 0$, there is explicit breaking of chiral symmetry with mass as a measure of the breaking of the symmetry [88].

Beside this, there is also a dynamical breaking of the chiral symmetry due to QCD vacuum. The QCD vacuum is a dynamical state which includes the creation of quark-antiquark pairs. Energy required to create such a pair is very small if quarks are massless. Since quarks are strongly interacted to each other, one expects a condensate of $q\overline{q}$ pairs. The differences in the masses of the hadrons, either meson or baryon can be explained by the spontaneously breaking of chiral symmetry due to QCD vacuum. e.g. π and ρ mesons have similar quark content but different masses. Quarks get a very large effective mass because of the dynamically chiral symmetry breaking.

This mechanism of spontaneous breaking of chiral symmetry due to the non zero value of $q\overline{q}$ is known as Nambu-Goldstone model [22,91]. According to this theorem, when a continuous symmetry is spontaneously broken by vacuum, massless particles known as Goldstone bosons are generated. Number of Goldstone bosons generated are equivalent to the number of broken generators. There are $N_f^2 - 1$ number of generated Goldstone bosons, so $N_f = 2$, we have three spin zero massless bosons. And for $N_f = 3$, there are eight pseudo-scalar bosons in QCD. Pions are identified as the Goldstone bosons for the first case and octet of light pseudo-scalar mesons for the second case.

1.8 Experimental Motivation

The aim of the experimental and theoretical particle physics is to know about the fundamental building block of matter by searching the new subatomic particles and to precisely measure the properties of the known particles and interactions. Experiments are done at large accelerator sites having several types of detectors. Each detector is specialized in detecting specific types of particles or characterizing their motion [1, 4, 9, 17, 25–29, 32, 33]. It is observed that overall interest in high energy physics had increased recently mainly due to the large media exposure of the modern experiments and their discoveries including Higgs boson [9,10], Pentaquarks [94,95], neutrino oscillations [96–98] and many more [92,93,99,100]. In 2015, Arthur McDonald and Takaaki Kajita were awarded the Nobel Prize for their discovery of neutrino oscillations, which make the neutrinos massive in nature, contradicting the massless neutrinos of the Standard Model. Thus, physics beyond standard model can be studied by working on these new achievements.

We can also explore the current array of particles in more depth to get a trace for what lies beyond the Standard Model. These traces will give a better preceptive of how the universe works, answering various questions like what is dark matter made of, why is the Higgs mass so light, what happened to the antimatter in the early universe, are all the forces unified into one force at high energy etc.

Due to the upcoming information about the new particles coming from the LHC, CLEO, BaBar, Belle, BESII/III, CMS etc. [9,10,25,28,68], hadrons are the current and interesting topic of research. Despite many mysteries, these experiments have provided a useful data which helped to explore the hadronic structure.

The emerging data from the experiments has also motivated the theoreticians [36, 42,44,47,75,76,80] to update the existing theoretical models to generate new models so that the newly observed particles can be explained theoretically.

1.9 Organization of Thesis

The thesis is organized as follows:

Chapter 2 gives the general introduction of the heavy quark spin and flavor symmetry in heavy-light mesons which led to the development of Heavy Quark Effective Theory. A general lagrangian is formulated in the limit $m_Q \to \infty$ and $m_q \to 0$, which results in the spin and flavor symmetry. Chiral perturbation theory is applied to study the leading order effective lagrangian, describing the interaction of light pseudo-scalar mesons (π, η, K) with the heavy-light meson fields. Various properties like two body strong decays, masses, hyperfine splittings and associated couplings are discussed for these heavy-light mesons.

In **Chapter 3**, a detail analysis is carried out for all the experimentally available non-strange and strange charm states $D_J^*(2460)$, $D_J(2560)$, $D_J^*(2680)$, $D_J(2740)$, $D_J^*(2760)$, $D_J(3000)$, $D_J^*(3000)$, $D_2^*(3000)$, $D_{sJ}(3040)$, $D_{s1}^*(2710)$, $D_{s1}^*(2860)$ and $D_{s3}^*(2860)$ for their properties, whose J^P's are yet to be confirmed. We compute the two body strong decays of these excited charm states decaying to ground state along with the emission of pseudo-scalar mesons to establish their positions in the charm spectra. This analysis helps in identifying the non-strange states $D_J^*(2460)$, $D_J(2560)$, $D_J^*(2680)$, $D_J(2740)$, $D_J^*(2760)$, $D_J(3000)$ and $D_J^*(3000)$ to be $1P_{\frac{3}{2}}2^+$, $2S_{\frac{1}{2}}0^-$, $2S_{\frac{1}{2}}1^-$, $1D_{\frac{5}{2}}2^-$, $1D_{\frac{5}{2}}3^-$, $2P_{\frac{1}{2}}1^+$ and $2P_{\frac{1}{2}}0^+$ as their J^P's. Our study for the non-strange charm mesons mainly focus on the prediction of J^P for the newly observed charm state $D_2^*(3000)$ seen by LHCb in 2016. Branching ratio BR=$\frac{\Gamma(D_2^*(3000)\to D^*\pi)}{\Gamma(D_2^*(3000)\to D\pi)}$ is analyzed, for choosing $1F_{\frac{5}{2}}(2^+)$ as the best possible assignment for this state. Similar analyses have been done for the strange charm states. The most suitable spin-parity assignment for $D_{sJ}(3040)$ is $2P_{\frac{1}{2}}1^+$. And the states $D_{s1}^*(2710)$, $D_{s1}^*(2860)$, $D_{s3}^*(2860)$ are assigned as $2S_{\frac{1}{2}}1^-$, $1D_{\frac{3}{2}}1^-$ and $1D_{\frac{5}{2}}3^-$ respectively. The present work estimates strong coupling constants g_{TH}, $\widetilde{g}_{HH}$, g_{YH}, g_{XH},

$\widetilde{g}_{SH}$ and g_{ZH} from all these recently observed charm states. In addition to this, hyperfine splittings are used to calculate the masses for their missing spin partners $2S_{\frac{1}{2}}0^-$, $2P_{\frac{1}{2}}0^+$ and $1D_{\frac{5}{2}}2^-$.

In **Chapter 4**, we analyze the recent experimentally available bottom states $B_1(5721)$, $B_2^*(5747)$, $B_{1s}(5830)$, $B_{2s}^*(5840)$, $B_J(5960)$ and $B_J(5840)$ for their HQET properties. The study of the masses and strong decays for these observed bottom states help in assigning their positions in the bottom spectra. The most suitable spin-parity for bottom state $B_J(5960)$ is $2S(1^-)$. And the states $B_1(5721)$, $B_2^*(5747)$, $B_{1s}(5830)$, $B_{2s}^*(5840)$ belongs to higher excited states of n=1 P-wave doublet $(1^+, 2^+)$. Our main interest in this chapter, is the spin-parity assignment of bottom state $B_J(5840)$, recently observed by LHCb in 2015. By analyzing the strong decay widths, the branching ratio $\frac{\Gamma(B_J(5840)\to B\pi)}{\Gamma(B_J(5840)\to B^*\pi)}$ with bottom masses of all the possible J^P's for $B_J(5840)$, it is concluded that the most suitable J^P is $1D1^-$. We also compute the coupling constants g_{TH}, $\widetilde{g}_{HH}$ and g_{XH} associated with the strong decays of bottom states through the emission of (π, η, K). We further aim to predict the decay width of few other unknown bottom states $B(2^1S_0)$, $B_s(2^3S_1)$, $B_s(2^1S_0)$, $B(1^1D_2)$, $B_s(1^3D_1)$ and $B_s(1^1D_2)$ which are the spin and strange partners of bottom states $B_J(5960)$ and $B_J(5840)$. The suitable suppression factor for isospin violating decays like excited stranged bottom state decaying to lower stranged bottom state along with pion have also been accounted. The results for various decays with their associated couplings are tabulated in this chapter.

In **Chapter 5**, masses and strong decays of radially excited non-strange and strange bottom state doublets $B(2S)$, $B(2P)$ along with n=1 orbitally excited doublets $B(1D)_{5/2}$ and $B(1F)_{5/2}$ are studied in detail. Masses for these bottom states are calculated using the heavy quark flavor symmetry for charm and bottom mesons implying $\Delta_F^{(b)} = \Delta_F^{(c)}$ and $\lambda_F^{(b)} = \lambda_F^{(c)}$. Here Δ_F is the spin averaged mass splittings

between the excited states and S-wave ground state and λ_F is the mass splittings between the spin partners of the same doublets. The effect of QCD and $1/m_Q$ corrections to the next to leading order lagrangian are also examined for both λ_F and Δ_F parameters. These corrections modify the heavy quark flavor parameters as $\Delta_F^{(b)} = \Delta_F^{(c)} + \delta\Delta_F$ and $\lambda_F^{(b)} = \lambda_F^{(c)}\delta\lambda_F$. It is observed that these corrections are less sensitive for n=2 masses as compared to n=1 masses. The various masses and their strong decays can be used to check the validity of the HQET framework.

Finally **Chapter 6**, concludes the work done in this thesis and summaries the results with possible extension for future reserach.

Bibliography

[1] Thomson, J.J. Cathode Rays. Philosophical Magazine, **44**, 293-316 (1897). http://dx.doi.org/10.1080/14786449708621070.

[2] E. Rutherford, Philosophical Magazine. Series 6, vol. **21**. May (1911).

[3] C. L Cowan Jr., F. Reines, F. B. Harrison et.al., Science. **124** (3212): 1034 (1956).

[4] E. D. Bloom et al. ,Phys. Rev. Lett. **23** (16), 930934 (1969).

[5] H.W.Kendall, Rev. Mod. Phys. **63**, 597 (1991).

[6] S. Weinberg, Phys. Rev. Lett. **19**, 1264 (1967).

[7] A. Salam, Conf. Proc. C680519, **367** (1968).

[8] S. Glashow, Nucl. Phys. **22**, 579 (1961).

[9] S.Chatrchyam et.al., [CMS Collaboration],Phys. Lett. B **716**, 30 (2012).

[10] G.Aad et.al., [ATLAS Collaboration],Phys. Lett. B **716**, 1 (2012).

[11] Lykken, J. D. CERN Yellow Report. CERN. pp. 101109 (2010). arXiv:1005.1676

[12] M. Gell-Mann, Phys. Lett. **8**, 214 (1964).

[13] G. Zweig, CERN Report 8419, TH401, (1964).

[14] G. Zweig, CERN Report 8419/TH.412 (1964).

[15] Gell-Mann, M. Nuovo Cim 4(Suppl 2): 848 (1956).

[16] K. Nishijima, Prog. Theor. Phys. **13**, 285(1955).

[17] M. Tanabashi et al.,[Particle Data Group Collaboration], Phys. Rev. D **98** 030001 (2018).

[18] O. W. Greenburg, Phys. Rev. Lett.**13**, 598(1964).

[19] K. G. Wilson, Phys. Rev. D **10**, 245 (1974).

[20] M. Neubert, Heavy Quark Effective Theory 39-78 hep-ph/9610385 CERN-TH-96-292 .

[21] Y. Nambu and G. Jona-Lasinio, Phys. Rev. **122**, 345 (1961).

[22] J. Goldstone, A. Salam and S. Weinberg, Phys. Rev. **127**, 965 (1962).

[23] G. Goldhaber et al., Phys. Rev. Lett. **37**, 255 (1976).

[24] I. Peruzzi et al., Phys. Rev. Lett. **37**, 569 (1976).

[25] S. Behrends et al. [CLEO Collaboration], Phys. Rev. Lett. **50**, 881 (1983).

[26] J.C. Anjos et al. [Tagged Photon Spectrometer], Phys. Rev. Lett. **62**, 1717 (1989)

[27] H. Albrecht et al. [ARGUS Collaboration], Phys. Lett. B **231**, 208 (1989).

[28] P. del Amo Sanchez et al. [BaBar Collaboration], Phys. Rev. D **82**, 111101 (2010).

[29] R. Aaij et al. [LHCb Collaboration], JHEP **09**, 145 (2013).

[30] R. Aaij et al. [LHCb Collaboration], Phys. Rev. D **94**, 072001(2016).

[31] R. Aaij et al. [LHCb Collaboration], JHEP **04**, 024 (2015).

[32] T.A. Aaltonen et al. [CDF Collaboration], Phys. Rev. D **90**, 012013 (2014), 1309.5961

[33] V.M. Abazov et al. [DØ Collaboration], Phys. Rev. Lett. **99**, 172001 (2007).

[34] R. Aaij et al. [LHCb Collaboration], Phys. Rev. Lett. **110**, 151803 (2013).

[35] T. Aaltonen et al. [CDF Collaboration], Phys. Rev. Lett. **100**, 082001 (2008).

[36] X.H. Zhong, Phys. Rev. D **82**, 114014 (2010).

[37] B. Chen, X. Liu, A. Zhang, Phys. Rev. D **92**, 034005 (2015).

[38] L.Y. Xiao, X.H. Zhong, Phys. Rev. D **90**, 074029 (2014).

[39] J.Z. Wang, D.Y. Chen, Q.T. Song et. al., Phys. Rev. D **94**, 094044 (2016).

[40] Z.G. Wang Commun.Theor.Phys. **66** 671 (2016).

[41] X.h. Zhong, Q. Zhao, Phys. Rev. D **78**, 014029 (2008).

[42] S. Godfrey, K. Moats, Phys. Rev. D **90**, 117501 (2014).

[43] Y. Sun, Q.T. Song, D.Y. Chen et. al., Phys. Rev. D **89**, 054026 (2014).

[44] Z.G. Wang, Eur. Phys. J. Plus **129**, 186 (2014).

[45] Q.F. L, T.T. Pan, Y.Y. Wang et.al., Phys. Rev. D **94**, 074012 (2016).

[46] A. Martin, Phys. Lett. B. **93**, 338 (1980).

[47] Bhavin Patel, P.C. Vinodkumar, J. Phys. G **36** 035003 (2009).

[48] D. Bettoni, EPJ Web of Conferences **73**, 01006 (2014).

[49] D. Ebert, R.N. Faustov and V. O. Galkin, Phys. Rev D **67**, 014027 (2003).

[50] J. Zeng, J. W. Van Orden and W. Roberts, Phys. Rev. D **52**, 5229 (1995).

[51] Yang Li, Pieter Maris, James P. Vary, Phys. Rev. D **96**, 016022 (2017).

[52] R. L. Jaffe, Phys. Rev. D **15**, 267 (1977).

[53] H. J. Lipkin, Phys. Lett. B **195** , 484 (1987).

[54] Z. Q. Liu, et al., Phys. Rev. Lett. **110**, 252002 (2013).

[55] T. Xiao, S. Dobbs, A. Tomaradze, K. K. Seth, Phys. Lett. B **727**, 366370 (2013).

[56] X. L.Wang, et al., Phys. Rev. D **91** 112007 (2015).

[57] R. Aaij, et al., Eur. Phys. J. C **78**, 1019 (2018).

[58] T. Aaltonen, et al., Mod. Phys. Lett. A **32**, 1750139 (2017).

[59] V. M. Abazov, et al., Phys. Rev. D **89**, 012004 (2014).

[60] J. P. Lees, et al.,Phys. Rev. D **86**, 051102 (2012).

[61] A. Bondar et al.,[Belle Collaboration] Phys. Rev. Lett. **108**, 122001 (2012).

[62] I. Adachi, et al., Phys. Rev. Lett. **108** , 032001 (2012).

[63] Hua-Xing Chen, Wei Chen, Xiang Liu et al., Phys. Rept. **639**, 1-121 (2016).

[64] A. Esposito et. al., Phys.Rept. **668**, 1-97 (2016).

[65] Xiaozhao Chen and Xiaofu L Phys. Rev. D **97**, 114005 (2018).

[66] Xiao zhao Chen , Xiao fu Lu, Eur. Phys. J. C **75**, 98 (2015).

[67] D. Ebert, R. N. Faustov, V. O. Galkin, Eur. Phys. J. C **58** 399-405 (2008).

[68] R. Aaij [LHCb collaboration], Phys. Rev. Lett. **115**, 072001 (2015).

[69] Eides, M.I., Petrov, V.Y. Polyakov, M.V. Eur. Phys. J. C **78**, 36 (2018).

[70] Scherer, Stefan et al. hep-ph/0505265v1, Report No. MKPH-T-05-08 (2005).

[71] Ecker Gerhard - Quantum chromodynamics, hep-ph/0604165 UWTHPH-2006-9

[72] A. V. Smilga: Lectures on Quantum Chromodynamics (World Scientific) (2001).

[73] David Bailin, Alexander Love, Introduction to Gauge Field theory, Institute of Physics Pub., (1986).

[74] Michael E. Peskin, Dan V. Schroeder: An Introduction to Quantum Field Theory (Frontiers in Physics) (HarperCollins Publishers) (1995).

[75] M. Neubert, Phys. Rep. **245** 259 (1994).

[76] M. A. Shifman, A. I. Vainshtein and V. I. Zakharov, Nucl. Phys. B **147**, 385, 448 (1979).

[77] Z. G. Wang and Z. B. Wang, Chin. Phys. Lett. **25**, 444-446 (2008).

[78] P. Colangelo et al.,1495-1576 hep-ph/0010175 CERN-TH-2000-296, BARI-TH-2000-394.

[79] D. Ebert, R. N. Faustov, V. O. Galkin, Phys. Rev. D **67**, 014027 (2003).

[80] Zalak Shah, Kaushal Thakkar, Ajay Kumar Rai, P. C. Vinodkumar, Eur. Phys. J. A **52**, 313 (2016).

[81] L. Giusti and S. Necco, JHEP **0704**, 090 (2007).

[82] Y. Maezawa et.al., Phys. Rev. D **75**, 074501 (2007).

[83] A. Chodos, R. L. Jaffe, K. Johnson, C. B. Thorn and V. F. Weisskopf, Phys. Rev. D **9**, 3471 (1974).

[84] R. Casalbuoni, A. Deandrea, N. Di Bartolomeo et. al., Phys. Rep. **281**, 145 (1977).

[85] E. Jenkins, Nucl. Phys. B **412**, 181 (1994).

[86] T. Mehen and R. Springer, Phys. Rev. D **72**, 034006 (2005).

[87] D. Kaplan, M. Savage, and M. Wise, Nucl.Phys. B **534**, 329 (1998).

[88] H. Sazdjian, EPJ Web of Conferences **137**, 02001 (2017).

[89] S. Scherer, Adv. Nucl. Phys. **27**, 277 (2003).

[90] M. E. Peskin, Les Houches Lectures, SLAC-PUB-3021 (1982).

[91] V. Koch, Int. J. Mod.Phys. E **6** 203-250 (1997).

[92] G. Bertone, D. Hooper and J. Silk, Phys. Rept. **405**, 279 (2005).

[93] P. A. R. Ade et al. [Planck Collaboration], Astron. Astrophys. **594**, A13 (2016).

[94] R. Aaij et al. [LHCb Collaboration], Phys. Rev. Lett. **117**, 082003 (2016); Errata Phys. Rev. Lett. **117**, 109902 (2016); Phys. Rev. Lett. **118**, 119901 (2017).

[95] A. Ali, J. S. Lange, and S. Stone, Prog. Part. Nucl. Phys. **97**, 123 (2017).

[96] Z.Maki, M.Nakagawa, and S. Sakata, Prog. Theor. Phys. **28** 870 (1962).

[97] B. Pontecorvo, Zh. Eksp. Teor. Fiz. **53**, 17171725 (1968).

[98] M. Kobayashi; T. Maskawa, Prog. Theor. Phys. **49** 652 (1973).

[99] F. Abe et al. [CDF Collaboration], Phys. Rev. Lett. **74**, 26262631 (1995).

[100] S. Abachi et al. [DØ Collaboration], Phys. Rev. Lett. **74**, 2632-2637 (1995).

[101] M. Ablikim et. al., [BESIII Collaboration], Phys. Rev. Lett. **106**, 072002 (2011).

[102] M. Ablikim et. al., Chin. Phys. C **36**, 1031-1039 (2012).

Chapter 2

Heavy Quark Effective Theory

2.1 Introduction

Recent experimental progress in meson spectra is challenging the naive quark model. The main challenge comes from the mesons containing heavy quark i.e. heavy-light $Q\overline{q}$ mesons and heavy heavy $Q\overline{Q}$ mesons. The properties of nearly all the light-light $q\overline{q}$ mesons have been successfully confirmed both experimentally and theoretically. At present heavy quark physics has become one of the rapidly growing areas of high energy physics. Recent experiments like LHCb, Belle, BESII/III, BaBar, CDF [1–4, 56, 57] etc. are producing a lot of information about heavy hadrons. Therefore, a much better theoretical approaches are required to understand the properties of heavy hadrons. The presence of the heavy quark degrees of freedom (DOF) in heavy mesons helps in understanding how the strong interactions binds the quarks within mesons, and thus helps in studying their QCD properties. This heavy quark DOF can be used to study the heavy hadrons by constructing effective field theories at both the quark level and hadron level. The well known effective theories are Heavy quark Effective Theory (HQET), Non-Relativistic QCD (NRQCD) and many more. These effective theories are always related to some scales which constrain their application region. In the effective theories, lagrangian is constructed using QCD symmetries and interaction terms are incorporated by

some expansion parameters. In the heavy-heavy sector, only few of the states like $B_c(6274), \eta_c(1S), J/\Psi(1S), \chi_{c0}(1P)$ have been experimentally observed, so their information is rather limited.

So we are inspired in studying the heavy-light charm (D) and bottom (B) mesons only. Study of heavy-light mesons has provided a better understanding of non-perturbative quantum chromodynamics. For this, we use two symmetries of the QCD, one in the infinite heavy quark (Q = c, d) mass limit ($m_Q \to \infty$) and the other in the chiral limit of light quark (q = u, d, s) ($m_q \to 0$), together to construct an effective theory commonly known as Heavy quark Effective Theory (HQET). In this chapter, we will discuss HQET as a quantum field theory to extract the properties of heavy-light D and B mesons. HQET is an effective theory formulated to obtain the QCD results for hadrons containing single heavy quark c or b strongly interacting by the exchange of gluons with the light DOF.

Heavy light meson $Q\overline{q}$ contains a heavy quark Q and antiquark $\overline{q}$, gluons, quark anti-quark pair. All the degrees of freedom other than heavy quark are referred as light degrees of freedom l or as brown muck. As discussed in chapter 1, QCD generates a non-perturbative scale $\Lambda_{QCD} \simeq 200$ MeV [22]. Size of the heavy-light meson $Q\overline{q}$ with $m_Q \gg \Lambda_{QCD}$ and $m_q \ll \Lambda_{QCD}$ is of the order of $\Lambda_{QCD}^{-1} \sim 1$ fm.

The heavy quark Q inside a hadronic bound state $Q\overline{q}$ interacts with the light constituents with the exchange of momentum much smaller than its mass m_Q [5–7]. The momentum of the heavy quark is given as

$$p_Q = m_Q v + K \tag{2.1}$$

where v is the velocity of the heavy quark and K is a small residual momentum which depicts the amount of the off shell of heavy quark due to its interaction with light degree of freedom. In the heavy-light systems, K is usually of the order of Λ_{QCD}, which is also the momentum of the light degrees of freedom. So the momentum exchange between the heavy and light constituent during strong interaction

is approximately Λ_{QCD}. As a result, the change in velocity of the heavy quark $\Delta v = \frac{p}{m_Q}$ is very small, implying a very crucial result that the velocity of the heavy quark does not change with time during the strong interactions.

Therefore, heavy quark moves with the hadron's velocity v. The QCD interactions does not affect the heavy quark's velocity at all. Any change in the trajectory of the heavy quark velocity is a result of external non QCD effects like weak and electromagnetic interactions.

The physical picture of heavy-light mesons can be interpreted as that of hydrogen atom, where in a first approximation, proton acts as a static source of EM fields. It only absorbs or emits photons, while other recoil effects are neglected. In heavy-light mesons, the heavy quark Q plays the part of proton and the light degrees of freedom (LDOF) acts as the electron cloud. The heavy quark is assumed to be static external source as compared to the light constituent, and it only transfers as a color triplet. The dynamics of the LDOF is still provided by its non-perturbative interactions among the constituents, but its interaction with the heavy quark Q has been oversimplified.

Therefore in this limit, heavy quark behaves as static, so the LDOF can not observe the mass of the heavy quark. This results in $U(N_h)$ (N_h is heavy flavors) heavy quark flavor symmetry (HQFS), describing that the dynamics of the heavy-light mesons is unchanged under the exchange of heavy quark flavour $b \longleftrightarrow c$. Also, in this limit, since the heavy quark interacts strongly only through the color exchange with gluons, thus making it independent of the orientation of the spin of the heavy quark $\uparrow Q \longleftrightarrow \downarrow Q, Q \in c, b$. This results in another SU(2) symmetry known as heavy quark spin symmetry (HQSS).

This SU(2) spin symmetry and $U(N_h)$ heavy quark flavor symmetry are embedded into a larger $SU(2N_h)$ spin-flavor symmetry [8–10]. Under this symmetry, $2N_h$ states of N_h heavy quarks with spin up and down transfer as the fundamental representation. Heavy-quark spin and flavor symmetry between charm and bottom mesons

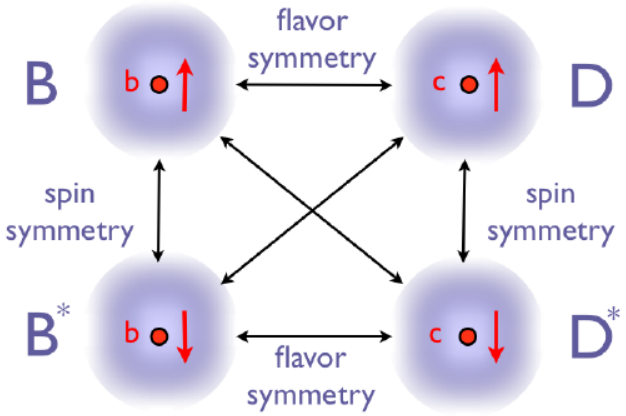

Figure 2.1: Heavy-quark spin and flavor symmetry between charm and bottom mesons.

are diagrammatically shown in Figure 2.1.

However, these symmetries faces $1/m_Q$ corrections due to the finite mass effects of the c and b quarks. In the next sections, we will construct a general lagrangian for HQET, and will study how the higher order expansion of HQET lagrangian in terms of inverse of heavy quark mass $1/m_Q$ results in breaking of this $SU(2N_h)$ symmetry of the heavy quark.

2.2 Quantum Numbers for Heavy-Light Mesons

Before studying the lagrangian for $Q\overline{q}$ systems, it is obligatory to know about the spectroscopy for the $Q\overline{q}$ mesons. There are various quantum numbers required to specify a heavy-light meson. The $Q\overline{q}$ state is notated as $nL_{S_l}J^P$, where n is the radial quantum number and P is the parity of the state. In the $m_Q \to \infty$ limit, spin of the heavy quark $\overrightarrow{S}_Q$ is conserved as $\overrightarrow{S}_Q = \frac{1}{2}$, so the total angular momentum of the light degrees of freedom $\overrightarrow{S}_l$ is written as

$$\overrightarrow{S}_l = \overrightarrow{S}_q + \overrightarrow{L} \tag{2.2}$$

with spin $\overrightarrow{S_q} = \frac{1}{2}$ and $\overrightarrow{L}$ being its orbital angular momentum [11,12]. The conserved operator $\overrightarrow{J}$, total angular momentum of the heavy-light system is therefore given as

$$\overrightarrow{J} = \overrightarrow{S}_l + \overrightarrow{S}_Q \tag{2.3}$$

The quantum numbers j, s_Q and s_l gives eigenvalues for the operators $\mathbf{J}^2, \mathbf{s}_\mathbf{Q}^2, \mathbf{s}_l^2$ as $\mathbf{J}^2 = j(j+1)$, $\mathbf{s}_\mathbf{Q}^2 = s_Q(s_Q+1)$ and $\mathbf{s}_l^2 = s_l(s_l+1)$ in the $Q\overline{q}$ state. Eq.(2.3) shows that, heavy light meson comes in doublets with states having total angular momentum $j_\pm = s_l \pm 1/2$. The ground state S-wave doublet for $L = 0$, has heavy quark spin $\overrightarrow{S}_Q = \frac{1}{2}$ and light degrees of freedom momentum $\overrightarrow{S}_l = \frac{1}{2}$; (from Eq.(2.2), $\overrightarrow{S}_l = 1/2 + 0 = \frac{1}{2}$).

Therefore J^P of the ground state is obtained as $\frac{1}{2} \otimes \frac{1}{2} = 0^- \oplus 1^-$, with P $= (-1)^{L+1}$ being the parity of the system. If the heavy quark Q is charm quark, the ground state doublet is represented as D and D^*. Similarly if Q is bottom quark, the states are represented as B and B^*. Mesons with light quark q = u and d form isodoublets, which are combined with isosinglets of q = s, to form SU(3) triplets. The field operators which annihilate these ground state heavy quark mesons are represented by $P^{(Q)}$ for spin 0 pseudoscalar and $P_\mu^{*(Q)}$ for spin 1 vector mesons.

Similarly for the low-lying excited P-wave mesons ($L = 1$), total angular momentum of the light degrees of freedom is given as

$$S_l = \tfrac{1}{2} \otimes 1 = \begin{cases} \frac{1}{2} \\ \frac{3}{2} \end{cases}$$

For the $S_l = \frac{1}{2}$ doublet, the degenerate states are $(0^+, 1^+)$, and for $S_l = \frac{3}{2}$, the degenerate states are $(1^+, 2^+)$ These states are represented as (P_0^*, P_1') and (P_1, P_2^*) for $S_l = \frac{1}{2}$ and $\frac{3}{2}$ respectively. In the HQ symmetry, 1^+ states of $S_l = \frac{1}{2}$ and $S_l = \frac{3}{2}$

doublets normally mix with an angle 35.3° [13], they can still be distinguished due to their different angular momentum of the light degrees of freedom and by their decay angular distributions. The experimentally available ground state and low lying excited charm and bottom states are listed in Table 2.1. Sometimes the word natural parity is used for the states having parity $P = (-1)^J$ such as for J^P's $= 0^+, 1^-, 2^+$, etc. and the word unnatural parity for states having $P = (-1)^{J+1}$ such as J^P's $= 0^-, 1^+, 2^-$, etc.

Table 2.1: Experimentally available S and low lying P wave charm and bottom meson states [14]. N: represents the notation for a particular state. All the masses are in MeV. States marked as "-" are yet to be experimentally confirmed.

State		Charm Mesons			Bottom Mesons		
		$c\overline{u}$	$c\overline{d}$	$c\overline{s}$	$b\overline{u}$	$b\overline{d}$	$b\overline{s}$
$J^P = 0^-_{\frac{1}{2}}$	N:	D^0	$D^{\pm}$	$D_s^{\pm}$	$B^{\pm}$	B^0	B_s^0
	Mass:	1864.83	1869.65	1968.34	5279.32	5279.63	5366.89
$J^P = 1^-_{\frac{1}{2}}$	N:	D^{*0}	$D^{*\pm}$	$D_s^{*\pm}$	$B^{*\pm}$	B^{*0}	B_s^{*0}
	Mass:	2006.85	2010.26	2112.20	5324.65	-	5415.40
$J^P = 0^+_{\frac{1}{2}}$	N:	D_0^{*0}	$D_0^{*\pm}$	$D_{s0}^{*\pm}$	$B_0^{*\pm}$	B_0^{*0}	B_{s0}^{*0}
	Mass:	2318	-	2317.70	-	-	-
$J^P = 1^+_{\frac{1}{2}}$	N:	$D_1^{\prime 0}$	$D_1^{\prime \pm}$	$D_{s1}^{\prime \pm}$	$B_1^{\prime \pm}$	$B_1^{\prime 0}$	$B_{s1}^{\prime 0}$
	Mass:	2420.80	-	2459.50	5725.90	5726.00	-

2.3 Representation of fields

In previous section, we have seen that each S_l value gives two degenerate states in the form of doublets. It is convenient to treat the degenerate states as a single quantity in terms of the fields that transform linearly under the heavy quark symmetries. So, in this section, we will express each doublet for L = 0,1,2,3 in terms of their effective fields.

The ground state S-wave doublet $(0^-, 1^-)$ contains a pseudoscalar meson (0^-) represented by P and a vector meson (1^-) represented by P^*_μ. Both these mesons can be framed in a single field "H" as a linear combination of both the vector field P^*_μ and pseudoscalar field P [8, 11, 15]. This combination is obtained as

$$H = \frac{i\not{D} + m_P}{2m_P}[\gamma^\mu P^*_\mu + iP\gamma^5] \tag{2.4}$$

where m_P is the mass of the heavy-light meson. In the static limit of heavy quark $m_P \to \infty$, the term $\frac{i\not{D}+m_P}{2m_P}$ changes to projection operator $\frac{1+\not{v}}{2}$. So the field H is now represented by

$$H = \frac{1+\not{v}}{2}[\gamma^\mu P^*_\mu + iP\gamma^5] \tag{2.5}$$

This field H annihilates the doublet with $S_l = 1/2$ and needs to transform as a bispinor under the lorentz transformation

$$H'(x') = D(\Lambda)H(x)D(\Lambda)^{-1}, \qquad x' = \Lambda x \tag{2.6}$$

where $D(\Lambda)$ is the 4×4 lorentz transformation matrix for spinors, so that

$$H(x) \to H'(x) = D(\Lambda)H(\Lambda^{-1}x)D(\Lambda)^{-1} \tag{2.7}$$

The projection term $\frac{1+\not{v}}{2}$ gives the particle component of the heavy quark Q and the relative phase between the P and P^*_μ states is arbitrary [24, 25, 31, 32]. The field represented in Eq.(2.5) is consistent under lorentz transformation as γ^5 converts the pseudoscalar field P and γ^μ converts the vector field P^*_μ into bispinors.

Using the relations $\not{v}(1 + \not{v}) = (1 + \not{v})$ and $v.P^* = 0$, this field also satisfies the relations

$$\not{v}H = H \qquad \text{and} \qquad H\not{v} = -H$$

The conjugate field for H represented by $\overline{H}$ is introduced as

$$\overline{H} = \gamma^0 H^\dagger \gamma^0 = [P^{*\dagger}_\mu \gamma^\mu + iP^\dagger \gamma^5]\frac{1+\not{v}}{2} \tag{2.8}$$

Because of $\gamma^0 D(\Lambda)^\dagger \gamma^0 = D(\Lambda)^{-1}$, conjugate field $\overline{H}$ also transforms as a bispinor

$$\overline{H}'(x) = D(\Lambda)\overline{H}((\Lambda)^{-1}x)D(\Lambda)^{-1} \tag{2.9}$$

and satisfies the relations

$$\overline{H}\not{v} = \overline{H} \qquad \text{and} \qquad \not{v}\overline{H} = -\overline{H}$$

Similarly, the P-wave doublets $(0^+, 1^+)_{1/2}$ and $(1^+, 2^+)_{3/2}$ are represented by "S" and "T" fields [32, 33] as

$$S = \frac{1+\not{v}}{2}\{P_1^{'\mu}\gamma_\mu\gamma_5 - P_0^*\} \tag{2.10}$$

$$T^\mu = \frac{1+\not{v}}{2}\{P_2^{*\mu\nu}\gamma_\nu - P_{1\nu}\sqrt{\frac{3}{2}}\gamma_5[g^{\mu\nu} - \frac{\gamma^\nu(\gamma^\mu - v^\mu)}{3}]\}. \tag{2.11}$$

satisfying

$$\not{v}S = S\not{v} = S, \quad \not{v}T^\mu = -T^\mu\not{v} = T^\mu, \quad \not{v}\overline{S} = \overline{S}\not{v} = \overline{S} \quad -\not{v}\overline{T}^\mu = \overline{T}^\mu\not{v} = \overline{T}^\mu$$

Field S is a linear combination of scalar P_0^* and axial vector state $P_1^{'\mu}$, whereas T field contains a combination of axial vector $P_{1\nu}$ and tensor $P_2^{*\mu\nu}$ states.

Heavy-light meson doublets for excited D-wave ($l = 2$) states are represented by (P_1^*, P_2) and (P_2', P_3^*) belonging to $J^P_{s_l} = (1^-, 2^-)_{\frac{3}{2}}$ and $(2^-, 3^-)_{\frac{5}{2}}$ respectively. And

the doublets of F-wave ($l = 3$) are represented by (P_2^*, P_3) and $(P_3^{'}, P_4^*)$ for $J^P_{s_l} = (2^+, 3^+)_{\frac{5}{2}}$ and $(3^+, 4^+)_{\frac{7}{2}}$ respectively. Similar to the Eqs.(2.5), 2.10, 2.11, these doublets are described by the effective super-field X_a, Y_a, Z_a and R_a [41, 47] as:

$$X_a^\mu = \frac{1+\not{v}}{2}\{P_{2a}^{\mu\nu}\gamma_5\gamma_\nu - P^*_{1a\nu}\sqrt{\frac{3}{2}}[g^{\mu\nu} - \frac{\gamma^\nu(\gamma^\mu + \gamma^\mu)}{3}]\} \tag{2.12}$$

$$Y_a^{\mu\nu} = \frac{1+\not{v}}{2}\{P_{3a}^{*\mu\nu\sigma}\gamma_\sigma - P_{2a}^{'\alpha\beta}\sqrt{\frac{5}{3}}\gamma_5[g^\mu_\alpha g^\nu_\beta - \frac{g^\nu_\beta\gamma_\alpha(\gamma^\mu - v^\mu)}{5} - \frac{g^\mu_\alpha\gamma_\beta(\gamma^\nu - v^\nu)}{5}]\} \tag{2.13}$$

$$Z_a^{\mu\nu} = \frac{1+\not{v}}{2}\{P_{3a}^{\mu\nu\sigma}\gamma_5\gamma_\sigma - P_{2a}^{*\alpha\beta}\sqrt{\frac{5}{3}}[g^\mu_\alpha g^\nu_\beta - \frac{g^\nu_\beta\gamma_\alpha(\gamma^\mu + v^\mu)}{5} - \frac{g^\mu_\alpha\gamma_\beta(\gamma^\nu + v^\nu)}{5}]\} \tag{2.14}$$

$$R_a^{\mu\nu\rho} = \frac{1+\not{v}}{2}\{P_{4a}^{*\mu\nu\rho\sigma}\gamma_5\gamma_\sigma - P_{3a}^{'\alpha\beta\tau}\sqrt{\frac{7}{4}}[g^\mu_\alpha g^\nu_\beta g^\rho_\tau - \frac{g^\nu_\beta g^\rho_\tau\gamma_\alpha(\gamma^\mu - v^\mu)}{7} - \frac{g^\mu_\alpha g^\rho_\tau\gamma_\beta(\gamma^\nu - v^\nu)}{7} - \frac{g^\mu_\alpha g^\nu_\beta\gamma_\tau(\gamma^\rho - v^\rho)}{7}]\} \tag{2.15}$$

The mentioned indices a or b in the subsequent fields are $SU(3)$ flavor index (u, d or s). For the radially excited states with radial quantum number n=2, the mesonic state is replaced by a tilde "$\sim$" sign on their head i.e. $\widetilde{P}, \widetilde{P}^*$ and so on. And the equation of effective fields for radially excited doublets remains same, but instead are replaced by $\widetilde{H}$, $\widetilde{S}$, $\widetilde{T}$, $\widetilde{X}$ etc.

2.4 Effective Feynman Rules in $m_Q \to \infty$ limit

The heavy quark symmetry can be embodied in the QCD to draw the Feynman diagrams with effective Feynman rules for heavy quark. The momentum of the

heavy-light meson $Q\overline{q}$ having mass M_Q and velocity v_μ is $p_\mu = M_Q v_\mu$. As discussed before, mass and momentum of the heavy quark is nearly same as that of the bound state $Q\overline{q}$ as in Eq.(2.1) [5, 16]. The four velocity of the heavy quark

$$v_Q^\mu = \frac{p^\mu}{m_Q} = v^\mu + \frac{k^\mu}{m_Q} \tag{2.16}$$

will also be same as that of the meson. So, the heavy quark is nearly on-shell and carries almost all of the bound state's momentum. QCD interactions does not alter the heavy quark velocity. This on shell condition simplifies the usual QCD fermion propagator $\frac{i}{\not{p}-m_Q}$ by

$$\frac{i}{\not{p}-m_Q} = \frac{i(\not{p}+m_Q)}{p^2-m_Q^2} = \frac{i(m_Q\not{v}+\not{k}+m_Q)}{2m_Q v.k+k^2} \simeq \frac{i}{v.k}\frac{1+\not{v}}{2} \tag{2.17}$$

The heavy quark propagator has a velocity dependent projection operator $P_+ = \frac{1+\not{v}}{2}$. The projection operator for the antiquark particle is defined as $P_- = \frac{1-\not{v}}{2}$. From these positive and negative energy projection operators P_+ and P_-, we obtain identities as

$$P_\pm P_\mp = 0, \qquad P_\pm^2 = P_\pm \qquad \text{and}$$
$$P_+\gamma_\mu P_+ = P_+ v_\mu P_+.$$

The last identity describes that the coupling of the heavy quark to gluons can also be simplified. At the leading order in $\frac{1}{m_Q}$, the quark gluon vertex of QCD $igT_a\gamma^\mu$ can be replaced as

$$igT_a\gamma^\mu = igT_a v^\mu \tag{2.18}$$

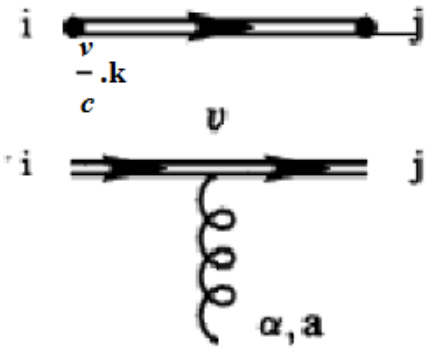

Figure 2.2: Modified Feynman rules for the heavy quark effective theory.

where g is the QCD strong coupling constant and T_a are the SU(3) color generators. These effective Feynman rules [17–19] for the heavy quark propagator and heavy quark gluon vertex are shown in Figure 2.2.

The heavy quark propagator in the above figure is represented by a double line to differentiate it from the QCD propagator.

The new Feynman rules are independent of the heavy quark mass term, explicitly depicting the heavy quark flavor symmetry. Also, as there is no gamma matrix in these modified rules, so the heavy quark spin symmetry is also apparent. In the heavy quark rest frame $v = (1,0,0,0)$, this projection operator becomes $\frac{1+\gamma^0}{2}$, which projects the quark component of four vector Dirac spinor. In this static frame, the phenomenon becomes non-relativistic, and hence the propagator and charge density can be approximated as [19],

$$\frac{i}{v.k} \to \frac{i}{k^0} = \frac{i}{E - m_Q} \tag{2.19}$$

$$-igv^\mu T_a = -ig\delta^{\mu 0} T_a. \tag{2.20}$$

These modified feymann rules will be used in the next section to derive the general lagrangian for the heavy quark effective theory.

2.5 General Lagrangian of HQET

Heavy quark symmetries can also be applied to the lagrangian level, by constructing an effective lagrangian in the inverse powers of m_Q. In the limit $m_Q \to \infty$, on shell condition of the heavy quark enables us to write the heavy quark field Q with four velocity v^μ in terms of the large h_ν^Q and small H_ν^Q velocity dependent components [5, 18, 19] as

$$Q = e^{-im_Q v.x}(h_\nu^Q + H_\nu^Q) \tag{2.21}$$

with

$$h_\nu(x) = e^{im_Q v.x}\frac{1+\not{v}}{2}Q(x) \tag{2.22}$$

$$H_\nu(x) = e^{im_Q v.x}\frac{1-\not{v}}{2}Q(x) \tag{2.23}$$

where the quark and antiquark components are denoted by $h_\nu(x)$ and $H_\nu(x)$ respectively. The exponential factor $\exp(im_Q v.x)$ ensures that the derivative applied to $h_\nu(x)$ produces momentum only of the order of k. Using the above definitions and the relation $v.v = 1$, we find the following relations:

$$\not{v}h_\nu^Q = h_\nu^Q \tag{2.24}$$

$$\not{v}H_\nu^Q = -H_\nu^Q \tag{2.25}$$

In the heavy quark rest frame i.e. $v^\mu = (1,0,0,0)$, h_v^Q gives the upper two components of the heavy quark field Q while H_v^Q gives the lower ones. h_v^Q annihilates a heavy quark with velocity v whereas H_v^Q creates a heavy anti-quark with velocity v. A

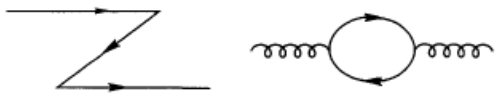

Figure 2.3: Virtual fluctuations involving pair creation of heavy quark.

general effective lagrangian in higher order of $\frac{1}{m_Q}$ is constructed for HQET by taking both the quark and anti-quark components [5, 20, 34]. In terms of both the quark and anti-quark components, QCD lagrangian for the heavy quark takes the form

$$\mathscr{L}_{QCD} = \overline{h}_\nu i\not{D} h_\nu + \overline{H}_\nu (i\not{D} - 2m_Q) H_\nu + \overline{h}_\nu (i\not{D} - 2m_Q) H_\nu + \overline{H}_\nu i\not{D} h_\nu \qquad (2.26)$$

Using the effective feymann rules and the relations of Eqs.(2.24),2.25), the first term for the above lagrangian changes as:

$$\overline{h}(\frac{1+\not{v}}{2})(i\gamma^\mu D_\mu)(\frac{1+\not{v}}{2})h = \overline{h}(iv.D)(\frac{1+\not{v}}{2})h = \overline{h}(iv.D)h \qquad (2.27)$$

and the $\mathscr{L}_{eff}$ becomes

$$\mathscr{L}_{eff} = \overline{h}_\nu iv.D h_\nu - \overline{H}_\nu (iv.D + 2m_Q) H_\nu + \overline{h}_\nu i\not{D}_\perp H_\nu + \overline{H}_\nu i\not{D}_\perp h_\nu \qquad (2.28)$$

where $D^\mu_\perp = D^\mu - v^\mu v.D$ is orthogonal to the heavy quark velocity i.e. $v.D_\perp = 0$. In the static limit of heavy quark, $D^\mu_\perp = (0, \overrightarrow{D})$ contains only the spatial components of the covariant derivative. In this lagrangian, h_v describes the massless degree of freedom and H_v field corresponds to an excitation with twice the heavy quark mass $2m_Q$, which is the energy required to create a heavy quark-antiquark pair. These fluctuations involving pair creation of heavy quark are described in Figure 2.3
Mass dependency of the heavy degree of freedom H_v are separated out for constructing an effective theory [21, 22]. On the classical level, H_v is eliminated using

the equation of motion for H_v as

$$\frac{\partial \mathscr{L}}{\partial \overline{H}} = -(iv.D + 2m_Q)H + (i\not{D}_\perp)h = 0 \tag{2.29}$$

which depicts that, the small component field H_v is indeed of the order of $\frac{1}{m_Q}$, given as

$$H_v = \frac{1}{2m_Q + iv.D} i\not{D}_\perp h_v \tag{2.30}$$

Therefore, the non local effective lagrangian in terms of the large component field h_v is

$$\mathscr{L}_{eff} = \overline{h}_v iv.D h_v + \overline{h}_v i\not{D}_\perp \frac{1}{2m_Q + iv.D} i\not{D}_\perp h_v \tag{2.31}$$

The second term in this equation describes the virtual fluctuations shown in Figure 2.3. Derivative expansion in powers of $\frac{i\not{D}_\perp}{m_Q}$ simplifies the above lagrangian as

$$\mathscr{L}_{eff} = \overline{h}_v iv.D h_v + \frac{1}{2m_Q} \sum_{m=0}^{\infty} \overline{h}_v i\not{D}_\perp (-\frac{iv.D}{2m_Q})^m i\not{D}_\perp h_v \tag{2.32}$$

Further using the standard γ matrix relations

$$\not{D}_\perp \not{D}_\perp = D_\perp^2 + \frac{1}{2}[\gamma_\mu, \gamma_\nu] D_\perp^\mu D_\perp^\nu = D_\perp^2 + \frac{1}{4}[\gamma_\mu, \gamma_\nu][D_\perp^\mu, D_\perp^\nu] \tag{2.33}$$

along with the identities $[D_\perp^\mu, D_\perp^\nu] = igG^{\mu\nu}$, $[\gamma_\mu, \gamma_\nu] = -\frac{i}{2}\sigma_{\mu\nu}$ and $\overline{h}\sigma_{\mu\nu}v^\mu h = 0$, the general HQET lagrangian to the order of $\frac{1}{m_Q}$ is obtained as

$$\mathscr{L}_{eff} = \overline{h}_v iv.Dh_v + \frac{1}{2m_Q}\overline{h}_v(iD_\perp)^2 h_v + \frac{g}{4m_Q}\overline{h}_v\sigma_{\mu\nu}G^{\mu\nu}h_v + \mathcal{O}(\frac{1}{m_Q^2}) \tag{2.34}$$

Or in general it is expressed as:

$$\mathscr{L}_{HQET} = \mathscr{L}_0 + \frac{1}{m_Q}\mathscr{L}_1 + \frac{1}{m_Q^2}\mathscr{L}_2 + ... \tag{2.35}$$

Retaining only the quark component h_ν^Q, effective lagrangian at the leading order in limit $m_Q \to 0$ is

$$\mathscr{L}_{eff} = \overline{h}_\nu iv.Dh_\nu = \overline{h}_\nu(iv^\mu\partial_\mu + gT_a v^\mu A_\mu^a)h_\nu \tag{2.36}$$

where $D_\mu = \partial_\mu - igT_a v^\mu A_\mu^a$ is the gauge covariant derivative [20–22]. This lagrangian is independent of the heavy quark mass, manifesting the heavy quark flavor symmetry. Also, the Dirac gamma matrices of the QCD Lagrangian are being replaced by the velocity v of the heavy quark, making this lagrangian invariant under the SU(2) spin symmetry group.

Therefore, the first term in Eq.(2.34) gives leading order lagrangian which preserves both flavor and spin symmetry of the heavy quark. The second term of this equation gives the heavy quark kinetic energy term which arises from the off shell residual momentum of heavy quark in the non relativistic model. This term breaks the flavor symmetry of the HQET but preserves the spin symmetry. The second higher order term in this lagrangian $g\sigma_{\mu\nu}G^{\mu\nu}$ gives the chromo-magnetic moment coupling of the heavy quark spin to the gluon field, which breaks both the spin and flavor symmetry [44–46].

2.6 Chiral Perturbation Theory

In the limit of light quark masses approaching to zero $m_u, m_d, m_s \to 0$, QCD lagrangian for these light quarks possess the $SU(3)_L \otimes SU(3)_R \otimes U(1)_V$ chiral symmetry. In reality, due to the finite masses of u,d and s quarks, this chiral symmetry is an approximate symmetry that is spontaneously broken down to $SU(3)_V$ subgroup. This results in the origin of eight Nambu-Goldstone bosons, which acquires the mass due to explicit breaking of this symmetry [24,25]. These bosons are identified as the light pseudo-scalar meson octet with $J^P = 0^-$ consisting of non-strange mesons as pions and eta (π, η) and strange mesons as kaons (K).

At low momentum, the interactions among these pseudo Goldstone bosons are described by the well known chiral perturbation theory [28, 34–36]. This theory describes these Goldstone bosons in a 3×3 unitary matrix $\Sigma \in \mathrm{SU}(3)$, defined as

$$\Sigma = \exp[\frac{2i\mathcal{M}}{f}] \tag{2.37}$$

where $\mathcal{M}$ is a 3×3 hermitian traceless matrix

$$\mathcal{M} = \begin{pmatrix} \frac{1}{\sqrt{2}}\pi^0 + \frac{1}{\sqrt{6}}\eta & \pi^+ & K^+ \\ \pi^- & -\frac{1}{\sqrt{2}}\pi^0 + \frac{1}{\sqrt{6}}\eta & K^0 \\ K^- & \overline{K}^0 & -\sqrt{\frac{2}{3}}\eta \end{pmatrix} \tag{2.38}$$

and f is the pion decay constant, which has value $f = 130$ MeV in the chiral limit. Under chiral symmetry $SU(3)_L \otimes SU(3)_R$, the octet field transforms as

$$\Sigma \to L\Sigma R^\dagger$$

with L and R representing the global elements of $SU(3)_L$ and $SU(3)_R$.

The interactions of the π, η, K with heavy-light meson fields is described as ξ, defined as $\Sigma = \xi^2$. This ξ field under the chiral limit $SU(3)_L \otimes SU(3)_R$ transforms as

$$\xi \to L\xi U^\dagger = U\xi R^\dagger$$

with U being the special unitary matrix depending on L, R and the mesonic field $\mathcal{M}$.

Matter fields for heavy-light mesons $Q\overline{q}$ may be included into the chiral theory [30,37–40]. At the leading order, the effective lagrangian describing the interactions of light pseudo-scalar mesons with the ground state heavy-light meson field "H" (eq:2.5) is given by

$$\mathcal{L}^{(H)} = -i\,Tr\overline{H}_a v.\partial H_a + i\,Tr\overline{H}_a H_b (v.V)_{ba} - g\,Tr\overline{H}_a H_b \gamma_\lambda \gamma_5 (A^\lambda)_{ba}, \tag{2.39}$$

where

$$V_\nu = \frac{1}{2}(\xi\partial_\nu\xi^\dagger + \xi^\dagger\partial_\nu\xi) \tag{2.40}$$

and

$$A_\lambda = \frac{i}{2}(\xi\partial_\lambda\xi^\dagger - \xi^\dagger\partial_\lambda\xi) \tag{2.41}$$

The indices a, b are flavor indices which depicts the light flavor quarks. This lagrangian is the most general lagrangian which is invariant under chiral symmetry $SU(3)_L \otimes SU(3)_R$. In heavy-light meson field H_a, factors of $\sqrt{m_p}$ and $\sqrt{m_{p^*}}$ have been absorbed in P_a and $P^*_{a\mu}$ fields to make lagrangian independent of a heavy quark mass. As a result heavy meson fields have a dimension of 3/2 [40]. This lagrangian gets modified when chiral symmetry is explicitly broken. The results due to this symmetry breaking are discussed in chapter 5 of the thesis.

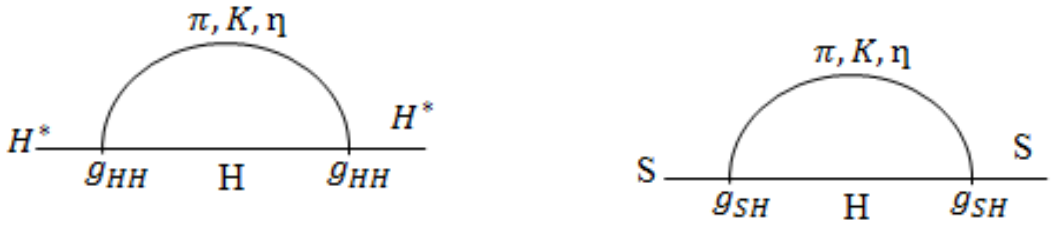

Figure 2.4: Two body interactions between ground-ground and lower excited-ground fields.

2.7 Leading Order Chiral lagrangian

We have seen, heavy-light meson doublets interacts with other doublet states through the exchange of light pseudo-scalar mesons (π, η, K). This interaction between doublets is represented in terms of their lagrangians [27]. The interaction can be within the ground states, excited states or between excited and ground states as shown in Figure 2.4, e.g. the states P_0^* and $P_1^{'}$ of low lying excited P-wave doublet $(0^+, 1^+)$ can interact among themselves $P_1^{'} \rightarrow P_0^* + p_M$, where p_M is the suitable light pseudo-scalar meson. These states can also interact with the ground state S-wave $(0^-, 1^-)$ doublet states P and P^*. In this thesis, our goal is to study the strong interactions of the higher excited states with the ground state H field through the emission of light pseudo-scalar mesons to extract properties like masses, decay widths, branching ratios, strong coupling constants etc.

At the leading order approximation, the heavy meson chiral lagrangians L_{HH}, L_{SH}, L_{TH}, L_{XH}, L_{YH}, L_{ZH} for the two-body strong interactions through light pseudoscalar mesons (π, K, η) are written as :

$$L_{HH} = g_{HH} Tr\{\overline{H}_a H_b \gamma_\mu \gamma_5 A^\mu_{ba}\} \tag{2.42}$$

$$L_{SH} = g_{SH} Tr\{\overline{H}_a S_b \gamma_\mu \gamma_5 A^\mu_{ba}\} + h.c. \tag{2.43}$$

$$L_{TH} = \frac{g_{TH}}{\Lambda} Tr\{\overline{H}_a T^\mu_b (iD_\mu \not{A} + i\not{D} A_\mu)_{ba} \gamma_5\} + h.c. \tag{2.44}$$

$$L_{XH} = \frac{g_{XH}}{\Lambda} Tr\{\overline{H}_a X^\mu_b (iD_\mu \not{A} + i\not{D} A_\mu)_{ba} \gamma_5\} + h.c. \tag{2.45}$$

$$L_{YH} = \frac{1}{\Lambda^2} Tr\{\overline{H}_a Y^{\mu\nu}_b [k^Y_1 \{D_\mu, D_\nu\} A_\lambda + k^Y_2 (D_\mu D_\lambda A_\nu + D_\nu D_\lambda A_\mu)]_{ba} \gamma^\lambda \gamma_5\} + h.c. \tag{2.46}$$

$$L_{ZH} = \frac{1}{\Lambda^2} Tr\{\overline{H}_a Z^{\mu\nu}_b [k^Z_1 \{D_\mu, D_\nu\} A_\lambda + k^Z_2 (D_\mu D_\lambda A_\nu + D_\nu D_\lambda A_\mu)]_{ba} \gamma^\lambda \gamma_5\} + h.c. \tag{2.47}$$

$$L_{RH} = \frac{1}{\Lambda^3} Tr\{\overline{H}_a R^{\mu\nu\rho}_b [k^R_1 \{D_\mu, D_\nu D_\rho\} A_\lambda + k^R_2 (\{D_\mu, D_\rho\} D_\lambda A_\nu + \{D_\nu, D_\rho\} D_\lambda A_\mu + \{D_\mu, D_\nu\} D_\lambda A_\rho)]_{ba} \gamma^\lambda \gamma_5\} + h.c. \tag{2.48}$$

In these equations $D_\mu = \partial_\mu + V_\mu$, $\{D_\mu, D_\nu\} = D_\mu D_\nu + D_\nu D_\mu$ and $\{D_\mu, D_\nu D_\rho\} = D_\mu D_\nu D_\rho + D_\mu D_\rho D_\nu + D_\nu D_\mu D_\rho + D_\nu D_\rho D_\mu + D_\rho D_\mu D_\nu + D_\rho D_\nu D_\mu$. Λ is the chiral symmetry breaking scale taken as 1 GeV. g_{HH}, g_{SH}, g_{TH}, g_{XH}, $g_{YH} = k^Y_1 + k^Y_2$, $g_{ZH} = k^Z_1 + k^Z_2$ and $g_{RH} = k^R_1 + k^R_2$ are the strong coupling constants involved. Here L_{FH} [F = H,S,T,X,Y,Z,R] is the chiral lagrangian resulting from the interaction of F = H,S,T,X,Y,Z,R fields with the ground state field H along with the emission of light pseudo-scalar mesons (π, η, K). These lagrangians are again replaced by

notation $L_{\widetilde{H}H}$, $L_{\widetilde{S}H}$, $L_{\widetilde{T}H}$ etc. for the radial excited states.

2.8 Decays of Heavy-light Mesons

Particle physics has discovered various new elementary particles. Quark level processes cannot be directly measured, because the strong interactions forms hadrons from underlying quarks. Therefore, the experiments measures the processes by which a particle decays. Decay of a particle is the spontaneous process in which particle tends to decay to the lowest possible energy state it can reach. Every particle can have various types of decay modes, i.e. different produced particles. A particle has a characteristic lifetime for which they usually live before decaying. The decay of a particle is expressed in terms of the half life, decay constant or mean lifetime. Lifetime of a particle is the inverse of the rate of its decay Γ.

The decay rate of particle depends on the interaction between the produced particles. Stronger is the interaction between the final particles, the more likely is the decay of initial paticle to occur, and thus shorter is the lifetime of the parent particle. The particles in the final state may themselves be unstable and can decay further to other particles.

Depending on the fundamental forces, the decay of a heavy-light $Q\overline{q}$ meson can be electromagnetically, weak or strong. There are various constraints that allows or forbids various types of decay modes. For an allowed decay mode, all quantum numbers like charge, baryon number, lepton number, strangeness, angular momentum, isospin, charge conjugation, parity should be conserved for a strongly decaying state. For a allowed electromagnetic decay, all quantum numbers except isospin need to be conserved. And the decay process to occur through weak interactions, except parity, isospin and charge conjugation all other quantum numbers should be conserved. The total decay width of a $Q\overline{q}$ system is given by

$$\Gamma_{Total}(Q\overline{q}) = \Gamma_{EM} + \Gamma_{Weak} + \Gamma_{Strong}$$

Since the coupling constant term for the weak and electromagnetic interactions is very small as compared to strong coupling constant, so the main contribution to the total decay width comes from the strong decays. Strong decays of the heavy-light mesons with the emission of light pseudo-scalar mesons $(\pi, \eta, K)$are particularly important, as they contribute maximum to the total decay width of the meson.
So, in this thesis, we will emphasize only on the strong decays of a $Q\overline{q}$ meson. The decay rates of D and B mesons are both experimentally and theoretically predicted with great interest. When discussing the heavy hadron decays, one treats the heavy quark(s) as a spectator(s). The decay amplitude relies on the coupling constants in the Lagrangian which are easy to determine from the known data. Along with the decay rates, branching ratios and fractions are also measured by various experimental collaborations like LHCb, BaBar, Belle, BESII/III, CDF etc., which are tested by the available theoretical models. Branching fraction of a decay gives the relative frequency of a particular decay mode. These strong decay rates may hold the key to yet unseen physics effects.
The two body strong decay of an excited heavy light meson to lower state heavy-light meson through the exchange of light pseudo-scalar mesons $(Q\overline{q})_i \rightarrow (Q\overline{q})_f + p(\pi, \eta, K)$is given as [41, 42]

$$\Gamma = \frac{1}{2J+1} \sum \frac{p_f}{8\pi M_i^2} |\mathscr{A}|^2 \tag{2.49}$$

with $\mathscr{A}$ being the scattering amplitude, i and f denotes the initial and final state of the heavy-light meson. The summation $\sum$ is over all the polarization vectors. And the term p_f denotes the momentum of the light pseudo-scalar meson given as

$$p_f = \frac{\sqrt{(M_i^2 - (M_f + M_p)^2)(M_i^2 - (M_f - M_p)^2)}}{2M_i} \tag{2.50}$$

This equation is obtained by observing the four momentum conservation in the decay. We will use the decay width formulae given in Eq.(2.49), to study the properties of the higher excited heavy-light charm and bottom mesons. Beside the decays to the light pseudo-scalar mesons, heavy-light system can also decay to vector mesons [26, 29, 43].

2.9 Two Body Strong Decays of Excited Mesons

Excited states can decay to the ground state through the emission of light pseudoscalar mesons (π, η, K) in various possible ways. The strong interactions are given by the most general chiral Lagrangian listed in previous section, which are invariant under the heavy quark, chiral, Lorentz, C, P and T transformations.
The effective chiral lagrangian $L_{HH}, L_{SH}, L_{TH}, L_{XH}, L_{YH}$ etc. are used to obtain the the scattering amplitudes $\mathscr{A}$ through their respective fields H,S,T,X,Y as the application of PCAC. More details regarding this derivation can be seen in the preliminaries of HQET. The calculated scattering amplitude is then used in Eq.(2.49) to compute the strong decay width of higher excited heavy-light mesons decaying to the ground state $(0^-, 1^-)$ doublet along with light pseudo-scalar meson (π, η, K). The decay width for various doublets are as:
$(0^-, 1^-) \to (0^-, 1^-) + M$

$$\Gamma(1^- \to 1^-) = C_M \frac{g_{HH}^2 M_f p_M^3}{3\pi f_\pi^2 M_i} \tag{2.51}$$

$$\Gamma(1^- \to 0^-) = C_M \frac{g_{HH}^2 M_f p_M^3}{6\pi f_\pi^2 M_i}$$

$$\Gamma(0^- \to 1^-) = C_M \frac{\widetilde{g}_{HH}^2 M_f p_M^3}{2\pi f_\pi^2 M_i}$$

$(0^+, 1^+) \to (0^-, 1^-) + M$

$$\Gamma(1^+ \to 1^-) = C_M \frac{g_{SH}^2 M_f (p_M^2 + m_M^2) p_M}{2\pi f_\pi^2 M_i} \tag{2.52}$$

$$\Gamma(0^+ \to 0^-) = C_M \frac{g_{SH}^2 M_f (p_M^2 + m_M^2) p_M}{2\pi f_\pi^2 M_i}$$

$(1^+, 2^+) \to (0^-, 1^-) + M$

$$\Gamma(2^+ \to 1^-) = C_M \frac{2 g_{TH}^2 M_f p_M^5}{5\pi f_\pi^2 \Lambda^2 M_i} \tag{2.53}$$

$$\Gamma(2^+ \to 0^-) = C_M \frac{4 g_{TH}^2 M_f p_M^5}{15\pi f_\pi^2 \Lambda^2 M_i}$$

$$\Gamma(1^+ \to 1^-) = C_M \frac{2 g_{TH}^2 M_f p_M^5}{3\pi f_\pi^2 \Lambda^2 M_i}$$

$(1^-, 2^-) \to (0^-, 1^-) + M$

$$\Gamma(1^- \to 0^-) = C_M \frac{4 g_{XH}^2}{9\pi f_\pi^2 \Lambda^2} \frac{M_f}{M_i} [p_M^3 (m_M^2 + p_M^2)] \tag{2.54}$$

$$\Gamma(1^- \to 1^-) = C_M \frac{2 g_{XH}^2}{9\pi f_\pi^2 \Lambda^2} \frac{M_f}{M_i} [p_M^3 (m_M^2 + p_M^2)]$$

$$\Gamma(2^- \to 1^-) = C_M \frac{2 g_{XH}^2}{3\pi f_\pi^2 \Lambda^2} \frac{M_f}{M_i} [p_M^3 (m_M^2 + p_M^2)]$$

$(2^-, 3^-) \to (0^-, 1^-) + M$

$$\Gamma(2^- \to 1^-) = C_M \frac{4g_{YH}^2}{15\pi f_\pi^2 \Lambda^4} \frac{M_f}{M_i}[p_M^7] \tag{2.55}$$

$$\Gamma(3^- \to 0^-) = C_M \frac{4g_{YH}^2}{35\pi f_\pi^2 \Lambda^4} \frac{M_f}{M_i}[p_M^7]$$

$$\Gamma(3^- \to 1^-) = C_M \frac{16g_{YH}^2}{105\pi f_\pi^2 \Lambda^4} \frac{M_f}{M_i}[p_M^7]$$

$(2^+, 3^+) \to (0^-, 1^-) + M$

$$\Gamma(2^+ \to 1^-) = C_M \frac{8g_{ZH}^2}{75\pi f_\pi^2 \Lambda^4} \frac{M_f}{M_i}[p_M^5(m_M^2 + p_M^2)] \tag{2.56}$$

$$\Gamma(2^+ \to 0^-) = C_M \frac{4g_{ZH}^2}{25\pi f_\pi^2 \Lambda^4} \frac{M_f}{M_i}[p_M^5(m_M^2 + p_M^2)]$$

$$\Gamma(3^+ \to 1^-) = C_M \frac{4g_{ZH}^2}{25\pi f_\pi^2 \Lambda^4} \frac{M_f}{M_i}[p_M^5(m_M^2 + p_M^2)]$$

$(3^+, 4^+) \to (0^-, 1^-) + M$

$$\Gamma(3^+ \to 1^-) = C_M \frac{36g_{RH}^2}{35\pi f_\pi^2 \Lambda^6} \frac{M_f}{M_i}[p_M^9] \tag{2.57}$$

$$\Gamma(4^+ \to 1^-) = C_M \frac{4g_{RH}^2}{7\pi f_\pi^2 \Lambda^6} \frac{M_f}{M_i}[p_M^9]$$

$$\Gamma(4^+ \to 0^-) = C_M \frac{16g_{RH}^2}{35\pi f_\pi^2 \Lambda^6} \frac{M_f}{M_i}[p_M^9]$$

In the above decay widths, M_i and M_f stands for initial and final meson mass, p_M and m_M are the final momentum and mass of the light pseudo-scalar meson respectively. The coefficient $C_{K^\pm}, C_{K^0}, C_{\overline{K}^0}, C_{\pi^\pm} = 1$, $C_{\pi^0} = \frac{1}{2}$ and $C_\eta = \frac{2}{3}$ or $\frac{1}{6}$.

Different values of C_η corresponds to the initial state being $c\overline{u}, c\overline{d}$ or $c\overline{s}$ respectively. All hadronic coupling constants depend on the radial quantum number. For the decay within n=1 they are noted as g_{HH}, g_{SH} etc., and the decay from n=2 to n=1 are represented by $\widetilde{g}_{HH}$, $\widetilde{g}_{SH}$. Higher order corrections for spin and flavor violation of order $\frac{1}{m_Q}$ are excluded to avoid new unknown coupling constants. Eqs.(2.51 - 2.57), shows that the decay width of any state depends on the initial and final meson masses, their strong coupling constants, pion decay constant, energy scale $\Lambda = 1$ GeV, mass and momentum of light pseudo-scalar mesons. The applications to charm and bottom meson decays have different aspects of advantages and drawbacks. In the case of the bottom meson decays, the expansion in $\Delta k/m_B$ converges quickly.

2.10 Masses of Heavy-Light Mesons

The constructed effective Lagrangians are used to extract various properties like masses, decays, hadron production etc. for the heavy-light D and B mesons. To study the behavior of the heavy-light mesons for their spectroscopy, masses are the second most important property to be studied [54]. From the effective lagrangian 2.34, mass for any $Q\overline{q}$ state to the first order of $1/m_Q$ is represented as :

$$M_X = m_Q + \overline{\Lambda} - \frac{\lambda_1}{2m_Q} + 4(S_Q.S_l)\frac{\lambda_2}{2m_Q}. \tag{2.58}$$

In this equation, m_Q is the mass of the heavy quark, $4(S_Q.S_l)$ is the Clebsch factor, The λ_1 and λ_2 are the non-perturbative parameters, whose values are expected to be of the order of Λ^2_{QCD} that can be estimated by fitting the theoretical and experimental data and their uncertainties. The parameter $\overline{\Lambda}$ is the energy of the light quark fields (i.e. brown muck), λ_1 term represents the kinetic energy of the heavy quark Q and the term λ_2 gives the chromomagnetic interaction energy. Masses are very important for studying the heavy-light mesons, as various other properties

like decays, splittings etc. are dependent on masses. The detailed study for the masses is presented in chapter 5.

2.10.1 Splittings

There are many implications of the mesonic masses in the heavy quark spin flavor symmetry. The basic property is that, hyperfine splitting i.e. mass splitting among the different doublets is independent of the heavy quark flavor. From the Table 2.1, the hyperfine splitting for the ground state charm and bottom meson are given as

$$D^{*+} - D^{+} = 140.61 \text{ MeV},$$
$$D^{*0} - D^{0} = 142.02 \text{ MeV},$$
$$B^{*+} - B^{+} = 45.33 \text{ MeV}$$

According to heavy quark spin symmetry, these hyperfine splittings should have given same values. But in reality, because of the finite masses of charm and bottom quarks, these doublets do not exactly degenerate [5, 15, 55]. The finite heavy quark mass makes hyperfine splittings to appear as proportional to $\frac{\Lambda_{QCD}}{m_Q}$ term. Therefore, larger bottom quark mass lowers the hyperfine splitting in B meson sector as compared to splittings in D meson sector as expected. It is natural to expect that, hyperfine splittings for P-wave mesons ($D_1^{'+} - D_0^{*+} = 102.80$ MeV) are smaller than the splittings in the ground state S-wave doublet. With increase in energy, the energy levels for the higher excited states get close to each other, therefore this hyperfine splitting is expected to be even much smaller for higher excited states.
The hyperfine splittings give more refined predictions for the vector meson mass m_V and pseudoscalar meson mass m_P in form of $m_V^2 - m_P^2$. This splitting for charm and bottom mesons gives $m_{D^*}^2 - m_D^2 = 0.54\ GeV^2$ and $m_{B^*}^2 - m_B^2 = 0.48\ GeV^2$ respectively, which is nearly same. In the case of the strange mesons, the hyperfine splittings are

$$D_s^* - D_s = 143.86 \text{ MeV},$$

$$B_s^* - B_s = 48.51 \text{ MeV}$$

These splittings show the similar behavior as that of non-strange sector. But due to the different flavored light quarks u,d and s, this splitting is not exactly same for non-strange and strange mesons.

Heavy quark flavor symmetry implies that, the difference of the non-strange and strange states for a given J^P is independent of the heavy quark flavor. We expect that to be $D_s - D \simeq B_s - B \simeq 100$ MeV. Experimentally, it is 103.51 MeV for charm ground state and 87.26 MeV for bottom ground state mesons.

Another implication of the heavy quark flavor symmetry is that, the energy for states with different quantum numbers of light DOF is same for both charm and bottom sector mesons. e.g. the excitation energy required to de-excite the P-wave state P_2^* ($J^P = 2^+$) to ground state P ($J^P = 0^-$) is approximately same for both charm and bottom mesons. i.e.,

$$D_2^* - D = 595.87 \text{ MeV}$$
$$B_2^* - B = 459.87 \text{ MeV}$$

2.11 Couplings

The strong decay rates mentioned in section 2.9 depend on the effective coupling constants. The value of the coupling in the decay rate of heavy-light hadrons is a very important input parameter for the description of the hadron processes. Therefore their confirmation, either by theoretical approaches or by experimental analysis, is relevant for checking the validity of effective theory. Effective coupling constant can be calculated directly by using the experimental meson width values. Theoretically, ground and low lying excited state couplings g_{HH} and g_{SH} are also calculated using different approaches of QCD sum rules [49,51–53], lattice QCD [48] and HHχPT [54]. Accuracy in the values of couplings is very important, as decay rates are directly related to the square of these couplings. so even a minor change in coupling values

can result in a major change in decay rates.

By using the heavy quark spin and flavor symmetry, the number of independent coupling constants are reduced to great extent. Heavy quark symmetry and decay widths of ground state mesons help in constraining the range of the strong coupling constants to be within 0 and 1 [50]. The value of the coupling constants for states of same doublet is considered to be equal for both charm and bottom mesons. So comparison of the coupling values predicted from both sectors individually, helps in testing the authenticity of the theory. By using this symmetry, we can also make predictions for decay widths for the unknown higher excited mesons.

However, model dependency in calculation of these couplings can be overcomed by considering the branching ratios of the widths in which the constants get canceled out.

In the next chapters, we will apply this heavy quark effective theory to study the charm and bottom meson spectra.

Bibliography

[1] R. Aaij et al. [LHCb Collaboration], JHEP **09**, 145 (2013).

[2] J. Brodzicka et al. [Belle Collaboration], Phys. Rev. Lett. **100**, 092001 (2008).

[3] P. del Amo Sanchez et al. [BaBar Collaboration], Phys. Rev. D **82**, 111101 (2010).

[4] T.A. Aaltonen et al. [CDF Collaboration], Phys. Rev. D **90**, 012013 (2014).

[5] M. Neubert: Phys. Rep. **245**, 259-395 (1994).

[6] N. Isgur and M. B. Wise, Adv. Ser. Direct. High Energy Phys. **10**, 549 (1992).

[7] H. Georgi,Heavy quark effective field theory, HUTP-91-A039 (1991).

[8] R. Casalbuoni, A. Deandrea et al., Phys. Rep. **281**, 145 (1977).

[9] E. Jenkins, Nucl. Phys. B **412**, 181 (1994).

[10] F. Hussain and G. Thompson, hep-ph/9502241, Report No. IC/95/15.

[11] A. V. Manohar, M. B. Wise, Camb. Monogr. Part. Phys. Nucl. Phys. Cosmol. **10**, 1-191 (2000).

[12] Andrey Grozin, "Heavy–Light Currents In: Heavy Quark Effective Theory", Springer Tracts in Modern Physics Volume 201, Springer, Berlin, Heidelberg (2004).

[13] T. Matsuki, T. Morii, and K.Seo, Prog. Theor. Phys. **124** 285 (2010).

[14] M. Tanabashi et al., [Particle Data Group Collaboration], Phys. Rev. D **98** 030001 (2018).

[15] A. F. Falk, B. Grinstein and M. E. Luke, Nucl. Phys. B **357** 185 (1991).

[16] H. Georgi, Phys. Left. B **240**, 447 (1990).

[17] A.G. Grozin, "Introduction to Heavy Quark Effective Theory" Budker-INP-1992-97, arxiv:hep-ph/9908366.

[18] MJ.Dugan, M. Golden and B. Grinstein, Phys. Lett. B **282**, 142 (1992).

[19] J M Flynn and N Isgur, J. Phys. G **18**, 1627-1644 (1992).

[20] Dedra Demaree, Heavy Quark Effective Field Theory, Mass Splittings and Decay Rates in B and D Mesons.

[21] T. Mannel, W. Roberts and Z. Ryzak, Nucl. Phys. B **368** 204 (1992).

[22] Matthias Neubert, C96-06-27.1,(Invited talk presented at the 20th Johns Hopkins Workshop on Current Problems in Particle Theory Heidelberg, Germany, 27-29 June 1996)arxiv:hep-ph/9610385.

[23] N. Di Bartolomeo, C93-06-01.1,(315-326), arxiv:hep-ph/19308285.

[24] M.A. Nowak, M. Rho and I. Zahed, Phys. Rev. D **48**, 4370 (1993).

[25] T. M. Yan, H. Y. Cheng et al., Phys. Rev. D **46**, 1148 (1992).

[26] R.Casalbuoni, A. Deandrea et al., Phys. Lett. B **292** 371 (1992).

[27] R. Casalbuoni, A. Deandrea et al., Phys. Lett. B **294** 106 (1992).

[28] R. Casalbuoni, A. Deandrea et al., Phys. Lett. B **299** 139 (1993).

[29] J. Schechter and A. Subbaraman, Phys. Rev. D **48** 332 (1993).

[30] M.B.Wise, Phys. Rev. D **45** R2188 (1992).

[31] D. Ebert, T. Feldmann et al., Nucl. Phys. B **434** 619 (1995).

[32] A. F. Falk, Nucl. Phys. B **378**, 79 (1992).

[33] U. Kilian, J. G. Korner and D. Pirjol, Phys. Lett. B **288** 360 (1992).

[34] P. Cho, Nucl. Phys. B **396**, 183-204, (1993).

[35] M. Creutz, Phys. Rev. Lett. **92**, 201601 (2004).

[36] A. F. Falk and M. E. Luke, Phys. Lett. B **292**, 119 (1992).

[37] J. Gasser and H. Leutwyler, Nucl. Phys. B **250** 465 (1985).

[38] S. Scherer, Adv. Nucl. Phys. **27** 277 (2003).

[39] Hooman Davoudiasl, Phys. Rev. D **54** 6830-6836 (1996).

[40] Mark B. Wise, Phys. Rev. D **45**, 7 (1992).

[41] Zhi-Gang Wang, Eur. Phys. J. Plus **129** 186 (2014) .

[42] P. Colangelo, F. De Fazio et al., Phys. Rev. D **86**, 054024 (2012).

[43] S. Campanella, P. Colangelo et al., Phys. Rev. D **98**, 114028 (2018).

[44] Hai-Yang Cheng, Fu-Sheng Yu, Phys. Rev. D **89**, 114017 (2014).

[45] G. Amoros, M. Beneke, M. Neubert, Phys. Lett. B **401**, 81 (1997).

[46] A. Upadhayay et al., Adv. High Energy Phys. **2014**, 619783 (2014).

[47] N. Isgur and M. B. Wise, Phys. Lett. B **237**, 527 (1990).

[48] D. Becirevic, E. Chang, and A. Le Yaouanc, arXiv:1203.0167 [hep-lat] , (2012).

[49] P. Colangelo, F. De Fazio et al., Phys. Rev. D **52**, 6422 (1995); P. Colangelo and F. De Fazio, Eur. Phys. J. C **4**, 503 (1998).

[50] I.W. Stewart, Nucl. Phys. B **529**, 62 (1998).

[51] M. E. Bracco, M. Chiapparini et al., Prog. Part. Nucl. Phys. **67** 1019 (2012).

[52] P. Colangelo et al., Phys. Lett. B **339**, 151 (1994).

[53] F.S. Navarra, M. Nielsen et al., Phys. Lett. B **489** 319-328 (2000).

[54] B. Ananthanarayan et al., Phys. Lett. B **651** 124-128 (2007).

[55] T. Matsuki, T. Morii and K. Sudoh, Phys. Lett. B **659** 593 (2008).

[56] M. Ablikim et. al., [BESIII Collaboration], Phys. Rev. Lett. **106**, 072002 (2011).

[57] M. Ablikim et. al., Chin. Phys. C **36**, 1031-1039 (2012).

Chapter 3

Analysis of Charmed Meson Spectra

3.1 Introduction

The excitation spectrum of heavy-light charm and bottom mesons has received considerable experimental and theoretical attention, as it provides opportunities to study the QCD properties with the help of different models. Experimental development of accelerators and detectors has resulted in the observation of precise data for many new excited hadrons. Mainly e^+e^-, $p\overline{p}$ and e^-p colliders have provided many open-flavored hadrons, especially the heavy-light mesons (H^Q). The heavy-light hadrons are usually detected in B (B_s) decays or in inclusive productions such as $e^+e^- \to Q\overline{Q} \to H^Q + X$, $pp \to H^Q + X$ and $ep \to H^Q + X$. Many new heavy-light states like $B_J(5840)$, $D_J^*(2650)^0$, $D_J^*(2760)^0$, $D_{sJ}(2860)$, $D_{s1}^*(2710)$, $B_1(5721)$, $B_2^*(5747)$, $D_J(2580)^0$, $D_J(2740)^0$, $D_2^*(3000)$, $B_J(5970)$ etc. have been observed by experimental collaborations like LHCb, BaBar, Belle, CLEO, CDF etc.

This vast available experimental information motivates the theorists not only to locate the available states but also to predict the masses and decay widths of missing spectra. As discussed in chapter 1, there are many effective theoretical approaches present in the literature to study the hadron properties. Some of the well known

methods reflecting the QCD aspects are effective lagrangian theories [33], Regge trajectory phenomenology [63], relativistic quark model [37, 38], constituent quark model etc. [47], quark pair creation (QPC) model [34,39,43]. In the present chapter, we will focus on the heavy-light charm mesons. Several properties like mass, decay width, angular momentum for the ground state, low lying and higher excited charm mesons are discussed in detail. The heavy-light mesons containing bottom quark as a heavy quark are investigated in next chapters. To examine the charm meson states, "Heavy Quark Effective Theory (HQET)" (discussed in previous chapter) is used as the basis of our framework.

Before starting the analysis of the charm meson spectra, let us first briefly look into the experimental information available for the charmed mesons to draw the interest towards the present study.

The ground state 1S non-strange and strange charmed mesons $D(1864)$, $D^*(2010)$, $D_s(1968)$ and $D_s^*(2112)$ have been well established and their masses and decay widths are listed in PDG [1]. The lowest lying charm meson D^0 is first observed in 1976 [2] followed by the vector meson D^* and strange mesons D_s and D_s^*, which are observed in 1977 [3, 4].

The first orbitally excited 1P non stranged charmed states ($D_0^*(2400)$, $D_1(2420)$) and ($D_1(2430)$, $D_2^*(2460)$) for J^P's $(0^+, 1^+)$ and $(1^+, 2^+)$ have been confirmed by many experiments and are listed in PDG. State $D_0^*(2400)$ is first announced by the Belle collaboration [5], which later got confirmed at BaBar [6], FOCUS [7] and Belle [8] experiments. Its spin partner $D_1(2420)$ is first reported in 1985 by the ARGUS collaboration [9] and has then confirmed by many experiments [5, 10–12]. The $D_1(2430)$ state of $S_l = 3/2$ doublet has similar mass of state $D_1(2420)$ for doublet $S_l = 1/2$, but has much larger decay width. This state is observed by Belle [5] and BaBar [13] collaborations. Its spin partner $D_2^*(2460)$ was first reported by TPS group [14], which later got confirmed by many other experiments [10–12].

The known stranged 1P charm states are ($D_{s0}^*(2317)$, $D_{s1}(2460)$) and ($D_{s1}(2536)$,

$D^*_{s2}(2573)$) for doublets $(0^+, 1^+)$ and $(1^+, 2^+)$ respectively. $D^*_{s0}(2317)$ is first observed by BaBar collaboration [15] in 2003, which has been then confirmed by Belle [16] and CLEO [17] experiments. CLEO collaboration [17] also observed $D_{s1}(2460)$ in the $D^{*+}_s\pi^0$ invariant mass spectrum, and it is then confirmed at BaBar [18] and Belle [19] experiments. The other $(1^+, 2^+)$ doublet state $D_{s1}(2536)$ is observed by ARGUS collaboration [20] followed by various other experimental groups [10,21,22]. The $J^P = 2^+$ state $D^*_{s2}(2573)$ is first seen by CLEO experiment [20] in 1994, which also provided the branching ratio

$$\frac{B(D^*_{s2}(2573)^+ \to D^{*0}K^+)}{B(D^*_{s2}(2573)^+ \to D^0K^+)} < 0.33 \tag{3.1}$$

The value for this branching ratio is also given by LHCb collaboration as $0.044 \pm 0.005 \pm 0.011$ [23].

Except the 1S and 1P charm mesons, the other orbitally excited (D,F,.. wave) or radially excited (n=2) charm mesons are still not confirmed by the experiments. With lot of upcoming experimental information for higher excited strange and non strange charm states, their J^P's are yet to be established. Charm states observed in the past decade are providing some hints in filling the missing charm spectra.

Recently, LHCb collaboration studied the resonant substructures $B^- \to D^+\pi^-\pi^-$ decays in the pp collision at 7 TeV center-of-mass energy. The masses and the widths of charm resonances with spins 1, 2 and 3 at high $D^+\pi^-$ masses are determined [24]. The study gives indication that, these resonances are mainly coming from the contribution of the $D^*_2(2460)$, $D^*_1(2680)$, $D^*_3(2760)$ and $D^*_2(3000)$ charmed mesons. The measured Breit-Wigner masses and widths of these charmed mesons are

$$\begin{aligned} D^*_2(2460) : M &= 2463.7 \pm 0.4 \pm 0.4 \pm 0.6 \text{ MeV}, \\ \Gamma &= 47.0 \pm 0.8 \pm 0.9 \pm 0.3 \text{ MeV}. \end{aligned} \tag{3.2}$$

$$D_1^*(2680) : M = 2681.1 \pm 5.6 \pm 4.9 \pm 13.1 \text{ MeV}, \quad (3.3)$$
$$\Gamma = 186.7 \pm 8.5 \pm 8.6 \pm 8.2 \text{ MeV}.$$

$$D_3^*(2760) : M = 2775.5 \pm 4.5 \pm 4.5 \pm 4.7 \text{ MeV}, \quad (3.4)$$
$$\Gamma = 95.3 \pm 9.6 \pm 7.9 \pm 33.1 \text{ MeV}.$$

$$D_2^*(3000) : M = 3214 \pm 29 \pm 33 \pm 36 \text{ MeV}, \quad (3.5)$$
$$\Gamma = 186 \pm 38 \pm 34 \pm 63 \text{ MeV}.$$

Also in 2010 and 2013, a great achievement has been made by BaBar and LHCb collaborations. LHCb collaboration observed two natural parity states $D_J^*(2650)^0$, $D_J^*(2760)^0$ and two unnatural parity states $D_J(2580)^0$ and $D_J(2740)^0$ by studying $D^+\pi^-$, $D^0\pi^+$ and $D^{*+}\pi^-$ invariant mass spectra [25]. Along with these states, LHCb has also observed $D_J(3000)^0$ in the $D^{*+}\pi^-$ final state and $D_J^*(3000)^+$ and $D_J^*(3000)^0$ in the $D^0\pi^+$ and $D^+\pi^-$ mass spectra respectively. BaBar collaboration in 2010, studied inclusive $e^+e^- \to c\bar{c}$ interaction and observed $D_J(2560)^0$, $D_J(2600)^+$, $D_J(2600)^0$, $D_J(2750)^0$, $D_J^*(2760)^0$ and $D_J^*(2760)^+$ charm states [26]. Masses and widths of charm resonances predicted by BaBar and LHCb are so close, that they are considered to be the same states. Masses and widths of these non-strange charm states observed by various collaborations are presented in Table 3.1.

In the strange charmed sector, a new state $D_{sJ}^*(2860)$ is first observed by the BaBar Collaboration in $D_{sJ}(2860) \to D^0K^+, D^+K^0$ with mass $M = 2856.6 \pm 1.5$ MeV and width $\Gamma = 48 \pm 7$ MeV [27]. It is supposed to have natural parity states i.e. $0^+, 1^-, 2^+, 3^-$ etc. But the assignment of $D_{sJ}(2860)$ as the 0^+ state has been ruled out after the observation of $D_{sJ}(2860) \to D^*K$ [28]. For this state, BaBar

Table 3.1: Experimental results of non-strange charm mesons from LHCb (2016) [24], LHCb (2013) [25] and BaBar (2010) [26]. Values corresponding to M: and Γ : represent masses and decay widths of the states in units of MeV. The "-" corresponds to the unobserved charm states at the experiments.

Charm State	LHCb(2013) [25]	BaBar(2010) [26]	LHCb(2016) [24]	Decay
$D_2^*(2460)$	-	-	M:$2463.7 \pm 0.4 \pm 0.4$ Γ : $47.0 \pm 0.8 \pm 0.9$	$D^{*+}\pi^-$
$D_J^*(2650)^0$	M:$2649.2 \pm 3.5 \pm 3.5$ Γ : $140.2 \pm 17.1 \pm 18.6$	M:$2608.7 \pm 2.4 \pm 2.5$ Γ : $93 \pm 6 \pm 13$	M:$2681.1 \pm 5.6 \pm 4.9$ Γ : $186.7 \pm 8.5 \pm 8.6$	$D^{*+}\pi^-$
$D_J^*(2760)^0$	M:$2761.1 \pm 5.1 \pm 6.5$ Γ : $74.4 \pm 3.4 \pm 37.0$	M:$2763.3 \pm 2.3 \pm 2.3$ Γ : $60.9 \pm 5.1 \pm 3.6$	M:$2775.5 \pm 4.5 \pm 4.5$ Γ : $5.3 \pm 9.6 \pm 7.9$	$D^{*+}\pi^-$
$D_J(2560)^0$	M:$2579.5 \pm 3.4 \pm 5.5$ Γ : $177.4 \pm 17.8 \pm 46.0$	M:$2539.4 \pm 4.5 \pm 6.8$ Γ : $130 \pm 12 \pm 13$	-	$D^{*+}\pi^-$
$D_J(2740)^0$	M:$2737.0 \pm 3.5 \pm 11.24$ Γ : $73.2 \pm 13.4 \pm 25.0$	M:$2752.4 \pm 1.7 \pm 2.7$ Γ : $71 \pm 6 \pm 11$	-	$D^{*+}\pi^-$
$D_J(3000)^0$	M:2971.8 ± 8.7 Γ : 188.1 ± 44.8	-	-	$D^{*+}\pi^-$
$D_J^*(2760)^0$	M:$2760.1 \pm 1.1 \pm 3.7$ Γ : $74.4 \pm 3.4 \pm 19.1$	-	-	$D^+\pi^-$
$D_J^*(3000)^0$	M:3008.1 ± 4.0 Γ : 110.5 ± 11.5	-	-	$D^+\pi^-$
$D_2^*(3000)$	-	-	M:$3214 \pm 29 \pm 33 \pm 36$ Γ : $186 \pm 38 \pm 34 \pm 63$	$D^+\pi^-$
$D_J^*(2760)^+$	M:$2771.7 \pm 1.7 \pm 3.8$ Γ : $66.7 \pm 6.6 \pm 10.5$	-	-	$D^0\pi^+$
$D_J^*(3000)^+$	M:3008.1 Γ : 110.5	-	-	$D^0\pi^+$

also measured the branching ratio R as

$$R = \frac{Br(D_{sJ}^*(2860) \to D^*K)}{Br(D_{sJ}^*(2860) \to DK)} = 1.10 \pm 0.15 \pm 0.19 \tag{3.6}$$

Along with the $D_{sJ}^*(2860)$ state, BaBar also observed two broad states $D_{s1}^*(2710)$ and $D_{sJ}(3040)$ in the DK and D^*K invariant mass spectrum with mass and widths as [27, 28]:

$$D_{s1}^*(2710) : M = 2688 \pm 4 \pm 3\text{MeV} \tag{3.7}$$
$$\Gamma = 112 \pm 7 \pm 36\text{MeV}$$

$$D_{sJ}(3040) : M = 3044 \pm 8 \pm 30\text{MeV} \qquad (3.8)$$
$$\Gamma = 239 \pm 35 \pm 42\text{MeV}$$

In Ref. [28], BaBar Collaboration reported the branching ratio for $D^*_{s1}(2710)$ state as

$$R = \frac{Br(D^*_{s1}(2710) \to D^*K)}{Br(D^*_{s1}(2710) \to DK)} = 0.91 \pm 0.13 \pm 0.12 \qquad (3.9)$$

In 2014, LHCb Collaboration also predicted a new resonance at 2.86 GeV in $\overline{D}^0 K^-$ invariant mass spectrum from decay channel $B^0_s \to \overline{D}^0 K^- \pi^+$, containing the mixture of spin 1 and spin 3 state components corresponding to $D^*_{s1}(2860)$ and $D^*_{s3}(2860)$ [29, 30], where the mass and width parameters are as:

$$D^*_{s1}(2860) : M = 2859 \pm 12 \pm 6 \pm 23\text{MeV} \qquad (3.10)$$
$$\Gamma = 159 \pm 23 \pm 27 \pm 72\text{MeV}$$

$$D^*_{s3}(2860) : M = 2860.5 \pm 2.6 \pm 2.5 \pm 6.0\text{MeV} \qquad (3.11)$$
$$\Gamma = 53 \pm 7 \pm 4 \pm 6\text{MeV}$$

Thus LHCb observed two new stranged charm states $D^*_{s1}(2860)$ and $D^*_{s3}(2860)$ with spin 1 and spin 3. Apart from these strange states, $D^*_{sJ}(2632)$ state is also observed by SELEX collaboration [41] in 2004. However, BaBar, FOCUS, CLEO collaborations [42] reported negative results in the search of this state. These experimentally seen strange charm states are tabulated in Table 3.2.

All these experimentally available charm states need to be assigned a position in the charm spectra. It is very crucial to assign a proper J^P to the heavy-light system in a given spectra, as large amount of experimental information like decay

Table 3.2: The experimental results of charm strange states $D^*_{sJ}(2860)$, $D^*_{s1}(2860)$, $D^*_{s3}(2860)$, $D^*_{s1}(2710)$ and $D_{sJ}(3040)$.

State	Mode of Decay	Mass(MeV)	Width(MeV)	Experiment
$D^*_{sJ}(2860)$	DK	2586.6 ± 1.5	47 ± 7	BaBar [27]
$D^*_{s1}(2860)$	D^0K^-	2859 ± 12	159 ± 23	LHCb [29,30]
$D^*_{s3}(2860)$	D^0K^-	2860.50 ± 2.6	53 ± 7	LHCb [29,30]
$D^*_{s1}(2710)$	DK	2688 ± 4	112 ± 7	BaBar [27]
$D_{sJ}(3040)$	D^*K	3044 ± 8	239 ± 35	BaBar [28]

width, branching ratios and hyperfine splitting are based on their J^P values. Various theoretical models have suggested different J^P states to the recently observed experimental charm mesons. In this chapter, we analyze the available theoretical and experimental data for the excited charm states to specify their proper J^P. In addition to this, we also attempt to fill the missing charm spectra by predicting the masses and strong decay widths for some of the unavailable non-strange and strange charm spectra.

The non-strange charm state $D^*_2(2460)$ is well established having $J^P = 2^+$ in the charm spectra [1,34]. The information provided by Babar (2010) and LHCb (2013) for the states $D^*_J(2680)$ and $D^*_J(2760)$ respectively, is confirmed in 2016 by LHCb, which suggested their J values to be 1 and 3 respectively. Theoretical study of these two states concluded their J^P to be 1^- for $n = 2$ S-wave and 3^- for $n = 1$ D wave respectively [31–35]. States $D_J(2560)^0$ and $D_J(2740)^0$ being the spin partners of $D^*_J(2680)^0$ and $D^*_J(2760)^0$, are assigned $J^P = 0^-$ for S-wave ($n = 2$) and 2^- for D-wave ($n = 1$) respectively. Higher charm states $D^*_J(3000)$ and $D_J(3000)$ are studied by various models like $^3P_0$ model, heavy quark effective theory, but their $J^{P'}s$ are not yet confirmed. Ref. [34] predicted the possible assignment for $D_J(3000)$ state is either $3S_{\frac{1}{2}}0^-$ or $1F_{\frac{5}{2}}3^+$ and $3S_{\frac{1}{2}}1^-$ for $D^*_J(3000)$ state. Where as authors in [36] assigned $D^*_J(3000)$ as the $1F_{\frac{5}{2}}2^+$ or $1F_{\frac{7}{2}}4^+$ state and $D_J(3000)$ as the $1F_{\frac{7}{2}}3^+$ or

$2P_{\frac{1}{2}}1^+$ state, and Ref. [40] has suggested various other possibilities for the $J^{P'}s$ of $(D_J^*(3000), D_J(3000))$ and concluded $2P(0^+, 1^+)$ to be the most favorable $nLJ^{P'}s$ in the charm spectra by evaluating their branching ratio.

The strange states $D_{sJ}^*(2860)$ and $D_{s1}^*(2710)$ have also gone through extensive discussions by various theoretical models, to find a place in strange charm spectrum. Various discussions suggest $D_{s1}^*(2710)$ to be suitable as radial excitation of S-wave i.e. $2S_{\frac{1}{2}}1^-$ [38,39] or as orbitally excited state with $l = 2$ i.e. $1D_{\frac{5}{2}}3^-$ [33,43,45]. Strange state $D_{sJ}^*(2860)$ is suggested to be either $1D_{\frac{5}{2}}3^-$ or $2P_{\frac{1}{2}}0^+$ state [33, 38, 39, 43–45]. All these different theoretical approaches calculated different values for the branching ratio $R = (\frac{Br(D_{sJ}^*(2860)\to D^*K)}{Br(D_{sJ}^*(2860)\to DK)})$ of $D_{sJ}^*(2860)$. HQET approach has predicted R to be $\approx$ 0.39 [33], while $^3P_0$ model calculated it to be R = 0.59 [43]. Both of these predicted value of R are far from the the experimental known branching ratio $R = 1.10$ [28]. All these approaches favored $D_{sJ}^*(2860)$ to be the 1^3D_3 state due to observed narrow decay width, at the cost of mismatch of R with its experimental value.

But after the observation of two independent states $D_{s1}^*(2860)$ and $D_{s3}^*(2860)$ by LHCb collaboration in 2014, it is speculated that it is the spin 3 resonance of $D_s^*(2860)$ that belongs to 1^3D_3 state, with a narrow width $\Gamma = 53$ MeV. Theoretically, branching ratio R can be matched with the experimental value, considering its contribution is coming from the spin 1 state of $D_{s1}^*(2860)$ resonance. Theoretical mass analysis, predicted the LHCb spin 1 resonance $D_{s1}^*(2860)$ to be either 1^3D_1 state of 1D family or to be a mixture of 1^3D_1 and 2^3S_1 states, since both have the same angular momentum. Ref. [39, 46] assign $D_{sJ}(2860)$ to be mixing state of $1^3D_1 - 2^3S_1$ with $D_{s1}^*(2700)$ to be its orthogonal partner, and Li and Ma in Ref. [46] obtained $R = 0.8$, which is very close to its experimental value of $R = 1.10$. X. H. Zhong and Q. Zhao by chiral quark model [47,48] studied the D_{sJ}^* state as the 1^3D_3 state with some $1^3D_2 - 1^1D_2$ mixing. Wang [49] tried to obtain this experimental R

value with some suitable hadronic coupling constants, that include chiral symmetry breaking corrections in heavy quark effective theory. Besides these studies, Vijande et al., assumes $D_{sJ}(2860)$ to be the multi-quark exotic state as $c\overline{s} - cn\overline{s}\ \overline{n}$ [50]. Stephen Godfrey by adopting the pseudoscalar emission decay model [51], Qing-Tao Song by QPC model [52], studied D^*_{sJ} as $1^3D_1 - 2^3S_1$. Various predictions are made to study the mixing effects in D^*_{sJ} state [53–56]. And lastly, the theoretical study for the strange state $D_{sJ}(3040)$ has suggested it to belong to either $2P_{\frac{1}{2}}1^+$ or $1D_{\frac{3}{2}}2^-$ or $1D_{\frac{5}{2}}2^-$ states [39, 48, 57–59]. In Ref. [39], Q.T. Song et al. also suggested that the $3S_{\frac{1}{2}}0^-$ assignment for $D_{sJ}(3040)$ state cannot be fully neglected.

Now, the main interest of theorists is focussed on newly observed non-strange charm state $D^*_2(3000)$, whose mass and decay widths are comparable with the former $D^*_J(3000)$ state. It is suggested by Zhi-Gang Wang in Ref. [60], that the energy difference between $D^*_2(3000)^0$ and $D^*_J(3000)^0$ is 206 MeV ($M_{D^*_2(3000)^0} - M_{D^*_J(3000)^0} = 206MeV$), which indicates them to be different particles. On the basis of the charm masses predicted by relativistic quark model [61], Wang suggested $D^*_2(3000)$ to be $1F_{\frac{5}{2}}2^+$ state [31, 60]. But, using the $^3P_0$ model, J.Z Wang et. al, suggested the most plausible assignment of $D^*_2(3000)$ to be the $3P_{\frac{3}{2}}2^+$ state, but then the other possibility like $2F_{\frac{5}{2}}2^+$ can not be completely excluded [62]. Thus, the clear picture of the J^P of $D^*_2(3000)$ is not yet available. Our present work is focussed on the above ambiguities and to come out with a clear picture of J^P for the $D^*_2(3000)$ state by examining its various properties like masses, branching ratios, decays etc.

On the basis of masses predicted by various theoretical models [34, 45, 61, 63–65], we expect $1F(2^+)$ and $2P(2^+)$to be the two most promising candidates for the J^P of $D^*_2(3000)$. $D^*_2(3000)$ is observed in the decay channel $D^+\pi^-$ but not in $D^{*+}\pi^-$, and hence $D^{*+}\pi^-$ decay mode must be suppressed. By analyzing the branching ratio BR=$\frac{\Gamma(D^*_2(3000)\to D^*\pi)}{\Gamma(D^*_2(3000)\to D\pi)}$ with their masses and strong decay widths, we further suggest

one of them to be the most appropriate J^P for the $D_2^*(3000)$ state and then determined its strong coupling constant.

As mentioned before, we use HQET model for studying the decay widths at the leading order approximations, because the mass and the spin degeneracy of heavy hadrons appears as approximate internal symmetry of the Lagrangian. Beside the fact that, HQET contains many unknown phenomenological constants, HQET in conjugation with the chiral perturbation theory χPT, has been successfully applied to study the strong decays of the heavy hadrons [66, 67]. However, heavy quark symmetry helps in reducing the parameters by imposing constraints on these constants, like that the range of the strong coupling constants is constrained to be within 0 and 1 by studying the decay widths and branching ratios of ground state charm mesons. [68]. The strong couplings can also be retrieved by comparing the theoretically observed strong decay widths with the experimentally available widths and masses.

In the next section 3.2, we examine the charm spectra for 1D, 1F, 2S, 2P states in both strange and non-strange sector. We study the strong decays and the branching ratios for the non-strange charm states $D_J^*(2460)$, $D_J(2560)$, $D_J(2740)$, $D_J(3000)$ with their spin partners $D_J^*(2680)$, $D_J^*(2760)$ and $D_J^*(3000)$ for J^P states $1P_{\frac{3}{2}}2^+$, $2S_{\frac{1}{2}}0^-$, $1D_{\frac{5}{2}}2^-$, $2P_{\frac{1}{2}}1^+$ and $2S_{\frac{1}{2}}1^-$, $1D_{\frac{5}{2}}3^-$, $2P_{\frac{1}{2}}0^+$ respectively. We discuss their strong coupling constants g_{TH}, $\widetilde{g}_{HH}$, g_{YH}, $\widetilde{g}_{SH}$ involved. We also suggest a suitable J^P to the newly observed charm state $D_2^*(3000)$.

In addition to this, we also study the strong decays for the unobserved spin and the strange partners of $D_2^*(3000)$ i.e. $D(1^1F_3)$, $D_s(1^1F_3)$ and $D_s(1^1F_2)$ in the framework of the HQET, which are experimentally unobserved but theoretically predicted. In the strange sector, we studied the strong decay widths for the strange states like $D_{sJ}(3040)$, $D_{s1}^*(2710)$, $D_{s1}^*(2860)$ and $D_{s3}^*(2860)$ for their J^P's $2P_{\frac{1}{2}}1^+$, $2S_{\frac{1}{2}}1^-$, $1D_{\frac{3}{2}}1^-$ and $1D_{\frac{5}{2}}3^-$ respectively. To get the complete picture of the stranged charm spectra, we have also predicted the masses and strong decay widths for their experimentally

missing spin partners $2P_{\frac{1}{2}}0^+$, $2S_{\frac{1}{2}}0^-$ and $1D_{\frac{5}{2}}2^-$. The section 3.3 of this chapter presents the conclusion of our study for charm mesons.

3.2 Numerical Analysis

The mass splitting between the higher excited charm states are closer than those of the lower states, so different orbital or radial J^P assignments are possible for single charm state, thus the observed state needs detailed investigations. For a particular J^P, various decay modes are possible. Among them, the dominant mode is decided on the basis of its contribution to the total decay widths among other partial widths. The properties of charm spectra are examined on the basis of information about its angular momentum, parity, spin, decay widths, branching ratios etc. Assigning a proper $J^{P'}s$ to the experimentally available states is essential, as it helps in retrieving many properties like decay width, strong coupling constant, branching ratios etc. To analyze the J^P's of charm states, we have divided this section in two parts, which separate the non-strange and strange charm states. The numerical masses of various mesons used in the calculation are tabulated in Table 3.3.

3.2.1 Non-Strange Charm States

In this section, we reanalyze the experimentally available data for the non-strange charm mesons $D_J^*(2460)$, $D_J(2560)$, $D_J(2740)$, $D_J^*(2680)$, $D_J^*(2760)$, $D_J(3000)$ and $D_J^*(3000)$. We have also predicted the masses and decay widths for other experi-

Table 3.3: Numerical value of the meson masses used in this work [1].

States	D^0	$D^{\pm}$	D^{*+}	D^{*0}	D_S^+	D_S^{*+}
Masses(MeV)	1864.86	1869.62	2010.28	2006.98	1968.49	2112.30
States	$\pi^{\pm}$	π^0	η	K^+	K^0	
Masses(MeV)	139.57	134.97	547.85	493.67	497.61	

mentally missing states in 1D, $1F_{5/2}$, 2S and 2P charm spectra. The charm states $D_J^*(2460)$, $D_J(2560)$, $D_J(2740)$, $D_J^*(2680)$, $D_J^*(2760)$, $D_J(3000)$ and $D_J^*(3000)$ discussed in previous section are analyzed on the basis of the available information on J values taken from LHCb in 2016. Hence we identify these states as:

$$D_J^*(2460) = (2^+)_{\frac{3}{2}} \text{with} \quad n = 1, L = 1 \tag{3.12}$$

$$(D_J(2560), D_J^*(2680)) = (0^-, 1^-)_{\frac{1}{2}} \text{with} \quad n = 2, L = 0 \tag{3.13}$$

$$(D_J(2740), D_J^*(2760)) = (2^-, 3^-)_{\frac{5}{2}} \text{with} \quad n = 1, L = 2 \tag{3.14}$$

$$D_J^*(3000)), (D_J(3000) = (0^+, 1^+)_{\frac{1}{2}} \text{with} \quad n = 2, L = 1 \tag{3.15}$$

The numerical value of the partial strong decay rates and the branching ratios for these charm states $D_2^*(2460)$, $D_0(2560)$, $D_2(2740)$, $D_1^*(2680)$, $D_3^*(2760)$, $D_1(3000)$ and $D_0^*(3000)$ are listed in Table 3.4. We have equated the resultant decay widths in Table 3.4 with their experimental data to obtain the coupling constants g_{YH}, g_{TH}, $\widetilde{g}_{HH}$ and $\widetilde{g}_{SH}$ which are listed in Table 3.5. The couplings $\widetilde{g}_{HH}, \widetilde{g}_{SH}$ are obtained by averaging the coupling values obtained from ($D_0(2560)$, $D_1^*(2680)$) and ($D_1(3000)$, $D_0^*(3000)$) respectively. We have neglected the small value of the coupling $g_{YH} = 0.10$, in comparison with its other theoretically predicted values [69]. The range in the coupling constant, comes from the error-bar in the experimental mass and decay width values. The obtained couplings are used later in this section to compute the total strong decay widths for the strange partners of these 2S, 2P and 1D states.

Table 3.4: Strong decay width of newly observed charm mesons $D_2^*(2460)$, $D_0(2560)$, $D_2(2740)$, $D_1^*(2680)$, $D_3^*(2760)$, $D_1(3000)$ and $D_0^*(3000)$. Ratio in 5^{th} column represents the $\widehat{\mathbf{\Gamma}} = \frac{\Gamma}{\Gamma(D_J^* \to D^{*+}\pi^-)}$ for the mesons. Fraction gives the percentage of the partial decay width with respect to the total decay width.

State	nLs_lJ^P	Decay channel	Decay Width (MeV)	Ratio	Fraction	Experimental value (MeV)
$D_2^*(2460)$	$1P_{3/2}2^+$	$D^{*+}\pi^-$	$56.55g_{TH}^2$	1	20.05	
		$D^{*+}\pi^0$	$29.76g_{TH}^2$	0.52	10.55	
		$D^{*+}\eta$	-	-	0	
		$D^+\pi^-$	$128.40g_{TH}^2$	2.27	45.52	
		$D^+\pi^0$	$67.06g_{TH}^2$	1.18	23.77	
		$D^+\eta$	$0.26g_{TH}^2$	0	0	
		Total	$282.04g_{TH}^2$			47.00 ± 0.80 [24]
$D_0(2560)$	$2S_{1/2}0^-$	$D^{*+}\pi^-$	$867.32\widetilde{g}_{HH}^2$	1	65.99	
		$D^{*+}\pi^0$	$443.03\widetilde{g}_{HH}^2$	0.51	33.71	
		$D^{*+}\eta$	$3.858\widetilde{g}_{HH}^2$	0	0.29	
		Total	$1314.22\widetilde{g}_{HH}^2$			177.40 ± 17.80 [25]
$D_1^*(2680)$	$2S_{1/2}1^-$	$D^{*+}\pi^-$	$889.34\widetilde{g}_{HH}^2$	1	32.41	
		$D^{*+}\pi^0$	$4451.87\widetilde{g}_{HH}^2$	0.50	16.56	
		$D^{*+}\eta$	$31.07\widetilde{g}_{HH}^2$	0.03	1.13	
		$D_s^{*+}K^-$	$78.40\widetilde{g}_{HH}^2$	0.08	2.87	
		$D^+\pi^-$	$682.53\widetilde{g}_{HH}^2$	0.76	25.01	
		$D^+\pi^0$	$346.56\widetilde{g}_{HH}^2$	0.38	12.70	
		$D^+\eta$	$48.05\widetilde{g}_{HH}^2$	0.05	1.76	
		$D_s^+K^-$	$200.49\widetilde{g}_{HH}^2$	0.22	7.34	
		Total	$2728.35\widetilde{g}_{HH}^2$			186.70 ± 8.50 [24]
$D_2(2740)$	$1D_{5/2}2^-$	$D^{*+}\pi^-$	$127.35g_{YH}^2$	1	64.79	
		$D^{*+}\pi^0$	$65.96g_{YH}^2$	0.51	33.55	
		$D^{*+}\eta$	$1.30g_{YH}^2$	0.01	0.97	
		$D_s^{*+}K^-$	$1.92g_{YH}^2$	0.01	0.97	
		Total	$196.55g_{YH}^2$			73.20 ± 13.40 [25]
$D_3^*(2760)$	$1D_{5/2}3^-$	$D^{*+}\pi^-$	$100.15g_{YH}^2$	1	21.10	
		$D^{*+}\pi^0$	$51.73g_{YH}^2$	0.51	10.90	
		$D^{*+}\eta$	$1.53g_{YH}^2$	0.01	0.32	
		$D_s^{*+}K^-$	$2.88g_{YH}^2$	0.02	0.60	
		$D^+\pi^-$	$191.14g_{YH}^2$	1.90	40.28	
		$D^+\pi^0$	$98.82g_{YH}^2$	0.98	20.82	
		$D^+\eta$	$7.05g_{YH}^2$	0.07	1.48	
		$D_s^+K^-$	$21.14g_{YH}^2$	0.21	4.45	
		Total	$474.47g_{YH}^2$			95.30 ± 9.60 [24]
$D_1(3000)$	$2P_{1/2}1^+$	$D^{*+}\pi^-$	$3325.52\widetilde{g}_{SH}^2$	1	41.96	
		$D^{*+}\pi^0$	$1674.26\widetilde{g}_{SH}^2$	0.50	21.12	
		$D^{*+}\eta$	$516.82\widetilde{g}_{SH}^2$	0.15	6.52	
		$D_s^{*+}K^-$	$2408.76\widetilde{g}_{SH}^2$	0.72	30.39	
		Total	$7925.36\widetilde{g}_{SH}^2$			188.10 ± 44.60 [25]
$D_0^*(3000)$	$2P_{1/2}0^+$	$D^+\pi^-$	$2315.81\widetilde{g}_{SH}^2$	0.50	20.26	
		$D^+\pi^0$	$4598.65\widetilde{g}_{SH}^2$	1	40.24	
		$D^+\eta$	$748.382\widetilde{g}_{SH}^2$	0.16	6.54	
		$D_s^+K^-$	$3763.23\widetilde{g}_{SH}^2$	0.81	32.93	
		Total	$11426.10\widetilde{g}_{SH}^2$			110.50 ± 11.50 [25]

Table 3.5: Comparison of various coupling constants available in the literature. Couplings in Ref. [69] and [35] are predicted by Z.G.Wang using charm and bottom mesons respectively.

Coupling constant	Our study	Work in [69]	Work in [35]
g_{TH}	0.40 ± 0.01	0.43 ± 0.05	0.43 ± 0.01
$\widetilde{g}_{HH}$	0.31 ± 0.05	0.14 ± 0.03	0.28 ± 0.01
g_{YH}	0.61 ± 0.05	0.53 ± 0.13	0.42 ± 0.02
$\widetilde{g}_{SH}$	0.12 ± 0.03	-	-

Next, we examine the newly observed charm state $D_2^*(3000)$. On the basis of the theoretically predicted masses [34, 45, 61, 63–65], $D_2^*(3000)$ is assumed to belong to either $1F_{\frac{5}{2}}(2^+)$ or $2P_{\frac{3}{2}}(2^+)$ state. The partial and the total decay widths for both these states are shown in Table 3.6.

To clear out the J^P state for $D_2^*(3000)$ between $1F(2^+)$ and $2P(2^+)$, we have observed the BR=$\frac{\Gamma(D_2^*(3000)\to D^*\pi)}{\Gamma(D_2^*(3000)\to D\pi)}$ for both these states with their masses. The graph for the BR with masses for these two J^P states $1F_{\frac{5}{2}}(2^+)$ and $2P_{\frac{3}{2}}(2^+)$ are shown in Figure 3.1.

The graph 3.1a shows, the value of BR for $2P_{\frac{3}{2}}(2^+)$ is equal to 1.06 corresponding to the mass 3214 MeV, predicting $D^*\pi$ to be dominant mode as compared to $D\pi$. And the graph 3.1b depicts the value of BR for $1F_{\frac{5}{2}}(2^+)$ state to be 0.40 for mass

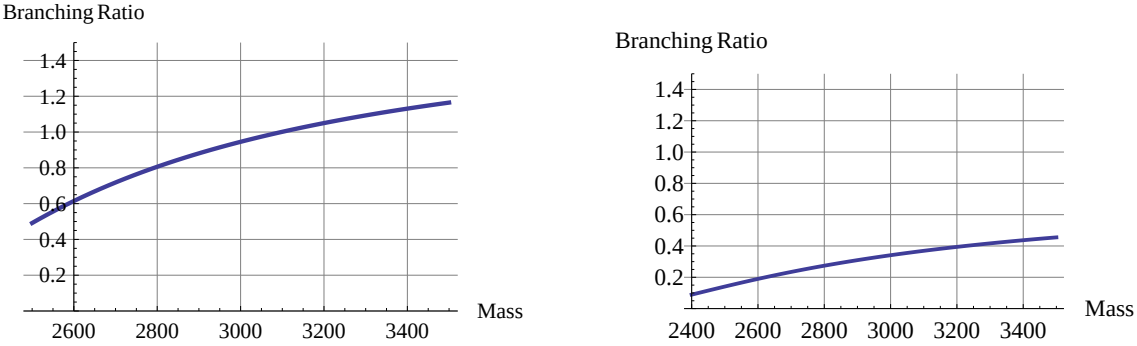

(a) Ratio for $2P(2^+)$ state

(b) Ratio for $1F(2^+)$ state

Figure 3.1: Branching ratio $\Gamma(D_2^*(3000)) \to \frac{D^*\pi}{D\pi}$ for two possible J^P's for $D_2^*(3000)$ state

Table 3.6: Strong decay width of $D_2^*(3000)$ with the J^P assignment as $1F_{\frac{5}{2}}(2^+)$ and $2P_{\frac{3}{2}}(2^+)$. Ratio represents $\widehat{\mathbf{\Gamma}} = \frac{\Gamma}{\Gamma(D_2^*(3000)\to D^{*+}\pi^-)}$ for $D_2^*(3000)$. Fraction gives the percentage of the particular decay width with respect to the total decay width.

nLs_lJ^P	Decay channel	Decay Width (MeV)	Ratio	Fraction	Experimental Value (MeV) [24]
$1F_{5/2}(2^+)$	$D^{*+}\pi^-$	$1046.53g_{ZH}^2$	1	13.60	
	$D^{*+}\pi^0$	$531.26g_{ZH}^2$	0.50	6.90	
	$D^{*+}\eta$	$109.14g_{ZH}^2$	0.10	1.41	
	$D_s^{*+}K^-$	$422.87g_{ZH}^2$	0.40	5.49	
	$D^+\pi^-$	$2630.35g_{ZH}^2$	2.51	34.20	
	$D^+\pi^0$	$1338.14g_{ZH}^2$	1.27	17.39	
	$D^+\eta$	$307.35g_{ZH}^2$	0.29	3.99	
	$D_s^+K^-$	$1304.87g_{ZH}^2$	1.24	16.96	
	Total				186 ± 38
$2P_{3/2}(2^+)$	$D^{*+}\pi^-$	$4075.15\widetilde{g}_{TH}^2$	1	24.69	
	$D^{*+}\pi^0$	$2060.89\widetilde{g}_{TH}^2$	0.50	12.48	
	$D^{*+}\eta$	$387.99\widetilde{g}_{TH}^2$	0.09	2.35	
	$D_s^{*+}K^-$	$1754.17\widetilde{g}_{TH}^2$	0.43	10.62	
	$D^+\pi^-$	$1952.32\widetilde{g}_{TH}^2$	0.94	23.36	
	$D^+\pi^0$	$3856.13\widetilde{g}_{TH}^2$	0.47	11.83	
	$D^+\eta$	$413.76\widetilde{g}_{TH}^2$	0.10	2.50	
	$D_s^+K^-$	$2002.65\widetilde{g}_{TH}^2$	0.49	12.13	
	Total				186 ± 38

3214 MeV, predicting $D\pi$ to be the dominant mode. Since $D^*\pi$ decay channel for $D_2^*(3000)$ is experimentally suppressed, therefore $1F(2^+)$ is considered to be the most favorable J^P for $D_2^*(3000)$. Along with the decay channels mentioned in Table 3.6, $D_2^*(3000)$ being $1F(2^+)$ also decays to $1P(1^+)$, $1P^{'}(1^+)$, $1D(2^-)$ and $1D^{'}(2^-)$ states along with pseudoscalar mesons (π, η, K). Since these decays occur via relative F-wave and D-wave, the contribution of their phase space to the decay widths are negligible. And therefore, these channels are suppressed.

Considering the decay channels mentioned in Table 3.6 to be the only dominant decay modes, the total decay width of $D_2^*(3000)$ comes out to be $7690.53g_{ZH}^2$. Along with the partial decay widths, Table shows the ratio $\widehat{\mathbf{\Gamma}} = \frac{\Gamma}{\Gamma(D_2^*(3000)\to D^{*+}\pi^-)}$ and the branching fraction for various decay channels of $D_2^*(3000)$ state. The results in this table reveals that, for $D_2^*(3000)$ state $D^+\pi^-$ and $D^0\pi^0$ are the main decay modes as

compared to the $D^{*+}\pi^-$ mode. The decay width obtained is finally compared with the experimental result, and the coupling constant g_{ZH} is obtained as

$$g_{ZH} = 0.15 \pm 0.02 \tag{3.16}$$

The information on the value of coupling g_{ZH} is very limited in literature, so theoretically extracting its value will be useful for finding partial and the total decay widths of unobserved charm states $D(1^1F_3)$, $D_s(1^1F_3)$ and $D_s(1^3F_2)$. Having similar angular momentum, F-wave states $1F(3^+)$ and $1F'(3^+)$ can be possibly a mixture of 1^1F_3 and 1^3F_3 with mixing angle $\theta_{1F} = -49.1^\circ$ [34].

Until now, the experimental information on the strong decay widths of $D(1^1F_3)$, $D_s(1^1F_3)$ and $D_s(1^3F_2)$ states is unavailable, so the prediction of their partial and total decay widths will be a motivation for future experiments. Mass of $D(1^1F_3)$ is predicted to be 3099 ± 25 MeV Ref. [61, 63–65]. Okubo Zweig Iizuka (OZI) allowed decay channels of $D(1^1F_3)$ are listed in the Table 3.7. Column 4 of the Table 3.7 gives the branching ratio of various partial decay widths for charm state $D(1^1F_3)$ with respect to its partial decay width $D^{*+}\pi^-$. Apart from the decay channels listed in Table 3.7, $D(1^1F_3)$ also decays to P-wave charm meson states through the light pseudo-scalar mesons. The decay occurs via. F-wave, and due to small phase space, these modes are suppressed and not considered in the present work. From the listed decay channels, $D^{*+}\pi^-$ comes out to be the dominant decay channel for $D(1^1F_3)$ with branching fraction 51.84%. Hence, the decay channel $D^{*+}\pi^-$ is suitable for the experimental search for the missing charm state $D(1^1F_3)$ in future. Using the strong coupling constant g_{ZH} from Eq.(3.16), total decay width for the charm state $D(1^1F_3)$ is obtained as 55.40 MeV. The partial decay widths predicted in this work are comparable with the values predicted in Ref. [34]. We will now proceed with the analysis of the strange charm states.

Table 3.7: Strong decay width of $D(1^1F_3)$, $D_s(1^1F_3)$ and $D_s(1^3F_2)$ charm mesons being the spin and strange partners of $1F(2^+)$. Ratio depicts the value $\widehat{\mathbf{\Gamma}} = \frac{\Gamma}{\Gamma(D_J^* \to D^{*+}\pi^-)}$ for $D(1^1F_3)$ and $\widehat{\mathbf{\Gamma}} = \frac{\Gamma}{\Gamma(D_{sJ}^* \to D^{*0}K^+)}$ for $D_s(1^1F_3)$ and $D_s(1^3F_2)$. Last column gives the branching fraction for these states.

nLs_lJ^P	Decay channel	Decay Width(MeV)	Ratio	Branching Fraction
$1F_{5/2}(3^+)$	$D^{*+}\pi^-$	29.03	1	51.84
	$D^{*+}\pi^0$	14.78	0.50	26.38
	$D^{*+}\eta$	2.57	0.09	4.75
	$D_s^{*+}K^-$	9.00	0.32	17.01
	Total	55.40	-	100
$1F_{s5/2}(3^+)$	$D^{*+}K^0$	42.41	0.97	35.15
	$D^{*0}K^+$	43.38	1	35.95
	$D_s^{*+}\eta$	14.81	0.34	12.27
	$D_s^{*+}\pi^0$	20.04	0.46	16.61
	Total	120.66	-	100
$1F_{s5/2}(2^+)$	$D^{*+}K^0$	16.61	0.97	9.29
	$D^{*0}K^+$	17.00	1	9.50
	$D_s^{*+}\eta$	5.78	0.34	3.23
	$D_s^{*+}\pi^0$	7.86	0.46	4.39
	D^+K^0	45.30	2.66	25.33
	D^0K^+	46.37	2.72	25.94
	$D_s^+\eta$	19.37	1.08	10.29
	$D_s^+\pi^0$	21.47	1.26	12.01
	Total	178.79	-	100

3.2.2 Strange Charm States

In this section, we reanalyze the previously available experimental and theoretical data on the strange charm states $D_{sJ}(3040)$, $D_{s1}^*(2710)$, $D_{s1}^*(2860)$, $D_{s3}^*(2860)$ which are identified as:

$$D_{sJ}(3040) = (1^+)_{\frac{1}{2}} \text{with} \quad n = 2, L = 1 \tag{3.17}$$

$$D_{s1}^*(2710) = (1^-)_{\frac{1}{2}} \text{with} \quad n = 2, L = 0 \tag{3.18}$$

$$D^*_{s1}(2860) = (1^-)_{\frac{3}{2}} \text{with} \quad n = 1, L = 2 \tag{3.19}$$

$$D^*_{s3}(2860) = (3^-)_{\frac{5}{2}} \text{with} \quad n = 1, L = 2 \tag{3.20}$$

The partial decay widths for the strong decays of these strange charm states decaying to the ground state $(0^-, 1^-)$ doublet are listed in Table 3.8. 4^{th} column of this table represents the branching ratio $\widehat{\mathbf{\Gamma}} = \frac{\Gamma}{\Gamma(D^*_{sJ} \to D^{*0} K^+)}$ for all the decay channels. And the 5^{th} column gives the contribution of a particular decay channel to the total strong decay width of the state. On equating the total decay widths with their experimental data, the strong coupling constants are obtained as:

$$\widetilde{g}_{SH} = 0.15 \pm 0.01 \tag{3.21}$$

$$\widetilde{g}_{HH} = 0.23 \pm 0.01 \tag{3.22}$$

$$g_{XH} = 0.12 \pm 0.01 \tag{3.23}$$

$$g_{YH} = 0.32 \pm 0.02 \tag{3.24}$$

The coupling constants $\widetilde{g}_{HH}$, $\widetilde{g}_{SH}$ and g_{YH} obtained for these strange states are compared with the same couplings obtained from the non-strange states. The comparison shows that, the predicted value of coupling $\widetilde{g}_{SH}$ is same for both strange and non-strange charm states. This similarity in the $\widetilde{g}_{SH}$ coupling value depicts the SU(3) chiral symmetry between (u,d) and s quark of $Q\overline{q}$ system.

Table 3.8: Strong decay width of charmed strange mesons $D_{sJ}(3040)$, $D^*_{s1}(2710)$, $D^*_{s1}(2860)$, $D^*_{s3}(2860)$. Ratio in the 5^{th} column depicts the $\widehat{\mathbf{\Gamma}} = \frac{\Gamma}{\Gamma(D^*_{sJ}\to D^{*0}K^+)}$ for the mesons. Fraction gives the percentage of the partial decay width with respect to the total decay width.

State	nLs_lJ^P	Decay channel	Decay Width (MeV)	Ratio	Fraction	Experimental value (MeV)
$D_{sJ}(3040)$	$2P_{1/2}1^+$	$D^{*+}K^0$	$3761.58\widetilde{g}^2_{SH}$	0.99	39.02	
		$D^{*0}K^+$	$3790.61\widetilde{g}^2_{SH}$	1	39.32	
		$D^{*+}_s\eta$	$485.90\widetilde{g}^2_{SH}$	0.12	5.04	
		$D^{*+}_s\pi^0$	$1600.17\widetilde{g}^2_{SH}$	0.42	16.60	
		Total	$9638.27\widetilde{g}^2_{SH}$			239 ± 35 [28]
$D^*_{s1}(2710)$	$2S_{1/2}1^-$	$D^{*+}K^0$	$300.11\widetilde{g}^2_{HH}$	0.94	15.42	
		$D^{*0}K^+$	$317.01\widetilde{g}^2_{HH}$	1	16.29	
		$D^{*+}_s\eta$	$3.17\widetilde{g}^2_{HH}$	0.00	0.16	
		$D^{*+}_s\pi^0$	$307.47\widetilde{g}^2_{HH}$	0.96	15.80	
		D^+K^0	$358.36\widetilde{g}^2_{HH}$	1.13	18.41	
		D^0K^+	$371.36\widetilde{g}^2_{HH}$	1.17	19.08	
		$D^+_s\eta$	$24.74\widetilde{g}^2_{HH}$	0.07	1.27	
		$D^+_s\pi^0$	$263.33\widetilde{g}^2_{HH}$	0.83	13.53	
		Total	$1945.59\widetilde{g}^2_{HH}$			112 ± 7 [27]
$D^*_{s1}(2860)$	$1D_{3/2}1^-$	$D^{*+}K^0$	$936.87g^2_{XH}$	0.98	8.90	
		$D^{*0}K^+$	$955.26g^2_{XH}$	1	9.07	
		$D^{*+}_s\eta$	$86.98g^2_{XH}$	0.09	0.82	
		$D^{*+}_s\pi^0$	$433.26g^2_{XH}$	0.45	4.11	
		D^+K^0	$3130.62g^2_{XH}$	3.27	29.74	
		D^0K^+	$3191.49g^2_{XH}$	3.34	30.32	
		$D^+_s\eta$	$342.89g^2_{XH}$	0.35	3.25	
		$D^+_s\pi^0$	$1448.06g^2_{XH}$	1.51	13.75	
		Total	$10525.50g^2_{XH}$			159 ± 23 [29, 30]
$D^*_{s3}(2860)$	$1D_{5/2}3^-$	$D^{*+}K^0$	$46.65g^2_{YH}$	0.93	9.47	
		$D^{*0}K^+$	$49.71g^2_{YH}$	1	10.09	
		$D^{*+}_s\eta$	$1.13g^2_{YH}$	0.02	0.22	
		$D^{*+}_s\pi^0$	$46.32g^2_{YH}$	0.93	9.40	
		D^+K^0	$121.21g^2_{YH}$	2.43	24.60	
		D^0K^+	$127.94g^2_{YH}$	2.57	25.97	
		$D^+_s\eta$	$6.16g^2_{YH}$	0.12	1.25	
		$D^+_s\pi^0$	$93.43g^2_{YH}$	1.87	18.96	
		Total	$492.58g^2_{YH}$			53 ± 7 [29, 30]

The other couplings $\widetilde{g}_{HH}$ and g_{YH} does not exactly match with the coupling values obtained from non-strange charm analysis. The value for the coupling $\widetilde{g}_{HH}$ is still very close for both the cases, which deviates only by 0.08 and can be very well compared with other theoretically predicted values [35, 69]. However, the coupling g_{YH} shows a large variation, where the maximum deviation is 0.26.

Apart from the decay channels mentioned in Table 3.8, state $D_{sJ}(3040)$ also decays to the D - wave charm states. But because of their small contribution, these decays are not considered in present work. $D^{*0}K^{+}$ and $D^{*+}K^{0}$ are seen as the dominating decay modes for $D_{sJ}(3040)$ with branching fraction 39.32 % and 39.02% respectively. Ref. [39] also shows $D^{*}K$ to be the dominating decay mode for $D_{sJ}(3040)$ belonging to $2P_{1/2}1^{+}$ state.

So the decay mode $D^{*0}K^{+}$ and $D^{*+}K^{0}$ are suitable for its further experimental confirmation.

Analysis for the strange state $D^{*}_{s1}(2710)$ shows that the $D^{0}K^{+}$ is the dominant decay mode for it, contributing 19.08% to its total decay width. The value of the experimental known branching ratio R = $\frac{Br(D^{*}_{s1}(2710)\rightarrow D^{*}K)}{Br(D^{*}_{s1}(2710)\rightarrow DK)}$ (Eq.(3.9)) obtained in our work is 0.84, which is very close to its experimental value of 0.91 predicted by BaBar [28]. Here $D^{*}K$ (DK) is taken as $D^{*+}K^{0} + D^{*0}K^{+}$ $(D^{+}K^{0} + D^{0}K^{+})$. Similar data obtained in the experimental and theoretical value of branching ratio R confirms the $J^{P} = 2S_{1/2}1^{-}$ assignment for $D^{*}_{s1}(2710)$ state.

Further, for the strange charm state $D^{*}_{s1}(2860)$, $D^{0}K^{+}$ is observed as the main decay mode followed by $D^{+}K^{0}$ having branching fraction of 30.32% and 29.74% respectively. Theoretically branching ratio R = $\frac{Br(D^{*}_{sJ}(2860)\rightarrow D^{*}K)}{Br(D^{*}_{sJ}(2860)\rightarrow DK)}$ for this state is computed as 0.29 which is very much deviating from its experimental value 1.10 [28]. The difference in these two R values can be justified by assuming that, instead of $D^{*}_{s1}(2860)$ belonging to a pure state $1D_{\frac{3}{2}}1^{-}$, this state is a mixture of $1D_{\frac{3}{2}}1^{-}$ and

$2S_{\frac{1}{2}}1^-$ with $D^*_{s1}(2710)$ as its orthogonal partner. This is represented as

$$\begin{pmatrix} D^*_{s1}(2710) \\ D_{s1}(2860) \end{pmatrix} = \begin{pmatrix} cos\theta & sin\theta \\ -sin\theta & cos\theta \end{pmatrix} \begin{pmatrix} 2^3S_1 \\ 1^3D_1 \end{pmatrix} \tag{3.25}$$

Now, branching ratio R depends on mixing angle θ, so by choosing a suitable mixing angle θ, the value for R can be matched with its experimental data. Such a mixing is allowed when spin symmetry violating 1/m effects are included, and both states 2^3S_1 and 1^3D_1 transform as $J^P = 1^-$ under the Lorentz group and differ only in their values of J^P_l. The mixing of these states has been studied in Ref. [39], which predicted that the experimental data for these two states can be retrieved around the mixing angle $\theta = 6.8° - 11.2°$.

Lastly for the charm state $D^*_{s3}(2860)$, D^0K^+ seems to be the main decay channel which contributes 25.97% to its total strong decay width. Apart from the decay modes listed in Table 3.8, $D^*_{s3}(2860)$ also decays to P - wave charm states, which due to their small phase space are not considered in the present work.

To complete the analysis of stranged charm spectra, we have also obtained the masses and decay widths for their missing spin partners $2S_{\frac{1}{2}}0^-$, $2P_{\frac{1}{2}}0^+$ and $1D_{\frac{5}{2}}2^-$. Until now, the experimental information on these states is unavailable, so prediction of the properties of these strange states will be a motivation to the further experimentalists. To calculate the masses, we have used the fact that, the hyperfine splittings between the spin partners within the same doublet are same for both strange and non-strange charm states. i.e. for any doublet

$$D^* - D = D^*_s - D_s \tag{3.26}$$

holds true. Using the above equality for the experimentally available non-strange and strange charm masses for $\widetilde{H}$, $\widetilde{S}$ and Y field states, masses for $2S_{\frac{1}{2}}0^-$, $2P_{\frac{1}{2}}0^+$

and $1D_{\frac{5}{2}}2^-$ are obtained as:

$$\begin{aligned} M(2S_{\frac{1}{2}}0^-) &= 2639.50\text{MeV} \\ M(2P_{\frac{1}{2}}0^+) &= 3080.30\text{MeV} \\ M(1D_{\frac{5}{2}}2^-) &= 2822.00\text{MeV} \end{aligned} \tag{3.27}$$

These masses are in the similar range with the other theoretically predicted masses [39, 63, 65, 70]. Calculated masses are only 0.84-3.86%, 0.43-2.76% and 1.51-1.88% deviating from the theoretical masses in Ref. [63], Ref. [65] and Ref. [70] respectively. As compared to the predictions in Ref. [39], masses for states $2S_{\frac{1}{2}}0^-$, $2P_{\frac{1}{2}}0^+$ and $1D_{\frac{5}{2}}2^-$ deviates by (0.28-0.81)%, (3.19-5.39)% and (13.04-16.33)% respectively. The calculated masses are further used to study their strong decays, branching ratios and fractions. Using Eqs.(2.51-2.57), the numerical value of the OZI allowed decay channels for these states are listed in Table 3.9. Using average value of the couplings $\widetilde{g}_{HH}$, $\widetilde{g}_{SH}$ and g_{YH} obtained from non-strange and strange charm mesons, total decay width of these states are obtained as:

$$\begin{aligned} \Gamma(2S_{\frac{1}{2}}0^-) &= 68.19\text{MeV} \\ \Gamma(2P_{\frac{1}{2}}0^+) &= 225.94\text{MeV} \\ \Gamma(1D_{\frac{5}{2}}2^-) &= 35.30\text{MeV} \end{aligned} \tag{3.28}$$

Decay width for $2S_{\frac{1}{2}}0^-$ state differs only by 7.87 MeV whereas for $2P_{\frac{1}{2}}0^+$ it deviates by 59.79 MeV from the results predicted in Ref. [39].

We have also studied the decay behavior of strange partners of $D_2^*(3000)$ and $D_3(3099)$ charm states i.e. $(D_{s2}^*, D_{s3}) = (2^+, 3^+)_{\frac{5}{2}}$ with n=1 and L=3. Masses for these strange charm states are taken as 3220.66 ± 9 MeV and 3232.50 ± 33 MeV from the theoretical work [61, 63–65]. OZI allowed two body strong decay channels

Table 3.9: Strong decay width of $2S_{\frac{1}{2}}0^-$, $2P_{\frac{1}{2}}0^+$ and $1D_{\frac{5}{2}}2^-$ as the spin partners of $D^*_{s1}(2710)$, $D_{sJ}(3040)$ and $D^*_{s3}(2860)$. Ratio in the 5th column depicts the $\widehat{\mathbf{\Gamma}} = \frac{\Gamma}{\Gamma(D^*_{sJ}\to D^{*0}K^+)}$ for the $2S_{\frac{1}{2}}0^-$ and $1D_{\frac{5}{2}}2^-$ mesons and $\widehat{\mathbf{\Gamma}} = \frac{\Gamma}{\Gamma(D^*_{sJ}\to D^{0}K^+)}$ for $2P_{\frac{1}{2}}0^+$. Fraction gives the percentage of the partial decay width with respect to the total decay width.

State	nLs_lJ^P	Decay channel	Decay Width(MeV)	Ratio	Fraction
$D_{s0}(2639.50)$	$2S_{1/2}0^-$	$D^{*+}K^0$	$275.12\widetilde{g}^2_{HH}$	0.92	29.40
		$D^{*0}K^+$	$296.83\widetilde{g}^2_{HH}$	1	31.72
		$D^{*+}_s\pi^0$	$363.55\widetilde{g}^2_{HH}$	1.22	38.86
		Total	$93.51\widetilde{g}^2_{HH}$		
$D^*_{s0}(3080.30)$	$2P_{1/2}0^+$	D^+K^0	$5155.02\widetilde{g}^2_{SH}$	0.98	38.48
		D^0K^+	$5212.65\widetilde{g}^2_{SH}$	1	38.98
		$D^+_s\eta$	$728.42\widetilde{g}^2_{SH}$	0.13	5.44
		$D^+_s\pi^0$	$2273.33\widetilde{g}^2_{SH}$	0.43	17.00
		Total	$13369.40\widetilde{g}^2_{SH}$		
$D^{'}_{s2}(2822)$	$1D_{5/2}2^-$	$D^{*+}K^0$	$51.86g^2_{YH}$	0.93	31.08
		$D^{*0}K^+$	$55.74g^2_{YH}$	1	33.41
		$D^{*+}_s\eta$	$0.89g^2_{YH}$	0.01	0.53
		$D^{*+}_s\pi^0$	$58.33g^2_{YH}$	1.04	34.96
		Total	$492.58g^2_{YH}$		

of these two states are also listed in Table 3.7. For D^*_{s2} and D_{s3} state, we observe D^0K^- and $D^{*0}K^-$ are observed as the dominant decay mode with branching fraction 25.94% and 35.95% respectively. In Ref. [39], DK and D^*K are also seen as one of the dominating decay modes for D^*_{s2} and D_{s3} states. These strange states also decay to P-wave charm meson states, but due to small phase space, these modes are suppressed in present work. Using g_{ZH} from Eq.(3.16), the total decay width for D^*_{s2} comes out to be 178.79 MeV and for D_{s3} it is 120.66 MeV. Since the sum of all the partial decay widths gives the total decay width for any state, therefore D^*_{s2} state is observed to be a broader state as compared to its spin partner D_{s3} which matches with the predictions of Ref. [39].

This analysis for the charm states in strange sector have helped in filling the charm spectra for $2S_{1/2}, 2P_{1/2}, 1D_{3/2}, 1D_{5/2}, 1F_{5/2}$ states.

3.3 Conclusion

In this chapter, we have examined the charm non-strange states $D_J^*(2460)$, $D_J(2560)$, $D_J^*(2680)$, $D_J(2740)$, $D_J^*(2760)$, $D_J(3000)$ and $D_J^*(3000)$ with their J^P as $1P_{\frac{3}{2}}2^+$, $2S_{\frac{1}{2}}0^-$, $2S_{\frac{1}{2}}1^-$, $1D_{\frac{5}{2}}2^-$, $1D_{\frac{5}{2}}3^-$, $2P_{\frac{1}{2}}1^+$ and $2P_{\frac{1}{2}}0^+$ respectively along with their strange partners $D_{sJ}(3040)$, $D_{s1}^*(2710)$, $D_{s1}^*(2860)$, $D_{s3}^*(2860)$ for their J^P's $2P_{\frac{1}{2}}1^+$, $2S_{\frac{1}{2}}1^-$, $1D_{\frac{3}{2}}1^-$ and $1D_{\frac{5}{2}}3^-$ respectively. We use the HQET lagrangian at the leading order approximation, to study the two body strong decay behavior of these charm states with the emission of light pseudo-scalar mesons (π, η, K). We have computed the branching ratios and the coupling constants g_{TH}, $\widetilde{g}_{HH}$, g_{YH}, g_{XH}, $\widetilde{g}_{SH}$ for the above said states, that can shed light on the present spectra and be helpful for future experimental findings.

Along with this, we have also tentatively identified the J^P for $D_2^*(3000)$ charm meson which is recently observed by the LHCb in 2016 [24]. We studied the branching ratio for this state and concluded its J^P to be $1F_{\frac{5}{2}}2^+$, and correspondingly obtained the coupling constant $g_{ZH} \simeq 0.15$. The obtained coupling constants g_{YH}, g_{ZH}, $\widetilde{g}_{HH}$ and $\widetilde{g}_{SH}$ helps in predicting the possible strong decay channels for the experimentally missing $D(1^1F_3)$, $D_S(1^1F_3)$ $D_S(1^3F_2)$, $D_S(1^1D_2')$, $D_S(2^1S_0)$ and $D_S(2^3P_0)$ states. The observation of $D_2^*(3000)$ as $1F_{\frac{5}{2}}2^+$ has opened a window to investigate the higher excitations of charm mesons at the LHCb, BaBar, BESIII. The prediction of masses and decay widths of these charm states have successfully provided the charm spectra for $1P_{3/2}$, $1D_{3/2}$, $1D_{5/2}$, $1F_{5/2}$, $2S_{1/2}$ and $2P_{1/2}$ states in both strange and non-strange spectra.

Bibliography

[1] M. Tanabashi et al. [Particle Data Group Collaboration], Phys. Rev. D **98**, 030001 (2018).

[2] I. Peruzzi et al., Phys. Rev. Lett. **37**, 569 (1976).

[3] G. Goldhaber et al., Phys. Lett. B **69**, 503 (1977).

[4] R. Brandelik et al. [DASP Collaboration], Phys. Lett. B **70**, 132 (1977).

[5] K. Abe et al. [Belle Collaboration], Phys. Rev. D **69**, 112002 (2004).

[6] B. Aubert et al. [BaBar Collaboration], Phys. Rev. D **79**, 112004 (2009).

[7] J.M. Link et al. [FOCUS Collaboration], Phys. Lett. B **586**, 11 (2004).

[8] D. Matvienko et al. [Belle Collaboration], Phys. Rev. D **92**, 012013 (2015).

[9] H. Albrecht et al. [ARGUS Collaboration], Phys. Rev. Lett. **56**, 549 (1986).

[10] S. Chekanov et al. [ZEUS Collaboration], Eur. Phys. J. C **60**, 25 (2009).

[11] P. Avery et al. [CLEO Collaboration], Phys. Lett. B **331**, 236 (1994), [Erratum: Phys. Lett.B **342**, 453 (1995)].

[12] K. Abe et al. [Belle Collaboration], Phys. Rev. Lett. **94**, 221805 (2005).

[13] B. Aubert et al. [BaBar Collaboration], Phys. Rev. D **74**, 012001 (2006).

[14] J.C. Anjos et al. [Tagged Photon Spectrometer Collaboration], Phys. Rev. Lett. **62**, 1717 (1989).

[15] B. Aubert et al. [BaBar Collaboration], Phys. Rev. Lett. **90**, 242001 (2003).

[16] D. Besson et al. [CLEO Collaboration], Phys. Rev. D **68**, 032002 (2003), [Erratum: Phys. Rev.D75,119908(2007)].

[17] K. Abe et al. [Belle Collaboration], Phys. Rev. Lett. **92**, 012002 (2004).

[18] B. Aubert et al. [BaBar Collaboration], Phys. Rev. D **74**, 032007 (2006).

[19] B. Aubert et al. [BaBar Collaboration], Phys. Rev. D **69**, 031101 (2004).

[20] Y. Kubota et al. [CLEO Collaboration], Phys. Rev. Lett. **72**, 1972 (1994).

[21] A. Heister et al. [ALEPH Collaboration], Phys. Lett. B **526**, 34 (2002).

[22] R. Aaij et al. [LHCb Collaboration], JHEP **02**, 133 (2016).

[23] R. Aaij et al. [LHCb Collaboration], Phys. Lett. B **698**, 14 (2011).

[24] R. Aaij et al. [LHCb Collaboration], Phys. Rev. D **94**, 072001 (2016).

[25] R. Aaij et al. [LHCb Collaboration], J. High Energy Phys. **09** 145 (2013).

[26] P. del Amo Sanchez et al. [BaBar Collaboration], Phys. Rev. D **82**, 111101 (2010).

[27] B. Aubert et al. [BaBar Collaboration],Phys. Rev. Lett. **97**, 222001 (2006).

[28] B. Aubert et al. [BaBar Collaboration], Phys. Rev. D **80**, 092003 (2009).

[29] R.Aaij et al. [LHCb Collaboration], Phys. Rev. Lett. **113**, 162001 (2014).

[30] R.Aaij et al. [LHCb Collaboration], Phys. Rev. D **90**, 072003 (2014).

[31] G. L. Yu, Z. G.Wang, and Z. Y. Li, Phys. Rev. D **94**, 074024 (2016).

[32] A. M. Badalian and B. L. G. Bakker, Phys. Rev. D **84**, 034006 (2011).

[33] P. Colangelo, F. De Fazio et al., Phys. Rev. D **86**, 054024 (2012).

[34] Q. T. Song, D. Y. Chen et al., Phys. Rev. D **92**, 074011 (2015).

[35] Z. G. Wang, Phys. Rev. D **88**, 114003 (2013).

[36] G. L. Yu, Z.-G. Wang et al., Chin. Phys. C **39**, 063101 (2015).

[37] T. Matsuki et al., Prog. Theor. Phys. **117** 1077 (2007).

[38] T. Matsuki et al., Eur. Phys. J. A **31**, 701 (2007).

[39] Q.T. Song et al., Phys. Rev. D **91**, 054031 (2015).

[40] M. Batra and A. Upadhyay, Eur. Phys. J. C **75**, 319 (2015).

[41] A.V. Evdokimov et al. [SELEX Collaboration], Phys. Rev. Lett. **93**, 242001 (2004).

[42] B. Aubert et al. [BaBar Collaboration], BABAR-CONF-04-045, SLAC-PUB-10633 (2004), arXiv: hep-ex/0408087.

[43] B. Zhang, X. Liu et al., Eur. Phys. J. C **50**, 617 (2007).

[44] P. Colangelo, F. De Fazioa, and S. Nicotria, Phys. Lett. B **642**, 48 (2006).

[45] D.-M. Li, B. Ma, and Y.-H. Liu, Eur. Phys. J. C **51**, 359 (2007).

[46] D.-M. Li and B. Ma, Phys. Rev. D **81**, 014021, (2010).

[47] X. H. Zhong andQ. Zhao, Phys. Rev. D **78**, 014029 (2008).

[48] X. H. Zhong and Q. Zhao, Phys. Rev. D **81**, 014031 (2010).

[49] Z.-G.Wang, Eur. Phys. J. C **75**, 25 (2015).

[50] J. Vijande, A. Valcarce, and F. FernLandez, Phys. Rev. D **79**, 037501 (2009).

[51] S. Godfrey and I. T. Jardine, Phys. Rev. D **89**, 074023 (2014).

[52] Q.T. Song, D.-Y. Chen et al., Eur. Phys. J. C **75**, 30 (2015).

[53] L. Yuan, B. Chen, and A. Zhang, arXiv:1203.0370 [hep-ph].

[54] F. E. Close, C. E. Thomas et al., Phys. Lett. B **647**, 159 (2007).

[55] D.M. Li, P.-F. Ji, and B. Ma, Eur. Phys. J. C **71**, 1582 (2011).

[56] B. Chen, X. Liu, and A. Zhang, Phys. Rev. D **92**, 034005 (2015).

[57] P. Colangelo, F. De Fazio, Phys. Rev. D **81**, 094001 (2010).

[58] B. Chen, L. Yuan et al., Phys. Rev. D **83**, 114025 (2011).

[59] Z.F. Sun, X. Liu, Phys. Rev. D **80**, 074037 (2009).

[60] Z. G. Wang, Commun. Theor. Phys. **66**, 671 (2016).

[61] S. Godfrey and K. Moats, Phys. Rev. D **93**, 034035 (2016).

[62] J.-Z.Wang, D.-Y. Chen et al., Phys. Rev. D **94**, 094044 (2016).

[63] D. Ebert, R. N. Faustov, and V. O. Galkin, Eur. Phys. J. C **66**, 197 (2010).

[64] S. Godfrey and N. Isgur, Phys. Rev. D **32**, 189 (1985).

[65] M. Di Pierro and E. Eichten, Phys. Rev. D **64**, 114004 (2001).

[66] J. L. Goity and W. Roberts, Phys. Rev. D **51**, 3459 (1995).

[67] A. Falk and T. Mehen, Phys. Rev. D **53**, 231 (1996).

[68] I.W. Stewart, Nucl. Phys. B **529**, 62 (1998).

[69] Z. G. Wang, Eur. Phys. J. Plus **129**, 186 (2014).

[70] V. Kher, N. Devlani et al., Chin. Phys. C **41**, 073101 (2017).

Chapter 4

Analysis of Higher Excited $1P_{3/2}$, $1D_{3/2}$ and $2S_{1/2}$ Doublets of Bottom Meson

4.1 Introduction

In the present chapter, we have examined the experimentally available bottom mesons $B_1(5721)$, $B_2^*(5747)$, $B_{s1}(5830)$, $B_{s2}^*(5840)$, $B_J(5960)$ and $B_J(5840)$. We have studied their properties like masses, strong decay widths, branching ratios etc. to assign them a particular J^P in the bottom sector. We have also predicted other unknown bottom states like $B(2^1S_0)$, $B_s(2^3S_1)$, $B(1^1D_2)$, $B_s(1^3D_1)$ etc. In particular, we aim in analyzing $1P_{3/2}$, $1D_{3/2}$ and $2H_{1/2}$ bottom doublets in both non-strange and strange sector. In the previous chapter, using the similar properties, we have studied the experimentally available non-strange charm mesons $D_J^*(2460)$, $D_J(2560)$, $D_J^*(2680)$, $D_J(2740)$, $D_J^*(2760)$, $D_J(3000)$, $D_J^*(3000)$ and strange charm states $D_{sJ}(3040)$, $D_{s1}^*(2710)$, $D_{s1}^*(2860)$, $D_{s3}^*(2860)$ [1–6].

To begin with this chapter, let us first review the experimental information available for the bottom mesons. This experimental study will raise the interest in the present analysis of bottom states. In bottom sector, only ground state and few of

the low lying excited bottom mesons are experimentally well known and are listed in PDG [7]. The ground state 1S bottom meson B is first observed by CLEO collaboration in 1983 [8] followed by the vector meson B^* in 1985 [9]. And the ground state, strange bottom mesons B_s and B_s^* are observed by CUSB-II collaboration in 1990 [10]. Experimental information for all these four states is tabulated in Table 4.1. There are many decay modes experimentally observed for these states. But weak decay $b \to cW^-$ is preferred for the pseudoscalar mesons B and B_s. Vector mesons B_s and B_s^* mainly decays through electromagnetic modes $B\gamma$ and $B_s\gamma$ respectively.

The first orbital excited bottom meson $B_J^*(5732)$, is observed by OPAL detector at LEP having mass $M = 5738^{+5}_{-6} \pm 7$ MeV and decay width $\Gamma = 18^{+15}_{-13}$ MeV [11]. The other orbitally excited 1P states $B_J(5721)$ and $B_2^*(5747)$ are first observed by DØ collaboration in 2007 for J^P's 1^+ and 2^+ [12]. This observation is also confirmed at LHCb [13] and CDF [14, 15] experiments. LHCb collaboration has also provided the following branching ratio's for $B_2^*(5747)$ state:

$$\frac{B_2^*(5747)^0 \to B^{*+}\pi^-}{B_2^*(5747)^0 \to B^+\pi^-} = 0.71 \pm 0.14 \pm 0.30 \tag{4.1}$$

$$\frac{B_2^*(5747)^+ \to B^{*0}\pi^+}{B_2^*(5747)^+ \to B^0\pi^+} = 1.0 \pm 0.5 \pm 0.8 \tag{4.2}$$

In the strange sector of bottom mesons, OPAL detector in the same experiment observed a strange state $B_{sJ}^*(5850)$ [11], which later in 2008 is separated into two states $B_{s1}(5830)$ and $B_{s2}^*(5840)$ by CDF collaboration [16]. These states are also confirmed by LHCb [17], DØ [18] and CDF [15] collaborations. In the bottom meson spectra, only the ground state mesons are known with confirmed J^P's. And the information for other higher excited bottom mesons above $B_J^*(5732)$ is rather limited

as compared to the charm mesons. However, the recent measurement of bottom mesons by LHCb has opened the gate to extend our understanding for the higher excited bottom states. Recently in 2013, a new state $B_J(5960)$ has been observed both in the $B^0\pi^+$ and $B^+\pi^-$ mass distribution by the CDF collaboration. The observed mass of this resonance is M = $5978 \pm 5 \pm 12$ MeV for the neutral state and M = $5961 \pm 5 \pm 12$ MeV for the charged state [15]. In 2015, LHCb has also reported the observation of new resonances $B_J(5960)^{0,+}$ in the pp collision data, at center-of-mass energies of 7 and 8 TeV [13] with results:

$$B_J(5960)^0 : M = 5969.2 \pm 2.9 \pm 5.1 \pm 0.2\text{MeV} \qquad (4.3)$$
$$\Gamma = 82.3 \pm 7.7 \pm 9.4\text{MeV}$$

$$B_J(5960)^+ : M = 5964.9 \pm 4.1 \pm 2.5 \pm 0.2\text{MeV} \qquad (4.4)$$
$$\Gamma = 63.0 \pm 14.5 \pm 17.2\text{MeV}$$

Besides the state $B_J(5960)$, LHCb also observed a new highly excited bottom resonance $B_J(5840)^{0,+}$ in the $B\pi$ mass distributions with mass and decay widths as:

$$B_J(5840)^0 : M = 5862.9 \pm 5.0 \pm 6.7 \pm 0.2\text{MeV} \qquad (4.5)$$
$$\Gamma = 127.4 \pm 16.7 \pm 34.2\text{MeV}$$

$$B_J(5840)^+ : M = 5850.3 \pm 12.7 \pm 13.7 \pm 0.2\text{MeV} \qquad (4.6)$$
$$\Gamma = 224.4 \pm 23.9 \pm 79.8\text{MeV}$$

The masses and the widths of the experimentally measured bottom states B, B^*, B_s, B_s^*, $B_J(5721)$, $B_2^*(5747)$, $B_J(5840)$, $B_J(5960)$, $B_{sJ}(5830)$ and $B_{s2}^*(5840)$ discussed above are listed in Table 4.1.

Table 4.1: Values of masses and decay widths of bottom mesons observed by various collaborations.

State	J^P	Mass (MeV)	Width (MeV)	Experiments	Decay Modes
$B(5279)^0$	0^-	5279.61 ± 0.16	-	CLEO [8]	$D\pi\pi$,$D^*\pi$
$B(5279)^\pm$	0^-	5279.29 ± 0.15	-	CLEO [8]	$D\pi$, $D^*\pi\pi$
$B(5324)^*$	1^-	5324.83 ± 0.32	-	CUSB [9]	Bγ
$B_s(5366)$	0^-	5366.79 ± 0.23	-	CUSB-II [10]	-
$B_s^*(5415)$	1^-	5415.40 ± 0.15	-	CUSB-II [10]	$B_s\gamma$
$B_J(5721)$	1^+	5727.7 ± 0.7	30.1 ± 1.5	LHCb [13]	$B^*\pi$
		5720.6 ± 2.4	-	D0 [12]	$B^*\pi$
		5725.3 ± 1.6	-	CDF [14]	$B^*\pi$
$B_2^*(5747)$	2^+	5739.44 ± 0.37	24.5 ± 1.0	LHCb [13]	$B^*\pi$,$B\pi$
		5746.8 ± 2.4	-	D0 [12]	$B^*\pi$,$B\pi$
		5740.2 ± 1.7	22.7 ± 3.2	CDF [14]	$B^*\pi$,$B\pi$
$B_J(5840)$	$-$	5862.9 ± 5.0	127.4 ± 16.7	LHCb [13]	$B\pi$
$B_J(5960)$	$-$	5978 ± 5	-	CDF [14]	$B\pi$
		5969.2 ± 2.9	82.3 ± 7.7	LHCb [13]	$B\pi$
$B_{s1}(5830)$	1^+	5828.40 ± 0.04	-	LHCb [17]	B^*K
		5828.3 ± 0.1	0.5 ± 0.3	CDF [15]	B^*K
		5829.4 ± 0.7	-	CDF [16]	B^*K
$B_{s2}^*(5840)$	2^+	5839.6 ± 1.1	-	D0 [18]	B^*K,BK
		5839.70 ± 0.7	-	CDF [16]	B^*K,BK
		5839.70 ± 0.1	1.40 ± 0.4	CDF [15]	B^*K,BK
		5839.99 ± 0.05	1.56 ± 0.13	LHCb [17]	B^*K,BK

Many theoretical predictions have been made for assigning a particular J^P's to these experimentally observed states. Different theoretical approaches include, the constituent quark model [19, 20], chiral quark model [21], effective lagrangian model [23], $^3P_0$ model [22], QCD sum rules [24], chiral particle decay [25] and semi-relativistic quark potential model [26, 27, 45]. Due to the different theoretical parameters present in these theoretical models, the predictions are not completely consistent with each other, hence a particular J^P is not confirmed for these experimentally observed bottom states. It is very crucial to assign a proper J^P to the heavy-light meson to know their properties like decay width, mass, branching ratios, strong coupling constant, hyperfine-splittings etc.

The states $B_J(5721)$ and $B_2^*(5747)$ are being analyzed theoretically by various models [26, 28–31] and have interpreted $B_2^*(5747)$ state to belong to 2^+. For the $B_J(5721)$ state, some of the theoretical work [23,26,30] favors it to be the spin partner of the $B_2^*(5747)$ state and hence as 1^+ for $S_l = 3/2$ P-wave bottom meson. And other papers [28,29,31] suggests $B_J(5721)$ to be the mixture of the $1P_{1/2}$ and $1P_{3/2}$ state. The other two bottom states $B_{s1}(5830)$ and $B_{s2}^*(5840)$, being the strange partners of $B_J(5721)$ and $B_2^*(5747)$ states, too belong to $1P_{s3/2}1^+$ and $1P_{s3/2}2^+$ J^P's respectively.

For the bottom state $B_J(5960)$, authors in Ref. [32] claimed, that the properties of $B(5970)$ seen by CDF collaboration [15] are consistent with the properties of $B_J(5960)$ measured by LHCb [13], so they might be similar state. The theoretical analysis made by studying decay widths for $B_J(5960)$ by QPC model [31] and HQET [34], favors it to belong to $2S1^-$ state. This prediction is also supported by work in [27, 33], where the authors have used the semi-relativistic quark potential model and relativistic quark model. The work [36], we presented in the next chapter deals with the masses that are predicted using the QCD and $1/m_Q$ corrections to the flavor independent parameters Δ_F and λ_F. Here also, $B_J(5960)$ is favored to be

2S1$^-$ state. But, Qi-Fang Lu et. al. in Ref. [29] studied masses and strong decays of $B_J(5960)$ states with different spin parity hypothesis and identified that, $B_J(5960)$ belongs to 1D3$^-$ state. A review on open charm and bottom systems by Hua-Xing Chen in Ref. [35] examines various theoretical results and concluded that $B_J(5960)$ belongs to 2S1$^-$ state. As most of the analysis favors the $2S1^-$ spin parity, thus $B_J(5960)$ is considered to be the radial excited $2S1^-$ state.

And lastly for the $B_J(5840)$ bottom state, two spin parity proposals have been put forward. First one is given by authors in [29], where they suggested it to belong to 2S0$^-$ state. This interpretation matches with the LHCb collaboration results [13]. Second possible J^P is given in [33], where authors suggested the $B_J(5840)$ state to be the member of 1P1$^+$ doublet with $S_l = 1/2$. Because of the ambiguity of various J^P states for $B_J(5840)$, it is motivation for us to look into its properties to assign it a proper position in the bottom meson spectra. In Ref. [29], the J^P for bottom state $B_J(5840)$ has been analysed by predicting the masses and decay widths using non-relativistic quark model and $^3P_0$ model respectively. Whereas the J^P of $B_J(5840)$ in Ref. [33] has been decided just on the basis of theoretically predicted bottom meson masses. In both the references, the models have some unknown parameters, which are fitted by using experimental data's like decay width of bottom state $B_2^*(5747)$ etc. So the accuracy of these predictions cannot be completely justified.

We use HQET as our framework to study the strong interactions among the heavy-light bottom mesons. As we have discussed in previous chapters, HQET has successfully explained the properties of heavy-light hadrons. The effectiveness of this theory lies on the fact that, heavy quark is treated as a dynamical degree of freedom. As a result, number of unknown parameters is greatly reduced by using the heavy quark SU(2N) flavor and spin symmetry.

In this chapter, we predicted J^P using the branching ratio $\frac{B\pi}{B^*\pi}$ which is free from any theoretical parameter, hence the predictions made by HQET are supposed to be more accurate and logical. This chapter is arranged as follows: section II rep-

Table 4.2: Numerical value of the meson masses used in this work [7].

States	B^0	$B^{\pm}$	B^*	B_s	B_s^*
Masses(MeV)	5279.58	5279.25	5325.20	5366.77	5415.40
States	$\pi^{\pm}$	π^0	η	K^+	K^0
Masses(MeV)	139.57	134.97	547.85	493.67	497.61

resents the numerical analysis to confirm the J^P for the bottom state $B_J(5840)$ by studying the branching ratio's with the masses for all the assigned J^P's states. This section also includes the reanalysis of bottom states $B_1(5721)$, $B_2^*(5747)$, $B_{s1}(5830)$, $B_{s2}^*(5840)$ and $B_J(5960)$ for their respective J^P's. In addition to this, we also study the strong decays for the experimentally unobserved but theoretically predicted states $B(2^1S_0)$, $B_s(2^3S_1)$, $B_s(2^1S_0)$, $B(1^1D_2)$, $B_s(1^3D_1)$ and $B_s(1^1D_2)$ in the framework of the HQET. Section III presents the conclusion of our work. The numerical masses of various mesons used in the calculation are listed in Table 4.2.

4.2 Numerical Analysis

To assign a particular J^P to the experimental available states is very important, as the J^P's helps in redeeming many crucial strong interaction properties of the states like their decay widths, masses, branching ratios, hadronic coupling constants etc. The recently observed state $B_J(5840)$ has gone through various theoretical analysis [29, 33] for its strong decay, but a unique J^P is not yet confirmed for it.

In this section, we confirm a particular J^P to the bottom state $B_J(5840)$ recently observed by LHCb. On the basis of the theoretically predicted masses Ref. [29, 33, 37–39], $B_J(5840)$ can be a member of the doublets for radially excited S-wave $2S(0^-, 1^-)$, or for orbitally excited D-wave doublets $1D(1^-, 2^-)$ or $1D(2^-, 3^-)$. These six possible J^P states are tabulated in Table 4.3 with their allowed strong decays to the ground state bottom mesons $1S(0^-, 1^-)$.

To choose the best possible J^P among these, we study the branching ratio

Table 4.3: Strong decay channels for all the six possible spin-parity J^P values for $B_J(5840)$ state. All the values are in MeV.

Decay Mode	$2S0^-$	$2S1^-$	$1D1^-$	$1D2^-_{3/2}$	$1D2^-_{5/2}$	$1D3^-$
$B^0\pi^0$	-	$220.64\widetilde{g}^2_{HH}$	$182.58g^2_{XH}$	-	-	$12.84g^2_{YH}$
$B^+\pi^-$	-	$439.40\widetilde{g}^2_{HH}$	$364.14g^2_{XH}$	-	-	$25.44g^2_{YH}$
$B^0\eta$	-	$12.47\widetilde{g}^2_{HH}$	$11.60g^2_{XH}$	-	-	$0.01g^2_{YH}$
B_sK	-	-	-	-	-	-
$B^*\pi^0$	$523.71\widetilde{g}^2_{HH}$	$347.46\widetilde{g}^2_{HH}$	$61.63g^2_{XH}$	$184.91g^2_{XH}$	$16.98g^2_{YH}$	$9.70g^2_{YH}$
$B^*\pi^+$	$1040.10\widetilde{g}^2_{HH}$	$690.08\widetilde{g}^2_{HH}$	$122.46g^2_{XH}$	$367.39g^2_{XH}$	$33.41g^2_{YH}$	$19.09g^2_{YH}$
$B^*\eta$	-	-	-	-	-	-
B^*_sK	-	-	-	-	-	-
Total	$1563.82\widetilde{g}^2_{HH}$	$1710.09\widetilde{g}^2_{HH}$	$742.43g^2_{XH}$	$552.30g^2_{XH}$	$50.40g^2_{YH}$	$67.09g^2_{YH}$
Ratio R_1	0	0.63	2.96	0	0	1.32

$$BR = R_1 = \frac{\Gamma(B_J(5840) \to B\pi)}{\Gamma(B_J(5840) \to B^*\pi)} \tag{4.7}$$

for all these suggested J^P's. This ratio R_1 is effective in distinguishing these six possible assignments, as this ratio R_1 gives result independent of the coupling constants $\widetilde{g}_{HH}$, g_{XH} and g_{YH}, thus making the predictions model independent. This ratio gives different values for all these six states, thus allowing us to assign a proper J^P for the bottom state $B_J(5840)$.

The calculation of the total decay widths for all these six classifications of $B_J(5840)$ requires the value of the coupling constants $\widetilde{g}_{HH}$, g_{XH} and g_{YH} which are experimentally unknown. Nevertheless, on the basis of the theoretically available values of these couplings, following justification can be provided.

- If $B_J(5840)$ is classified as the one of the member of the doublet $2S(0^-, 1^-)$, then the total decay width for these states comes out to be 150.28 MeV and 165.13 MeV respectively for $2S0^-$ and $2S1^-$. This prediction is made using the theoretical data $\widetilde{g}_{HH} = 0.31$ [41]. Both these decay widths match very well with the experimentally observed broad decay width of 127 MeV for $B_J(5840)$.

Theoretically $2S1^-$ is known to be the suitable J^P for experimental bottom state $B_J(5970)$. And, according to conservation laws, experimental observed decay mode $B^0\pi^+$ is not possible for $2S0^-$. Hence the possibility of these both J^P's $2S0^-$ and $2S1^-$ are excluded.

- If $B_J(5840)$ is the member of the doublet $1\mathrm{D}(1^-, 2^-)$ with $s_l^P = 3/2^-$, then the total strong decay width comes out to be 42.76 MeV and 31.81 MeV for J^P 1^- and 2^- respectively. For this, g_{XH} is taken as 0.24 which is obtained using the charm state $D_1^*(2760)$ information observed by LHCb in 2016 [43]. The 0 R_1 value and the narrow decay width for state $1\mathrm{D}2^-$ also rules out this option for the $B_J(5840)$.

- The last possibility for $B_J(5840)$ can be the member of the doublets $1\mathrm{D}(2^-, 3^-)$. Using the available data for coupling constant $g_{YH} = 0.61$ [41], the total decay widths for J^P states 2^- and 3^- comes out to be 18.75 MeV and 24.96 MeV respectively. Even for such high value of g_{YH}, the decay widths are very narrow. So, the classification of $B_J(5840)$ as member of $1\mathrm{D}(2^-, 3^-)$ is completely ruled out.

The only available option of spin parity for $B_J(5840)$ is $1D(1^-)_{3/2}$. We have also plotted the graphs for the R_1 with their masses for all six possible J^P states, shown in Figure 4.1. It is worth noticing that the Fig. 4(a) shows, the R_1 remains 0 for the entire mass range which depicts that $B\pi$ decay mode is either suppressed or not allowed for J^P's $2S0^-$, $1D_{3/2}2^-$ and $1D_{5/2}2^-$. The graph 4(b), 4(c) and 4(d) shows the variation of R_1 with the masses and give the values of R_1 as 0.63, 2.96 and 1.32 for the J^P states $2S1^-$, $1D1^-$ and $1D3^-$ respectively, corresponding to the $M(B_J(5840)) = 5862.90$ MeV. The values 2.96 for $1D1^-$ and 1.32 for $1D3^-$ point towards the dominancy of $B\pi$ mode, whereas the value 0.63 for the $2S1^-$ directs the dominancy of $B^*\pi$ decay mode.

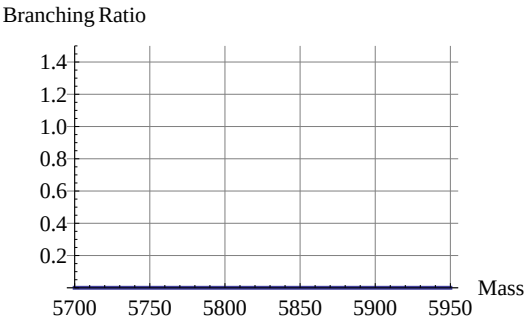

(a) Ratio for $2S(0^-)$, $1D(2^-)_{3/2}$ and $1D(2^-)_{5/2}$ state

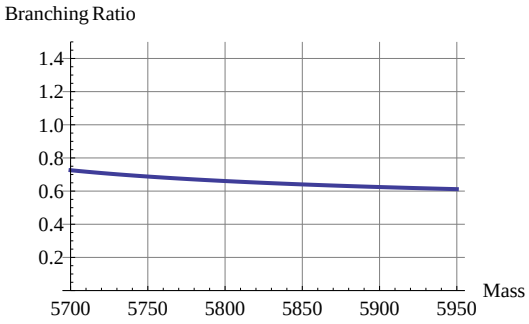

(b) Ratio for $2S(1^-)$ state

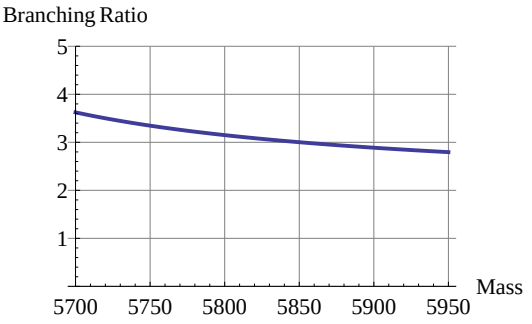

(c) Ratio for $1D(1^-)$ state

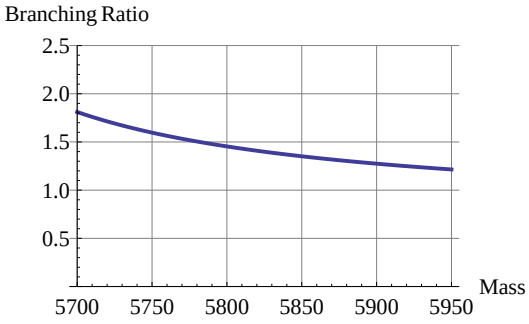

(d) Ratio for $1D(3^-)$ state

Figure 4.1: Branching ratio $\Gamma(B_J(5840)) \to \frac{B\pi}{B^*\pi}$ for all six possible J^P's for $B_J(5840)$ state, where three possible J^P's are shown in the same Fig 4.1a

It is interesting to notice that, the ratio R_1 of $B_J(5840)$ for J^P state $1D(1^-)_{3/2}$ also comes out to be maximum with value of 2.96, thus favoring $1D(1^-)_{3/2}$ as the most favorable J^P for $B_J(5840)$.

However, if we consider the fact that photon from the $B^* \to B\gamma$ is too low in energy to be detected and B^* mesons are partially reconstructed as B mesons. Then the J^P option for $B_J(5840)$ belonging to $2S0^-$ cannot be fully ignored because of its large decay width. The identification of $B_J(5840)$ as $2S0^-$ is also supported by the work in [13, 29]. So, in future one may expect that, experimental information about the decay modes for $B_J(5840)$ broadens up, to clearly identify the exact J^P for this state. As LHCb experiment observed only $B^0\pi^+$, so in this chapter, we expect $B_J(5840)$ to belong to $1D(1^-)_{3/2}$ J value.

4.2.1 Prediction of Spin and Strange partners for $B_J(5840)$

On the basis of the spin parity assignment of $B_J(5840)$, it is interesting to look for some features of its spin and strange partners. As discussed, $B_J(5840)$ is assigned as the orbitally excited D-wave state with J^P as $1\mathrm{D}1^-$. Using the Eq.(2.54), the complete picture of the partial decay widths for $B(1^1D_2)$, $B_s(1^3D_1)$ and $B_s(1^1D_2)$ being the spin and strange partners of $B_J(5840)$ state are listed in Table 4.4. Along with the partial decay widths, table also shows the branching ratio $\widehat{\mathbf{\Gamma}} = \frac{\Gamma}{\Gamma(B_J(5840)\to B^{*+}\pi^-)}$ for non strange states, ratio $\widehat{\mathbf{\Gamma}} = \frac{\Gamma}{\Gamma(B^*_{sJ}\to B^{*0}K^+)}$ for strange states and branching fractions for all the mentioned decay modes. Apart from the decay channels mentioned in this table, $B_J(5840)$ being $1D(1^-)$ also decays to $1P(1^+)$, $1P^{'}(1^+)$ and $1P(2^+)$ states along with pseudoscalar mesons (π, η, K). Since these decays occur via D-wave, so their contribution is relatively suppressed. Here, we mentioned only the dominant decay modes of $B_J(5840)$, with which total decay width comes out to be $742.43 g^2_{XH}$.

The information in the Table 4.4 reveals that, for $B_J(5840)$ state $B^+\pi^-$ and $B^0\pi^0$ are the main decay modes as compared to the $B^{*+}\pi^-$ and $B^{*0}\pi^0$ mode. The experimental decay width information of $B_J(5840)$ gives coupling constant g_{XH} to be

$$g_{XH} = 0.41 \pm 0.02. \tag{4.8}$$

This information can be a beneficial in finding total and the partial decay widths of unobserved highly excited 1D-wave bottom states.

Theoretically, mass of the spin partner of $B_J(5840)$ i.e. $B(1^1D_2)$ is obtained as 5967.20±30 MeV from Ref. [26,29,33,37–39]. Column 5 of the table gives the ratio of the partial decay widths for $B(1^1D_2)$ decaying to various channels to its decay width of $B^{*-}\pi^+$. Apart from the decay channels ($B^*\pi^0$, $B^*\eta$, B_s^*K) listed in this table, $B(1^1D_2)$ also decays to P-wave bottom meson states $1P(0^+)$, $1P(1^+)$, $1P^{'}(1^+)$ and $1P(2^+)$ which occurs via D-wave, and thus due to the small phase space, these decay modes are suppressed when compared with its decay to ground state S-wave mesons and hence are not shown in Table 4.4. From the listed decay channels, $B^{*-}\pi^+$ comes out to be the dominant decay mode for $B(1^1D_2)$ with branching fraction 60.34%. Hence, the decay mode $B^{*-}\pi^+$ can be a motivation for the experimental search for the missing bottom state $B(1^1D_2)$. Using the value of the coupling constant g_{XH} obtained from Eq.(4.8), total decay width of the bottom state $B(1^1D_2)$ is obtained as 241.33 MeV. This value is in same range as given in Ref. [29] with 3.87 % deviation. Masses for the strange partners of these bottom states are taken as 6083.06 MeV and 6057.50 MeV from the theoretical work [29, 33, 37–39]. Strange bottom states decaying to decay modes represented by "†" in Tables 4.4, 4.5, 4.6 are the isospin violating processes, so the final decay widths are multiplied by suppression factor ϵ^2. This suppression factor ϵ results from the $\pi^0 - \eta$ mixing [25] defined as $\epsilon =$

Table 4.4: Strong decay width of newly observed bottom mesons $B_J^*(5840)$ and its spin and strange partners $B(1^1D_2)$, $B_s(1^1D_2)$ and $B_s^*(1^3D_1)$. Ratio in 5^{th} column represents the $\widehat{\mathbf{\Gamma}} = \frac{\Gamma}{\Gamma(B_J^{(*)} \to B^{*+}\pi^-)}$ for the non-strange mesons and $\widehat{\mathbf{\Gamma}} = \frac{\Gamma}{\Gamma(B_{sJ}^* \to B^{*0}K^+)}$ for the strange mesons. Branching fraction (B.R) gives the percentage of the partial decay width with respect to the total decay width. † represents the isospin violating processes.

State	nLs_lJ^P	Decay channel	Decay Width (MeV)	Ratio	B.F %	Compared value (MeV)
$B_J(5840)$	$1D_{3/2}1^-$	$B^*\pi^+$	$122.46g_{XH}^2$	1	16.49	
		$B^*\pi^0$	$61.63g_{XH}^2$	0.50	8.30	
		$B^0\pi^0$	$182.58g_{XH}^2$	1.49	24.59	
		$B^+\pi^-$	$364.14g_{XH}^2$	2.97	49.04	
		$B^0\eta$	11.60	0.09	1.56	
		Total	$742.43g_{XH}^2$			127.40 Ref.[1]
$B_J(5967)$	$1D_{3/2}2^-$	$B^*\pi^+$	$866.42g_{XH}^2$	1	60.34	
		$B^*\pi^0$	$435.16g_{XH}^2$	0.50	30.31	
		$B^*\eta$	$94.61g_{XH}^2$	0.10	6.58	
		B_s^*K	$39.42g_{XH}^2$	0.04	2.74	
		Total	$1435.69g_{XH}^2$			250.69 Ref.[2]
$B_{sJ}(6083)$	$1D_{s(3/2)}1^-$	$^\dagger B_s^*\pi^0$	$0.01g_{XH}^2$	-	-	
		$B_s^*\eta$	$12.39g_{XH}^2$	0.04	0.50	
		$B^{*0}K^0$	$300.48g_{XH}^2$	0.98	12.30	
		$B^{*-}K^+$	$305.62g_{XH}^2$	1	12.51	
		$^\dagger B_s^0\pi^0$	$0.04g_{XH}^2$	-	-	
		$B_s\eta$	$49.01g_{XH}^2$	0.16	2.00	
		B^+K^-	$894.37g_{XH}^2$	2.92	36.62	
		B^0K^0	$879.81g_{XH}^2$	2.87	36.03	
		Total	$2441.72g_{XH}^2$			213.38 Ref.[2]
$B_{sJ}(6057)$	$1D_{s(3/2)}2^-$	$^\dagger B_s^*\pi^0$	$0.04g_{XH}^2$	-	-	
		$B_s^*\eta$	$23.62g_{XH}^2$	0.03	1.61	
		$B^{*-}K^+$	$724.42g_{XH}^2$	1	49.66	
		$B^{*0}K^0$	$710.60g_{XH}^2$	0.98	48.71	
		Total	$1458.66g_{XH}^2$			198.64 Ref.[2]

$\frac{\sqrt{3}}{4}\frac{m_d-m_u}{m_s-(m_u+m_d)/2} = 1.00 \times 10^{-2}$.

Referring to the branching fractions in Table 4.4, B^+K^0 and $B^{*-}K^+$ seems to be the dominant decay modes with contribution 36.62% and 49.66% for strange states B^*_{s1} and B_{s2} respectively. These states also allow decays to P-wave bottom mesons, but are relatively suppressed. Hence the total decay width for these strange state comes out to be

$$\Gamma(B^*_{s1}) = 410.45 MeV. \tag{4.9}$$

$$\Gamma(B_{s2}) = 245.20 MeV. \tag{4.10}$$

The result concludes, B^*_{s1} to be a broader state as compared to its spin partner B_{s2}.

Moreover, if we use the coupling $g_{XH} = 0.45$ obtained in Ref. [42], the decay widths for states $B(1^1D_2), B_s(1^3D_1)$ and $B_s(1^1D_2)$ deviate from our results by 16%. Theoretically, this coupling values are also obtained as 0.45 [42], 0.53 [44] and 0.19 [30] from the charm states $D_{sJ}(2860), D_J(2600)$ and bottom state $B_J(5960)$ assuming them to be in $1D1^-$ state. As the $D_J(2600)$ and $B_J(5960)$ belong to $2S1^-$, so the last two values of coupling $g_{XH} = 0.53$ and 0.19 predicted from $D_J(2600)$ and $B_J(5960)$ are not useful for our study.

4.2.2 Analysis for bottom states $B_1(5721)$, $B^*_2(5747)$, $B_{s1}(5830)$ and $B^*_{s2}(5840)$

We also analyze the bottom states $B_1(5721)$, $B^*_2(5747)$, $B_{s1}(5830)$ and $B^*_{s2}(5840)$ for their J^P's. On the basis of their available theoretical and experimental information, $B_1(5721)$, $B^*_2(5747)$, $B_{s1}(5830)$ and $B^*_{s2}(5840)$ are identified as the P- wave bottom mesons with $S_l = 3/2$.

$$(B_1(5721), B_2^*(5747)) = (1^+, 2^+)_{3/2} \text{with } n = 1, L = 1. \tag{4.11}$$

$$(B_{s1}(5830), B_{s2}^*(5840)) = (1^+, 2^+)_{3/2} \text{with } n = 1, L = 1. \tag{4.12}$$

We study their strong decay widths and calculated various branching ratios involved. Using Eq.(2.53), the numerical value of the partial decay widths for bottom states $B_1(5721)$, $B_2^*(5747)$, $B_{s1}(5830)$ and $B_{s2}^*(5840)$ are given in Table 4.5. The obtained decay widths are then compared with the experimental data to obtain the strong coupling constant g_{TH}. Since the strange states $B_{s1}(5830)$ and $B_{s2}^*(5840)$ are very narrow, we exclude them to calculate the coupling constant g_{TH}. g_{TH} comes out to be 0.50 ± 0.01 and 0.37 ± 0.01 for bottom states $B_1(5721)$ and $B_2^*(5747)$ respectively. This is consistent with other theoretical values of g_{TH} in Ref. [41], [30], [40] (mentioned in Table 3.5) obtained from charm mesons. Here, the consistency in the hadronic coupling constant g_{TH} beautifully describes the heavy quark symmetry for the charm and the bottom mesons. Even if we include the above strange states, the change in the coupling value is negligible. We also obtained the ratios R_2, R_3 and R_4 as

$$R_2 = \frac{\Gamma(B_1(5721))}{\Gamma(B_1(5721)) + \Gamma(B_2^*(5747))} = 0.60 \tag{4.13}$$

$$R_3 = \frac{\Gamma(B_2^* \to B^*\pi)}{(\Gamma(B_2^* \to B^*\pi) + \Gamma(B_2^* \to B\pi))} = 0.46 \tag{4.14}$$

$$R_4 = B_2^*(5747) \to \frac{B^{*+}\pi^-}{B^+\pi^-} = 0.85 \tag{4.15}$$

which are consistent with their experimental value of $R_2 = 0.47 \pm 0.06$ and $R_3 = 0.47 \pm 0.09$ observed by D$\emptyset$ collaboration [12] and $R_4 = 0.71 \pm 0.14$ measured by LHCb [13]. Table 4.5 also shows the decay widths of the strange bottom states

Table 4.5: Strong decay width of newly observed bottom mesons $B_1(5721)$ and $B_2^*(5747)$ and their strange partners $B_{s1}(5830)$ and $B_{s2}^*(5840)$. Ratio in 5^{th} column represents the $\widehat{\mathbf{\Gamma}} = \frac{\Gamma}{\Gamma(B_J^{(*)} \to B^{*+}\pi^-)}$ for the non-strange mesons and $\widehat{\mathbf{\Gamma}} = \frac{\Gamma}{\Gamma(B_{sJ}^* \to B^{*0}K^+)}$ for the strange mesons. Branching fraction (B.F) gives the percentage of the partial decay width with respect to the total decay width. Decay width marked as "-" represents very small, but non zero contribution.

State	nLs_lJ^P	Decay channel	Decay Width (MeV)	Ratio	B.F %	Experimental value(MeV)
$B_1(5721)$	$1P_{3/2}1^+$	$B^*\pi^+$	$74.83g_{TH}^2$	1	66.16	
		$B^*\pi^0$	$38.25g_{TH}^2$	0.51	33.82	
		Total	$113.09g_{TH}^2$			30.1 Ref.[1]
$B_2^*(5747)$	$1P_{3/2}2^+$	$B^*\pi^+$	$52.47g_{TH}^2$	1	30.65	
		$B^*\pi^0$	$26.78g_{TH}^2$	0.51	15.64	
		$B^0\pi^0$	$30.91g_{TH}^2$	0.58	18.05	
		$B^+\pi^-$	$61.02g_{TH}^2$	1.16	35.64	
		Total	$171.18g_{TH}^2$			24.5 Ref.[1]
$B_{s1}(5830)$	$1P_{s3/2}1^+$	$B^{*+}K^0$	–	-	-	
		$B^{*-}K^+$	–	-	-	
		Total	-			0.5 Ref.[3]
$B_{s2}^*(5840)$	$1P_{s3/2}2^+$	$B^{*+}K^0$	$0.20g_{TH}^2$	0.59	2.18	
		$B^{*-}K^+$	$0.34g_{TH}^2$	1	3.71	
		B^+K^-	$3.97g_{TH}^2$	11.40	43.38	
		B^0K^0	$4.64g_{TH}^2$	13.33	50.71	
		Total	$9.15g_{TH}^2$			1.40 Ref.[3]

$B_{s1}(5830)$ and $B^*_{s2}(5840)$. Decay widths marked as "-" for $B_{s1}(5830)$ state decaying to $B^{*+}K^-$ and $B^{*-}K^0$ has very small contribution of the order of 10^{-10} MeV. The suppression factor $\epsilon^2 = 1 \times 10^{-4}$ neglects the contribution of decay modes $B^*_s\pi^0$ and $B_s\pi^0$ for these strange bottom states. Thus, negligible values of the decay widths for $B_{s1}(5830)$ state is consistent with its very small decay width 0.5 MeV measured by CDF collaboration [15] in 2014. Table 4.5 reveals that $B^{*+}\pi^-$ and $B^+\pi^-$ are main decay modes for $B_1(5721)$ and $B^*_2(5747)$ with branching fraction 66.16% and 35.64% respectively. Similarly, B^0K^0 is observed to be the dominant decay mode for strange state $B^*_{s2}(5840)$.

4.2.3 Prediction of Spin and Strange partners for $B_J(5970)$

Now, we will proceed in the similar manner to study the spin and strange partners for bottom state $B_J(5970)$. As we have discussed, $B_J(5970)$ is fitted to be the radially excited state with J^P 1^-. Table 4.6 shows the partial decay widths for $B_J(5970)$ along with its spin and strange partners $B(2^1S_0)$, $B_s(2^3S_1)$ and $B_s(2^1S_0)$. Along with the partial decay widths, table also shows the branching ratio $\widehat{\mathbf{\Gamma}} = \frac{\Gamma}{\Gamma(B_J^{(*)} \to B^{*+}\pi^-)}$ and $\widehat{\mathbf{\Gamma}} = \frac{\Gamma}{\Gamma(B^*_{sJ} \to B^{*0}K^+)}$ for the non-strange and strange states $B(2^1S_0)$, $B(2^3S_1)$ and $B_s(2^3S_1)$, $B_s(2^1S_0)$ respectively.

From the experimental decay widths of $B_J(5970)$, we obtain the strong coupling constant $\widetilde{g}_{HH}$ as

$$\widetilde{g}_{HH} = 0.15 \pm 0.01. \tag{4.16}$$

Using HQET, this coupling constant $\widetilde{g}_{HH}$ is also predicted as 0.14 [30], 0.31 [41], 0.28 [23] and 0.40 [44]. The first value is obtained from bottom state $B_J(5960)$ and other three values are obtained from the charm state sector by assuming the charm

Table 4.6: Strong decay width of bottom meson $B_J(5970)$ with its spin and strange partners $B(2^1S_0)$, $B_s(2^1S_0)$ and $B_s(2^3S_1)$. Ratio in 5^{th} column represents the $\widehat{\mathbf{\Gamma}} = \frac{\Gamma}{\Gamma(B_J^{(*)} \to B^{*+}\pi^-)}$ for the non-strange mesons and $\widehat{\mathbf{\Gamma}} = \frac{\Gamma}{\Gamma(B_{sJ}^* \to B^{*0}K^+)}$ for the strange mesons. Branching fraction (B.F) gives the percentage of the partial decay width with respect to the total decay width. † represents the isospin violating processes.

State	nLs_lJ^P	Decay channel	Decay Width (MeV)	Ratio	B.F %	Compared value (MeV)
$B_0(5881)$	$2^1S_0 0^-$	$B^*\pi^+$	$1148.08\widetilde{g}_{HH}^2$	1	66.48	
		$B^*\pi^0$	$577.80\widetilde{g}_{HH}^2$	0.50	33.27	
		$B^*\eta$	$1.00\widetilde{g}_{HH}^2$	0.00	0.05	
		B_s^*K	-	-	-	
		Total	$1726.89\widetilde{g}_{HH}^2$			-
$B_J(5970)$	$2^3S_1 1^-$	$B^*\pi^+$	$1178.23\widetilde{g}_{HH}^2$	1	36.30	
		$B^*\pi^0$	$591.95\widetilde{g}_{HH}^2$	0.50	18.23	
		$B^*\eta$	$122.22\widetilde{g}_{HH}^2$	0.10	3.76	
		B_s^*K	$69.94\widetilde{g}_{HH}^2$	0.05	2.15	
		$B^0\pi^0$	$359.11\widetilde{g}_{HH}^2$	0.30	11.06	
		$B^+\pi^-$	$716.21\widetilde{g}_{HH}^2$	0.60	22.06	
		$B^0\eta$	$113.37\widetilde{g}_{HH}^2$	0.09	3.49	
		B_sK	$94.43\widetilde{g}_{HH}^2$	0.08	2.90	
		Total	$3245.49\widetilde{g}_{HH}^2$			82.30 Ref.[1]
$B_{s0}(5976.0)$	$(2^1S_0)0^-$	$B^{*0}K^0$	$521.96\widetilde{g}_{HH}^2$	0.96	47.48	
		$B^{*+}K^-$	$539.41\widetilde{g}_{HH}^2$	1	49.07	
		$^\dagger B_s^*\pi^0$	$0.05\widetilde{g}_{HH}^2$	-	-	
		$B_s^*\eta$	$7.85\widetilde{g}_{HH}^2$	0.01	0.71	
		Total	$1099.25\widetilde{g}_{HH}^2$			75.80 Ref.[4]
$B_s^*(6007.8)$	$2^3S_1 1^-$	B^0K^0	$342.71\widetilde{g}_{HH}^2$	0.97	24.48	
		B^+K^-	$350.66\widetilde{g}_{HH}^2$	1	25.05	
		$^\dagger B_s\pi^0$	$0.02\widetilde{g}_{HH}^2$	-	-	
		$B_s\eta$	$58.29\widetilde{g}_{HH}^2$	0.16	4.16	
		$B^{*0}K^0$	$474.96\widetilde{g}_{HH}^2$	1.35	33.93	
		$B^{*+}K^-$	$486.47\widetilde{g}_{HH}^2$	1.38	34.76	
		$^\dagger B_s^*\pi^0$	$0.04\widetilde{g}_{HH}^2$	-	-	
		$B_s^*\eta$	$36.98\widetilde{g}_{HH}^2$	0.10	2.64	
		Total	$1399.45\widetilde{g}_{HH}^2$			114.0 Ref.[4]

states to be in $2S0^-$ state.

From the listed decay channels mentioned in Table 4.6, $B^{*-}\pi^+$ comes out to be the dominant decay mode for $B_J(5970)$ and its spin partner $B(2^1S_0)$ with branching fraction 36.30% and 66.48% respectively.

Apart from the decay channels listed in table, we also find their partial decays to $1P(0^+)$, $1P(2^+)$, $1D(1^-)$ and $1D(3^-)$ states, but due to the small phase space, these decay modes are suppressed and are not considered in this work. For their strange partners, we observe $B^{*+}K^-$ as the dominant decay mode for B^*_{s1} and B_{s0} bottom states. Thus, this decay mode is suitable for the experimental search for these missing radially excited strange bottom mesons B^*_{s1} and B_{s0}. Using the result in Eq.(4.16), their total decay widths corresponding to the mass $M(B_0) = 5881.00$ MeV, $M(B^*_{s1}) = 6007.80$ MeV and $M(B_{s0}) = 5976.00$ MeV [27, 29, 33, 37–39] are obtained as

$$\Gamma(B_0) = 38.85 MeV \tag{4.17}$$

$$\Gamma(B^*_{s1}) = 31.48 MeV \tag{4.18}$$

$$\Gamma(B_{s0}) = 24.73 MeV \tag{4.19}$$

This shows that the strange partners follow the same pattern as the non-strange bottom states. B^*_{s1} state is seen to be broader as compared to its spin partner B_{s0}. From the other theoretically available values of $\widetilde{g}_{HH}$, the upper most value is 0.40, predicted from charm states [44]. The decay rates of these states obtained using this higher coupling deviates a lot from results in Eqs.(4.17-4.19). For example, width of B_0 changes to 254 MeV from 38 MeV. However, if we use the coupling value $\widetilde{g}_{HH} = 0.14$ [30] obtained from bottom sector, it give decay widths as 33.84 MeV, 21.54 MeV, 27.42 MeV for states $B(2^1S_0), B_s(2^1S_0), B_s(2^3S_1)$, which deviates by 12% from our results. If we look at the leading order terms of coupling constants, it will remain same for both charm and bottom sectors. It may vary if we go for

corrections upto $1/m_Q$ order. Coupling constant calculated from the experimental charm information may vary the theoretically predicted bottom results.

4.3 Conclusion

In the present chapter, we have used the effective chiral lagrangian, and studied the two body strong decay behavior of bottom mesons with the emission of light pseudo-scalar mesons (π, η, K). In particular, we have identified the six possible spin parity assignments for $B_J(5840)$ state, observed by LHCb in 2015 [13]. We have analyzed the total decay widths and branching ratio (R_1) $\frac{B\pi}{B^*\pi}$ for all these six assignments in Table 4.3 and concluded that, the most favorable J^P value for $B_J(5840)$ state is $1D1^-$, but the assignment $2S0^-$ cannot be fully ignored. The ratio R_1 has very different value for $B_J(5840)$ belonging to these two J^P's, so experimental measurement of such ratio in the future will be very helpful in clearly identifying one of them to be the most favorable J^P for $B_J(5840)$.

We have also obtained coupling constants g_{XH}, $\widetilde{g}_{HH}$ and g_{TH} governing the strong decays of bottom states through the light pseudo-scalar mesons. These obtained couplings allowed us to compute the strong decay widths of the experimentally missing bottom states $B(2^1S_0)$, $B_s(2^3S_1)$, $B_s(2^1S_0)$, $B(1^1D_2)$, $B_s(1^3D_1)$ and $B_s(1^1D_2)$ states. Along with this, we examine the recently observed bottom state $B_J(5721)$ and $B_2^*(5747)$ and their strange partners $B_{sJ}(5830)$ and $B_{s2}^*(5840)$ for their J^P's as $1P_{3/2}1^+$ and $1P_{3/2}2^+$ respectively. Thus, these predictions have opened a window to investigate the higher excitations of bottom mesons at the LHCb, D$\emptyset$, CDF.

In this chapter, we have analyzed the $1P_{3/2}$, $1D_{3/2}$ and $2S_{1/2}$ bottom doublets, the other higher excited bottom doublets $1D_{5/2}$, $1F_{5/2}$, $2S_{1/2}$, $2P_{1/2}$ and $2P_{3/2}$ are discussed in the next chapter.

Bibliography

[1] R. Aaij et al. [LHCb collaboration], Phys. Rev. D **94**, 072001 (2016).

[2] R. Aaij et al. [LHCb collaboration], J. High Energ. Phys. **2013** 145.

[3] P. del Amo Sanchez et al. [BaBar collaboration], Phys. Rev. D **82**, 111101 (2010).

[4] R. Aaij et al. [LHCb collaboration], Phys. Rev. Lett. **113**, 162001 (2014).

[5] R. Aaij et al. [LHCb collaboration], Phys. Rev. D **90**, 072003 (2014).

[6] B. Aubert et al. [BaBar collaboration], Phys. Rev. D **80**, 092003 (2009).

[7] M. Tanabashi et al. [Particle Data Group Collaboration], Phys. Rev. D **98** 030001(2018).

[8] S. Behrends, et al., [CLEO Collaboration], Phys. Rev. Lett. **50** 881884 (1983).

[9] K. Han, et al., Phys. Rev. Lett. **55** 36 (1985).

[10] J. Lee-Franzini, U. Heintz et al., Phys. Rev. Lett. **65** 29472950 (1990).

[11] R. Akers et al. [OPAL Collaboration], Z. Phys. C **66**, 19 (1995).

[12] V. M. Abazov et al. [DØ Collaboration], Phys. Rev. Lett. **99** 172001 (2007).

[13] R. Aaij et al. [LHCb Collaboration], J. High Energ. Phys. **04**, 024 (2015).

[14] T. Aaltonen et al. [CDF Collaboration], Phys. Rev. Lett. **102** 102003 (2009).

[15] T. A. Aaltonen et al. [CDF Collaboration],Phys. Rev. D **90**, 012013 (2014).

[16] T. Aaltonen, et al., [CDF Collaboration], Phys. Rev.Lett. **100** 082001 (2008).

[17] R. Aaij, et al., [LHCb Collaboration], Phys. Rev. Lett. **110** 151803 (2013).

[18] V. M. Abazov, et al., [D0 Collaboration], Phys. Rev. Lett. **100** 082002 (2008).

[19] S. Godfrey and N. Isgur,Phys. Rev. D **32**, 189 (1985).

[20] D. Ebert, R. N. Faustov and V. O. Galkin, Eur. Phys. J. C **66**, 197 (2010).

[21] L. Y. Xiao and X. H. Zhong, Phys. Rev. D **90**, 074029 (2014).

[22] Z. G. Luo, X. L. Chen and X. Liu, Phys. Rev. D **79**, 074020 (2009).

[23] P. Colangelo et. al., Phys. Rev. D **86**, 054024 (2012).

[24] P. Gelhausen, A. Khodjamirian et al., Eur. Phys. J. C **74**, 2979 (2014).

[25] T. Matsuki and K. Seo, Phys. Rev. D **85** 014036 (2012).

[26] T. Matsuki et al., Prog. Theor. Phys. **117** 1077 (2007).

[27] T. Matsuki et al., Eur. Phys. J. A **31** 701 (2007).

[28] X.-H. Zhong, Q. Zhao, Phys. Rev.D **78** 014029 (2008) .

[29] Q.-F. Lu, T.-T. Pan et al., Phys. Rev. D **94** 074012 (2016).

[30] Z.-G. Wang, Eur. Phys. J. Plus **129** 186 (2014) .

[31] Y. Sun, Q.-T. Song et al., Phys. Rev. D **89** 054026 (2014).

[32] S. Godfrey, K. Moats, E. S. Swanson, Phys. Rev. D **94** 054025 (2016).

[33] Jing-Bin Liu, Cai-Dian Lu, Eur. Phys. J. C **77** 312 (2017).

[34] H. Xu. et. al., Phys. Rev. D **89** 097502 (2014).

[35] Hua-Xing Chen et. al., Rept. Prog. Phys. **80** 076201 (2017).

[36] Gupta P., Upadhyay A. Eur. Phys. J. A **54** 160 (2018).

[37] J. Zeng, J. W. Van Orden and W. Roberts, Phys. Rev. D **52**, 5229 (1995).

[38] M. Di Pierro and E. Eichten, Phys. Rev. D **64**, 114004 (2001).

[39] T. A. Lahde, C. J. Nyfalt and D. O. Riska, Nucl. Phys. A **674**, 141 (2000).

[40] Z. G. Wang, Phys. Rev. D **88**, 114003 (2013).

[41] P.Gupta and A. Upadhyay, Phys. Rev. D **97**, 014015 (2018).

[42] P. Colangelo, F. De Fazio and S. Nicotri, Phys. Lett. B **642** 48-52 (2006).

[43] R. Aaij, et al., [LHCb Collaboration],Phys. Rev. D **91** 092002 (2015), [Erratum: Phys. Rev. D **93**, 119901 (2016)].

[44] M. Batra, A. Upadhayay, Eur.Phys. J. C **75**, 319 (2015).

[45] T. Matsuki and K. Seo, Prog. Theor. Phys. **118**, 1087 (2007).

Chapter 5

Masses and Strong Decays of Bottom states $B(2S)$, $B(2P)$, $B(1D)_{5/2}$ and $B(1F)_{5/2}$ Doublets

5.1 Introduction

From the previous two chapters, it is observed that, the heavy-light mesons ($Q\overline{q}$) which contain heavy quark Q and light anti-quark $\overline{q}$ have received considerable experimental and theoretical attention due to the existence of heavy quark and chiral symmetry. The study of heavy light mesons provide a better understanding of non-perturbative quantum chromodynamics (QCD). Many new discoveries have filled the charm and bottom meson spectroscopy. The ground state charm mesons such as $D(1S)$, $D(1P)$, $D_s(1S)$ and $D_s(1P)$ are well established and are listed in particle data group [1]. New candidates for higher radial and orbital excitations in the charm spectra include newly observed mesons like $D_0(2560)$, $D_1^*(2680)$, $D_2(2740)$, $D_3^*(2760)$, $D_J(3000)$, $D_2^*(3000)$ and $D_J^*(3000)$ and strange states $D_{s1}(2860)$, $D_{s3}(2860)$ and $D_s(3040)$ [2–6]. The properties of these charm states have been discussed in chapter 3 of this thesis.

Observing the bottom spectroscopy in chapter 4, it is realized that unlike the success

in charm sector, experimental information on higher excited bottom states is scare. Till now, only ground state bottom mesons for $B(1S)$ and excited P-wave mesons $B(1P)$ with $S_l = 3/2$ along with their strange partners are experimentally available [8–12]. Recently in 2015, LHCb has observed new bottom mesons, which have diverted theorists interest towards the bottom sector. LHCb collaboration studied $B^+\pi^-$ and $B^0\pi^-$ mass distributions by analyzing the p-p collisions at center-of-mass energies of 7 and 8 TeV and observed four bottom states $B_1(5721)$, $B_2^*(5747)$, $B_J(5840)^{0,+}$ and $B_J(5960)^{0,+}$ [13]. The results for $B_J(5960)^{0,+}$ are reported as : $M = 5969.20 \pm 2.9 \pm 5.1$ MeV and decay width $\Gamma = 82.3 \pm 7.7 \pm 9.4$ MeV. Also in 2013, the CDF collaboration studied the $B^0\pi^+$ and $B^+\pi^-$ mass distributions and have observed neutral bottom state $B_J^0(5970)$ with mass $M = 5978 \pm 5 \pm 12$ MeV and decay width $\Gamma = 70^{+30}_{-20} \pm 30$ MeV [14]. Since, this resonance decays in $B\pi$ final state, this state is supposed to have a natural spin parity state. The properties of $B_J(5970)$ state observed by CDF collaboration are consistent with $B_J(5960)$ state observed by LHCb collaboration, so they are assumed to be the same state. Theoretically, these states are studied by using various models like relativistic quark model [15], effective Lagrangian approach [16], quark model [17] etc. Being the fact that, $B(5960)$ decays to $B\pi$ final states and its mass being close to the mass of 2^3S_1 state given in Ref's [18–20], this state is considered to belong to n=2, with $J^P = 1^-$ S-wave state in the bottom spectroscopy. $B_1(5721)$ and $B_2^*(5747)$ are observed to belong to the bottom states $B(1^1P_1(1^+))$ and $B(1^3P_2(2^+))$ respectively. Beside these recently observed states, the information on other higher orbital and radial excited bottom states is still unknown. All these experimentally observed states $B_1(5721)$, $B_2^*(5747)$, $B_{1s}(5830)$, $B_{2s}^*(5840)$, $B_J(5840)$ and $B_J(5960)$ filling the J^P states $1P_{3/2}$, $1D_{3/2}$ and $2H_{1/2}$ have been studied in chapter 4.

Now, to complete the bottom spectra, we aim on predicting the properties of experimentally missing higher excited bottom states $B(1D)_{5/2}$, $B(1F)_{5/2}$ and radially excited $B(2S)$, $B(2P)$ states with their strange partners. This prediction will be

useful for both finding and understanding these excited bottom mesons in future. We will enlighten some of the properties like masses, strong decay widths, branching ratios, branching fractions, strong coupling constants for these radial excited bottom states. For this, we use HQET discussed in chapter 2, as our framework that includes $SU(2N_f)$ heavy quark spin-flavor symmetries.

In the heavy quark limit, we expect that the mass splittings between different doublets and the partial decay widths are independent of heavy quark flavor [21]. The flavor symmetry implies that the spin averaged mass splittings between the higher states and the ground state i.e. Δ_F and the mass splittings between the spin partners of the doublets i.e. λ_F are flavor independent i.e. $\Delta_F^{(b)} = \Delta_F^{(c)}$ and $\lambda_F^{(b)} = \lambda_F^{(c)}$. We apply this heavy quark symmetry on the experimental available data for n=1 and n=2 charm mesons to predict the properties of the corresponding bottom meson spectroscopy. We provide the mass spectra and strong decays for the bottom sector that will not only help in identifying the recent observed experimental bottom mesons, but will also help in validating the authenticity of the HQET model. This chapter is organized as follows: Section 2 gives the brief review of the heavy quark symmetry parameters and the possible QCD and $1/m_Q$ correction's to them. Section 3 represents the numerical analysis, where we have calculated the masses based on the heavy quark symmetry and the corrections involved for the bottom states $B(2S)$, $B(2P)$, $B_s(2S)$, $B_s(2P)$, $B(1D)_{5/2}$ and $B(1F)_{5/2}$. Next, we use these calculated masses as an application, to predict the strong decay widths in terms of their couplings. Section 4 presents the conclusion of our work.

5.2 Masses of heavy-light mesons in HQET

In HQET, spin and parity of the heavy quark decouples from the light degrees of freedom as they interact through the exchange of soft gluons only. As discussed in chapter 2, HQET is developed by expanding the QCD lagrangian in power of $1/m_Q$, in which heavy quark symmetry breaking terms are studied order by order.

Applying finite heavy quark mass corrections, HQET lagrangian to order of $1/m_Q$ is

$$\mathcal{L} = \overline{H}_v(iv.D)H_v + \overline{H}_v\frac{(iD_\perp)^2}{2m_Q}H_v + \overline{H}_v\frac{g\sigma_{\mu\nu}G^{\mu\nu}}{4m_Q}H_v + \mathrm{O}(\frac{1}{m_Q^2}). \tag{5.1}$$

Where, $D_\perp^\mu = D^\mu - v^\mu v.D$ is orthogonal to heavy quark velocity v, and $G^{\mu\nu} = T_a G_a^{\mu\nu} = \frac{i}{g_s}[D^\mu, D^\nu]$ is the gluon field strength tensor. In the limit $m_Q \to \infty$, only first term H_0 i.e. $\overline{h}(iv.D)h$ survives. The second term $D_\perp^2$ is arising from the off shell residual momentum of the heavy quark in the non relativistic model and it represents the heavy quark kinetic energy $\frac{p_Q^2}{2m_Q}$ [24]. This term breaks the flavor symmetry because of the explicit dependence on m_Q, but does not break the spin symmetry of the HQET. The third term in the above equation i.e. $g\sigma_{\mu\nu}G^{\mu\nu}$ represents the magnetic moment interaction coupling of the heavy quark spin to the gluon field. This term breaks both the flavor and spin symmetry and is known as chromo-magnetic term.

When the hadron state $|H^{(Q)}\rangle$ is applied at the leading order operator H_0 of the lagrangian in Eq.(5.1), hadron mass gets the contribution as

$$\overline{\Lambda} \equiv \frac{1}{2}\langle H^{(Q)} \mid H_0 \mid H^{(Q)}\rangle \tag{5.2}$$

At $1/m_Q$ order, hadron masses gets additional contribution from the expectation values of the higher terms of lagrangian 5.1. The matrix elements of the $1/m_Q$ order are represented in terms of two non-perturbative parameters λ_1 and λ_2 as

$$2\lambda_1 = \langle H_Q|\overline{Q}(iD_\perp)^2 Q|H_Q\rangle \tag{5.3}$$

$$16(S_Q.S_l)\lambda_2(m_Q) = \alpha(\mu)\langle H_Q|\overline{Q}\sigma.GQ|H_Q\rangle. \tag{5.4}$$

Therefore, mass of heavy-light meson to the first order of $1/m_Q$ is given as :

$$M_X = m_Q + \overline{\Lambda} - \frac{\lambda_1}{2m_Q} + 4(S_Q.S_l)\frac{\lambda_2}{2m_Q}. \tag{5.5}$$

In this equation, $-4(S_Q.S_l)$ is the Clebsch factor, having value -3 or 1 for J = 0 or 1 respectively for $S_l = 1/2$ and having values -5 or 3 for J = 1 or 2 for $S_l = 3/2$.

The parameter $\overline{\Lambda}$ is the energy of the light quark fields (i.e. brown muck), λ_1 term represents the kinetic energy of the heavy quark Q and the term λ_2 gives the chromomagnetic interaction energy [25–27]. Since value of kinetic energy of the heavy quark is positive, the value of the parameter λ_1 should be negative. $\overline{\Lambda}$ is the HQET parameter whose value is same for all the particles in a spin-flavor multiplet. $\overline{\Lambda}$ does not depend on the light quark flavor if there is $SU(3)$ symmetry, but for the breaking of this symmetry $\overline{\Lambda}$ is different for strange and non-strange heavy -light mesons and is denoted by $\overline{\Lambda}_s$ and $\overline{\Lambda}_{u,d}$ respectively.

In the limit $m_Q \to \infty$, only the first term of the HQET lagrangian will have the effect of interaction. Based on various fields defined in chapter 2, the kinetic terms of the heavy meson doublets and of the Σ field of light pseudo-scalar mesons are as [21] :

$$\begin{aligned}\mathcal{L} = {} & iTr[\overline{H_b}v^\mu D_{\mu ba}H_a] + \frac{f_\pi^2}{8}Tr[\partial^\mu\Sigma\partial_\mu\Sigma^\dagger] + Tr[\overline{S_b}(iv^\mu D_{\mu ba} - \delta_{ba}\Delta_S)S_a] \\ & + Tr[\overline{T_b}^\alpha(iv^\mu D_{\mu ba} - \delta_{ba}\Delta_T)T_{\alpha a}] + Tr[\overline{X_b}^\alpha(iv^\mu D_{\mu ba} - \delta_{ba}\Delta_X)X_{\alpha a}] \\ & + Tr[\overline{Y_b}^{\alpha\beta}(iv^\mu D_{\mu ba} - \delta_{ba}\Delta_Y)Y_{a\alpha\beta}] + Tr[\overline{Z_b}^{\alpha\beta}(iv^\mu D_{\mu ba} - \delta_{ba}\Delta_Z)Z_{a\alpha\beta}]\end{aligned} \tag{5.6}$$

where the operator D is given as:

$$D = -\delta_{ba}\partial^{\mu} + \mathcal{V}_{\mu ba} = -\delta_{ba}\partial^{\mu} + \frac{1}{2}(\xi^{\dagger}\partial_{\mu}\xi + \xi\partial_{\mu}\xi^{\dagger})_{ba}. \tag{5.7}$$

The mass parameter Δ_F describes the mass splitting between the higher mass doublets (F) and the ground state H field doublet. This mass parameter Δ_F (F = S,T,X,Y,Z) can be written in terms of the spin average mass of these doublets as:

$$\Delta_F = \overline{M}_F - \overline{M}_H, \quad F = S, T, X, Y, Z \tag{5.8}$$

where

$$\overline{M}_H = (3m^{(Q)}_{P^*_1} + m^{(Q)}_{P_0})/4, \tag{5.9}$$

$$\overline{M}_S = (3m^{(Q)}_{P'_1} + m^{(Q)}_{P^*_0})/4, \tag{5.10}$$

$$\overline{M}_T = (5m^{(Q)}_{P^*_2} + 3m^{(Q)}_{P_1})/8 \tag{5.11}$$

$$\overline{M}_X = (5m^{(Q)}_{P_2} + 3m^{(Q)}_{P^*_1})/8 \tag{5.12}$$

$$\overline{M}_Y = (7m^{(Q)}_{P^*_3} + 5m^{(Q)}_{P'_2})/12 \tag{5.13}$$

$$\overline{M}_Z = (7m^{(Q)}_{P_3} + 5m^{(Q)}_{P^*_2})/12 \tag{5.14}$$

The mass degeneracy within the spin members of the doublets also breaks at the $1/m_Q$ corrections to the heavy quark limit. This correction is in the form of

$$\mathcal{L}_{1/m_Q} = \frac{1}{2m_Q}\{\lambda_H Tr[\overline{H}_a\sigma^{\mu\nu}H_a\sigma_{\mu\nu}] + \lambda_S Tr[\overline{S}_a\sigma^{\mu\nu}S_a\sigma_{\mu\nu}] + \lambda_T Tr[\overline{T}^{\alpha}_a\sigma^{\mu\nu}T^{\alpha}_a\sigma_{\mu\nu}]\}$$

$$+ \lambda_X Tr[\overline{X}^{\alpha}_a\sigma^{\mu\nu}X^{\alpha}_a\sigma_{\mu\nu}]\} + \lambda_Y Tr[\overline{Y}^{\alpha\beta}_a\sigma^{\mu\nu}Y^{\alpha\beta}_a\sigma_{\mu\nu}]\} + \lambda_Z Tr[\overline{Z}^{\alpha\beta}_a\sigma^{\mu\nu}Z^{\alpha\beta}_a\sigma_{\mu\nu}]\} \tag{5.15}$$

where $\lambda_H, \lambda_S\lambda_T, \lambda_X, \lambda_Y$ and λ_Z are the hyperfine splittings between the spin partners in each doublet with

$$\lambda_H = \frac{1}{8}(M^2_{P^*_1} - M^2_{P_0}), \tag{5.16}$$

$$\lambda_S = \frac{1}{8}(M^2_{P'_1} - M^2_{P^*_0}), \tag{5.17}$$

$$\lambda_T = \frac{3}{16}(M^2_{P^*_2} - M^2_{P_1}) \tag{5.18}$$

$$\lambda_X = \frac{3}{16}(M^2_{P_2} - M^2_{P^*_1}) \tag{5.19}$$

$$\lambda_Y = \frac{5}{24}(M^2_{P^*_3} - M^2_{P'_2}) \tag{5.20}$$

$$\lambda_Z = \frac{5}{24}(M^2_{P_3} - M^2_{P^*_2}). \tag{5.21}$$

Flavor symmetry implies

$$\Delta_F^{(c)} = \Delta_F^{(b)} \tag{5.22}$$

$$\lambda_F^{(c)} = \lambda_F^{(b)} \tag{5.23}$$

i.e. Δ_F parameter which represents the splittings between higher and the ground state doublets and parameter λ_F which represents the hyperfine splittings between spin partners, are same for both charm and bottom mesons.

This symmetry is broken by the higher order $1/m_Q$ terms in the HQET lagrangian. The parameters Δ_F and λ_F get modified by extra term $\delta\Delta_F$ and $\delta\lambda_F$ [25].

The hyperfine splitting term λ_F which originates from the chromomagnetic interaction is dominated by the QCD corrections and the $1/m_Q$ effect is neglected [26].

QCD corrections change the λ_F relation to

$$\lambda_F^{(b)} = \lambda_F^{(c)}(\frac{\alpha_s(m_b)}{\alpha_s(m_c)})^{9/25}. \tag{5.24}$$

For any doublet F, difference of the spin averaged masses at $1/m_Q$ order is

$$\overline{M}_F - \overline{M}_H = \overline{\Lambda}_F - \overline{\Lambda}_H - \frac{\lambda_1^F}{2m_Q} + \frac{\lambda_1^H}{2m_Q} \tag{5.25}$$

which modifies the parameter Δ_F by $\delta\Delta_F$, i.e.

$$\Delta_F^{(b)} = \Delta_F^{(c)} + \delta\Delta_F, \qquad \text{with} \qquad \delta\Delta_F = (\lambda_1^F - \lambda_1^H)[\frac{1}{2m_c} - \frac{1}{2m_b}]. \tag{5.26}$$

In HQET, strange states possess the property that for a given state, strange quark shifts the mass by the same amount for both fundamental mode n=1 and radially excited mode n = 2, i.e.

$$M_{P_S} - M_P = \widetilde{M}_{P_S} - \widetilde{M}_P. \tag{5.27}$$

Masses of the heavy hadrons can be used to calculate other properties like strong decays, radiative decays, magnetic moments etc. Strong interactions are very important for the study of heavy hadrons containing one heavy and one light quark in the non-perturbative regime. In the next section, we will use this heavy quark symmetric parameters Δ_F and λ_F to predict the masses and strong decay widths for the bottom states $B(1D)_{5/2}$, $B(1F)_{5/2}$, $B(2S)$ and $B(2P)$.

5.3 Numerical Analysis

The masses, decay widths and $J^{P'}s$ for the experimentally available radial excited charm mesons $D_0(2560)$, $D_1^*(2680)$, $D_J(3000)$, $D_J^*(3000)$ have been analyzed with various theoretical approaches [7, 28–30]. In particular the predicted J^P values for $(D_J(2560), D_J^*(2680))$ are given as $(0^-, 1^-)_{\frac{1}{2}}$ for n=2 and L=0 and J^P for states $(D_J^*(3000)), (D_J(3000))$ are given as $(0^+, 1^+)_{\frac{1}{2}}$ for n=2 and L=1.

In bottom sector, only one radially excited bottom state i.e. $B_J(5970)$, is experimentally known, whose J^P is associated with 1^- [16, 35] for $\widetilde{B}_1^*(2S)$ state. Other radially excited bottom states ($B(2S)$, $B(2P)$, $B_s(2S)$ and $B_s(2P)$) are still unavailable. In this section, we aim to predict the masses, decay widths, branching ratios of these missing radially excited bottom states B(2S) and B(2P) in the framework of HQET. To study the behavior of the heavy-light mesons for their spectroscopy, masses are the most important property to be studied, so we start our calculations by predicting the masses of these bottom meson states. To calculate these masses, we use the flavor symmetry property of the heavy quarks $\lambda_F^{(b)} = \lambda_F^{(c)}$ and $\Delta_F^{(b)} = \Delta_F^{(c)}$. This flavor symmetry parameters are defined in terms of the spin averaged mass splittings between the higher the ground state doublet, represented by Δ_F and λ_F which is the mass splittings between the spin partners of the doublets. From the LHCb data [2], mass splittings Δ_F and hyperfine splittings λ_F for recently observed 2S and 2P charm mesons states comes out to be:

$$\Delta_{\widetilde{H}}^{(c\overline{u})} = 660.33 \pm 3.8 MeV,\ \lambda_{\widetilde{H}}^{(c\overline{u})} = (213.43 \pm 3.9 MeV)^2$$

$$\Delta_{\widetilde{S}}^{(c\overline{u})} = 1009.44 \pm 6.12 MeV,\ \lambda_{\widetilde{S}}^{(c\overline{u})} = (164.72 MeV \pm 2.4)^2$$

$$\Delta_{\widetilde{T}}^{(c\overline{u})} = 1034.19 \pm 1.2 MeV,\ \lambda_{\widetilde{T}}^{(c\overline{u})} = (208.41 MeV \pm 1.4)^2$$

for the n=2 odd parity, low lying even parity and for the excited even parity $c\overline{u}$ mesons. The charm mesons for n=2, P-wave with $j = 3/2$ are experimentally

unavailable, so we have taken the theoretical masses for $(\widetilde{D}_1, \widetilde{D}_2^*)$ having values (2932.50, 3020.60)MeV [18, 19, 31, 32, 35]. In this, we have taken the SU(2) isospin symmetry for the non-strange charm mesons, i.e. M($c\overline{u}$) = M($c\overline{d}$). The small statistical errors in Δ_F and λ_F ($F = \widetilde{H}, \widetilde{S}, \widetilde{T}$) for the non-strange radial excited charm mesons reflect the precision of the LHCb results [2].

Calculated bottom masses obtained using these symmetries are listed in the 2^{nd} row of Table 5.1. Here, mass of bottom state $\widetilde{B}_1^*$ for n=2 and $J^P = 1^-$ comes out to be 5981.50 MeV, which is very close to experimentally observed mass 5978 MeV and 5969.20 MeV for bottom state $B_J(5970)$ observed by CDF and LHCb collaboration respectively. Closeness in the experimentally observed mass for bottom state $\widetilde{B}_1^*$ and the mass obtained by HQET shows the authenticity of this heavy quark symmetry. Since the experimental information on radial excited bottom states is limited, the authenticity of this symmetry cannot be completely justified just on the basis of one experimental available bottom state.

Based on these limitations, we have also compared the predicted masses for other n=2 bottom states with some of the theoretically available data. The masses calculated using the heavy quark symmetry in our work are in agreement with the masses obtained by the potential model in Ref. [35]. Masses of the non-strange bottom field $\widetilde{H}$ deviate by 0.4 % and 0.5% when compared with the masses in Ref. [35] for $\widetilde{B}_0$ and $\widetilde{B}_1^*$ states respectively. Similar pattern is observed for P-wave masses where the deviations are below 1%.

We have obtained a set of bottom spectra for n=2 using flavor symmetry which upto a very good approximation matches with other theoretical data as discussed above.

Now, we would like to look into the QCD and $1/m_Q$ corrections in the HQET lagrangian. QCD and $1/m_Q$ corrections are applied to a scale of Λ_{QCD}/m_Q, where they can be an important input to decide the level of breaking of symmetry. The

corrections to Δ_F and λ_F (where F = $\widetilde{H}$, $\widetilde{S}$, $\widetilde{T}$) parameters are coming in the form of

$$\lambda_F^{(b)} = \lambda_F^{(c)}\delta\lambda_F \qquad \Delta_F^{(b)} = \Delta_F^{(c)} + \delta\Delta_F \tag{5.28}$$

where $\delta(\lambda_F) = (\frac{\alpha_s(m_b)}{\alpha_s(m_c)})^{9/25}$ and $\delta\Delta_F = (\lambda_1^F - \lambda_1^H)[\frac{1}{2m_c} - \frac{1}{2m_b}]$.

The λ_F parameter originates from the chromomagnetic interaction, thus only QCD corrections are dominated and $1/m_Q$ effect is small. For applying the QCD corrections to the spin hyperfine splitting relation λ_F, the values of the parameter $\alpha_s(m_b)$ and $\alpha_s(m_c)$ are taken as 0.22 and 0.36 [26]. The leading QCD correction to the λ_F relation comes out to be

$$\delta(\lambda_F) = (\frac{\alpha_s(m_b)}{\alpha_s(m_c)})^{9/25} = 0.83.$$

We then obtain:

$$\lambda_{\widetilde{H}}^b = (194.44 \pm 3.9)^2 MeV^2, \tag{5.29}$$

$$\lambda_{\widetilde{S}}^b = (150.06 \pm 2.19)^2 MeV^2, \tag{5.30}$$

$$\lambda_{\widetilde{T}}^b = (189.87 \pm 1.27)^2 MeV^2 \tag{5.31}$$

Table 5.1: Predicted values of the radially excited non-strange 2S and 2P bottom meson states. All the masses are in MeV units.

	$0^-(2^1S_0)$	$1^-(2^3S_1)$	$0^+(2^3P_0)$	$1^+(2^1P_1)$	$1^+(2^3P_1)$	$2^+(2^3P_2)$
Without corrections	5950.96	5981.50	6335.83	6318.67	6336.30	6354.56
Corrections inλ_F	5954.68	5980.26	6333.74	6319.37	6338.16	6353.45
Corrections in Δ_F	5928±13	5959±13	6291±37	6274±37	6306±9	6324±9
Correction in both parameters λ_F and Δ_F	5932±13	5957±13	6289±37	6274±37	6308±9	6323±9
Ref. [31]	5985	6019	6264	6278	6296	6292
Ref. [19]	5976	5992	6318	6321	6345	6359
Ref. [35]	6003	6029	6367	6375	6387	6382

The calculated bottom meson masses inherited with this QCD correction are tabulated in the 3^{rd} row of the Table 5.1. The results obtained with this correction

are deviating by 1 or 2 MeV except for the $\widetilde{B}_1^*$ state, where the deviation is of 4 MeV value. The experimental mass 5978 MeV observed by CDF collaboration for bottom state $B_J(5970)$ is now deviating by 2 MeV from the mass obtained by applying the QCD correction to the λ_F. Thus the gap between experimental and theoretical HQET mass has been reduced when the correction has been introduced. While studying this correction, we realize that these kind of correction for n=2 bottom mesons are showing similar pattern of behavior but with a reduced effect, when compared with results for n=1 bottom states. Specifically in Ref. [33], most of the bottom masses are deviating from their values by at 6-7 MeV. This is something we expect when we study the properties of the heavier mesons for higher excited states.

Now, in the next section, we will study the effect of QCD and $1/m_Q$ corrections to other heavy flavor symmetry in the form of $\delta\Delta_F$, where $F = \widetilde{H}, \widetilde{S}, \widetilde{T}$. This kind of analysis is already performed for n=1 states in Ref. [25], where the value of $\delta\Delta_{\widetilde{S}} \sim \mathcal{O}(-35)$ MeV

Since the experimental information on the radial excited bottom state masses is unavailable, so we cannot predict the exact value for these corrections $\delta\Delta_F$ for n=2. However, by using the available theoretical masses for these radial excited charm and bottom states, we have estimated a range to this correction $\delta\Delta_F$ for n=2, that modifies Δ_F as:

$$\Delta^b_{\widetilde{H}} = 638.58 \pm 13.75 MeV, \tag{5.32}$$

$$\Delta^b_{\widetilde{S}} = 965.09 \pm 37.15 MeV, \tag{5.33}$$

$$\Delta^b_{\widetilde{T}} = 1004.56 \pm 9.2 MeV, \tag{5.34}$$

Masses obtained by this correction are tabulated in 4^{th} row of Table 5.1. The Table shows that the correction $\delta\Delta_F$ to $\Delta_F^{(b)} = \Delta_F^{(c)}$ results in proportionate reduction in the bottom masses.

Masses tabulated in 5^{th} row of Table 5.1 are calculated by applying corrections to both the parameters i.e.$\delta\lambda_F$ and $\delta\Delta_F$ simultaneously. Since the effect of corrections to λ_F is small, so the resultant masses are close to the masses obtained by applying corrections to the Δ_F parameter.

In the strange sector, the experimentally known radially excited charm mesons are $D_{sJ}(2700)$ and $D_{sJ}(3040)$ [5,6]. The J^P for these states are theoretically [36–39] given as $(1^-)_{\frac{1}{2}}$ (n=2, L=0) for $D_{sJ}(2700)$ and $(1^+)_{\frac{1}{2}}$ (n=2, L=1)for $D_{sJ}(3040)$ state. The other strange 2S and 2P charm and bottom mesons are still unknown. Here, we have predicted the unavailable 2S and 2P charm masses using Eq.(5.27). The obtained strange charm masses are listed in Table 5.2 and are matched with other theoretical data.

Table 5.2: Predicted values of the radially excited strange 2S and 2P charm meson states. All the masses are in MeV units.

$J^P(n^{2s+1}L_J)$	Our	Ref. [35]	Ref. [19]	Ref. [34]
$0^-(2^1S_0)$	2682.96	2680	2688	2673
$1^-(2^3S_1)$	2754.63	2719	2731	2732
$0^+(2^3P_0)$	3007.80	3022	3054	3005
$1^+(2^1P_1)$	3009.90	3081	3154	3018
$1^+(2^3P_1)$	3089.61	3092	3067	3038
$2^+(2^3P_2)$	3127.71	3109	3142	3048

In the same way, strange bottom masses are calculated and are reported in Table 5.3. The 2^{nd} row of the table gives the masses without any correction and the masses listed in row 3^{rd} and 4^{th} include the corrections to the λ_F and to Δ_F relation respectively. This is followed by the masses in 5^{th} row which gives the masses obtained by using corrections to both the λ_F and Δ_F relations simultaneously. In general, QCD correction to λ_F relation changes the bottom masses by few MeV. Correction to Δ_F relation results in deviating the mass of S-wave bottom states by 0.22% . And the masses for P-wave get deviated by 0.77% and 0.58% respectively for $S_l = 1/2^+$ and $S_l = 3/2^+$.

Table 5.3: Predicted values of the radially excited strange 2S and 2P bottom meson states. All the masses are in MeV units.

	$0^-(2^1S_0)$	$1^-(2^3S_1)$	$0^+(2^3P_0)$	$1^+(2^1P_1)$	$1^+(2^3P_1)$	$2^+(2^3P_2)$
Without corrections	6039.67	6071.85	6335.72	6336.72	6429.02	6447.41
Corrections inλ_F	6043	6070.54	6335.84	6336.68	6430.89	6446.29
Corrections in Δ_F	6025±6	6058±6	6286±8	6287±8	6391±20	6410±20
Correction in both parameters λ_F and Δ_F	6029±6	6056±6	6286±8	6287±8	6393±20	6409±20
Ref. [31]	5886	5920	6163	6175	6194	6188
Ref. [19]	5890	5906	6221	6209	6281	6260
Ref. [35]	5926	5947	6297	6295	6311	6299

Now we study the various other properties of bottom mesons like strong decay widths, branching ratios, strong coupling constants. We apply the effective Lagrangian approach to calculate the OZI allowed two body strong decay widths and the various branching ratios involved with the bottom states $B(2S)$, $B(2P)$, $B_s(2S)$ and $B_s(2P)$. The numerical value of the partial and total decay widths of 2S and 2P family obtained using Eqs.(2.51-2.53)are collected in Table 5.4, 5.5, 5.6, where Table 5.4 and 5.5 are for the n=2, S and P wave bottom meson with $S_l = 1/2$, and the Table 5.6 is for the other P wave bottom meson states having $S_l = 3/2$. As followed in the previous chapter, strange bottom states decaying to decay modes represented by "†" in Tables 5.4, 5.5, 5.6, 5.8 are the isospin violating processes, so the final products are multiplied by suppression factor ϵ^2 [41].

For the radially ground state S-wave bottom states, Table 5.4 reveals $B^*\pi^-$ mode to be the dominant decay mode both for $\widetilde{B}_1^*$ and $\widetilde{B}_0$ bottom states with branching fraction of 37.97% and 64.16% respectively. And for their strange partners, $B^{*+}K^-$ is seen to be the leading decay mode with branching fraction 27.39% and 47.31% for $\widetilde{B}_{s1}^*$ and $\widetilde{B}_{s0}$ state respectively. Hence the decay modes $B^*\pi^-$ and $B^{*+}K^-$ are suitable for the experimental search of the missing non-strange and strange 2S bottom meson states. Total decay width for bottom state $\widetilde{B}_1^*$ is 64.32 MeV, which matches with its experimental value of 70 MeV [14](observed by CDF Collaboration), where

Table 5.4: Strong decay width of non-strange and strange n=2 S-wave bottom mesons $B(2^3S_1)$, $B(2^1S_0)$, $B_s(2^3S_1)$ and $B_s(2^1S_0)$. Ratio in 5^{th} column represents the $\widehat{\mathbf{\Gamma}} = \frac{\Gamma}{\Gamma(B_J^{(*)} \to B^{*+}\pi^-)}$ for the non-strange mesons and $\widehat{\mathbf{\Gamma}} = \frac{\Gamma}{\Gamma(B_{sJ}^* \to B^{*0}K^+)}$ for the strange mesons. Fraction gives the percentage of the partial decay width with respect to the total decay width. † represents the isospin violating processes.

State	nLs_lJ^P	Decay channel	Decay Width(MeV)	Ratio	Fraction
$\widetilde{B}_1^*(5981.50)$	$2S_{1/2}1^-$	$B^*\pi^+$	$1246.27\widetilde{g}_{HH}^2$	1	37.97
		$B^*\pi^0$	$626.01\widetilde{g}_{HH}^2$	0.50	19.07
		$B^*\eta$	$37.18\widetilde{g}_{HH}^2$	0.02	1.13
		B_s^*K	$96.36\widetilde{g}_{HH}^2$	0.07	2.93
		$B^0\pi^0$	$377.54\widetilde{g}_{HH}^2$	0.30	11.50
		$B^+\pi^-$	$753.14\widetilde{g}_{HH}^2$	0.60	22.94
		$B^0\eta$	$32.41\widetilde{g}_{HH}^2$	0.02	0.98
		B_sK	$112.72\widetilde{g}_{HH}^2$	0.09	3.43
		Total	$3281.67\widetilde{g}_{HH}^2$		
$\widetilde{B}_0(5950.96)$	$2S_{1/2}0^-$	$B^*\pi^+$	$1629.05\widetilde{g}_{HH}^2$	1	64.16
		$B^*\pi^0$	$818.67\widetilde{g}_{HH}^2$	0.50	32.24
		$B^*\eta$	$33.15\widetilde{g}_{HH}^2$	0.02	1.30
		B_s^*K	$57.78\widetilde{g}_{HH}^2$	0.03	2.27
		Total	$2538.67\widetilde{g}_{HH}^2$		
$\widetilde{B}_{s1}^*(6071.85)$	$2S_{s1/2}1^-$	B^0K^0	$520.79\widetilde{g}_{HH}^2$	0.65	17.84
		B^+K^-	$529.94\widetilde{g}_{HH}^2$	0.66	18.15
		$^\dagger B_s\pi^0$	$0.03\widetilde{g}_{HH}^2$	-	-
		$B_s\eta$	$134.70\widetilde{g}_{HH}^2$	0.16	4.61
		$B^{*0}K^0$	$784.86\widetilde{g}_{HH}^2$	0.98	26.88
		$B^{*+}K^-$	$799.72\widetilde{g}_{HH}^2$	1	27.39
		$^\dagger B_s^*\pi^0$	$0.06\widetilde{g}_{HH}^2$	-	-
		$B_s^*\eta$	$148.94\widetilde{g}_{HH}^2$	0.18	5.10
		Total	$2918.98\widetilde{g}_{HH}^2$		
$\widetilde{B}_{s0}(6039.67)$	$2S_{s1/2}0^-$	$B^{*0}K^0$	$924.75\widetilde{g}_{HH}^2$	0.97	46.27
		$B^{*+}K^-$	$945.50\widetilde{g}_{HH}^2$	1	47.31
		$^\dagger B_s^*\pi^0$	$0.08\widetilde{g}_{HH}^2$	-	-
		$B_s^*\eta$	$128.26\widetilde{g}_{HH}^2$	0.13	6.41
		Total	$1998.52\widetilde{g}_{HH}^2$		

strong coupling constant $\widetilde{g}_{HH}$ is used as 0.14 [23]. This coupling for the other S-wave bottom states gives decay width $\Gamma(\widetilde{B}_0) = 49.48$ MeV, $\Gamma(\widetilde{B}^*_{s1}) = 57.21$ MeV and $\Gamma(\widetilde{B}_{s0}) = 39.17$ MeV.

Similarly, for n=2 low lying P-wave bottom states$(0^+, 1^+)$, Table 5.5 shows that the dominant decay modes for bottom state $\widetilde{B}^*_0$ and $\widetilde{B}'_1$ are $B^+\pi^-$ and $B^{*+}\pi^-$ respectively. These decay modes contribute 42.15% and 42.83% to the total decay widths of $\widetilde{B}^*_0$ and $\widetilde{B}'_1$ state. And for the strange states $\widetilde{B}^*_{s0}$ and $\widetilde{B}'_{s1}$, B^-K^+ and $B^{*-}K^+$ decay modes emerge as the prominent modes for their experimental exploration in future. Using the coupling constant $\widetilde{g}_{SH} = 0.12$, the total decay width for these $S_l = 1/2$ P-wave bottom states are obtained as: $\Gamma(\widetilde{B}^*_0) = 242.70$ MeV, $\Gamma(\widetilde{B}'_1) = 203.46$ MeV, $\Gamma(\widetilde{B}^*_{s0}) = 235.97$ MeV and $\Gamma(\widetilde{B}'_{s1}) = 207.80$ MeV.

Apart from the mentioned partial decay widths, these bottom states also decays to D-wave bottom mesons. But these decays are suppressed in our calculations because of their small contribution.

Lastly, for the other P-wave bottom states having $S_l = 3/2$, Table 5.6 points $B^*\pi^+$ and B^*K^- decay modes to be the best suitable for the study of the missing non-strange states $(\widetilde{B}_1, \widetilde{B}^*_2)$ and strange states $(\widetilde{B}_{s1}, \widetilde{B}^*_{s2})$ respectively. While observing the total decay width values from Table, we notice that lower values of coupling constant $\widetilde{g}_{TH}$ will give realistic decay width value for these states. Assuming that the coupling constant $\widetilde{g}_{SH}$ and $\widetilde{g}_{TH}$ will not vary much for higher excited states, total decay width corresponding to the coupling constant $\widetilde{g}_{TH} = 0.12$ value are obtained as $\Gamma(\widetilde{B}_1) = 188.69$ MeV, $\Gamma(\widetilde{B}^*_2) = 226.39$ MeV, $\Gamma(\widetilde{B}_{s1}) = 208.22$ MeV and $\Gamma(\widetilde{B}^*_{s2}) = 252.80$ MeV.Thus the states $\widetilde{B}^*_2$ and $\widetilde{B}^*_{s2}$ are observed to be broader states as compared to their spin partner states $\widetilde{B}_1$ and $\widetilde{B}_{s1}$ respectively. Here, we need to emphasize that the estimated total width of these states does not include the contribution from the decays to n=1 D-wave bottom mesons since the phase space is very small for these decay states.

Table 5.5: Strong decay width of non-strange and strange n=2 P-wave with $S_l = 1/2$ bottom mesons $B(2^3P_0)$, $B(2^1P_1)$, $B_s(2^3P_0)$ and $B_s(2^1P_1)$. Ratio in 5^{th} column represents the $\widehat{\mathbf{\Gamma}} = \frac{\Gamma}{\Gamma(B_J^{(*)} \to B^{*+}\pi^-)}$ for the non-strange mesons and $\widehat{\mathbf{\Gamma}} = \frac{\Gamma}{\Gamma(B_{sJ}^* \to B^{*0}K^+)}$ for the strange mesons. Fraction gives the percentage of the partial decay width with respect to the total decay width. † represents the isospin violating processes.

State	nLs_lJ^P	Decay channel	Decay Width(MeV)	Ratio	Fraction
$\widetilde{B}_0^*(6335.83)$	$2P_{1/2}0^+$	$B^-\pi^+$	$7087.60\widetilde{g}_{SH}^2$	1	42.15
		$B^0\pi^0$	$3542.06\widetilde{g}_{SH}^2$	0.49	21.06
		$B^0\eta$	$1063.91\widetilde{g}_{TH}^2$	0.15	6.32
		B_sK	$5118.49\widetilde{g}_{TH}^2$	0.72	30.44
		Total	$16812.10\widetilde{g}_{SH}^2$		
$\widetilde{B}_1^{'}(6318.67)$	$2P_{1/2}1^+$	$B^*\pi^+$	$6052.72\widetilde{g}_{SH}^2$	1	42.83
		$B^*\pi^0$	$3027.69\widetilde{g}_{SH}^2$	0.50	21.42
		$B^*\eta$	$890.83\widetilde{g}_{TH}^2$	0.14	6.30
		B_s^*K	$4158.15\widetilde{g}_{TH}^2$	0.68	29.42
		Total	$14129.40\widetilde{g}_{SH}^2$		
$\widetilde{B}_{s0}^*(6335.72)$	$2P_{s1/2}0^+$	$^\dagger B_s\pi^0$	$0.28\widetilde{g}_{SH}^2$	-	-
		$B_s\eta$	$3308.90\widetilde{g}_{TH}^2$	0.50	20.19
		B^+K^0	$6530.27\widetilde{g}_{SH}^2$	0.99	39.85
		B^-K^+	$6547.13\widetilde{g}_{SH}^2$	1	39.95
		Total	$16386.83\widetilde{g}_{SH}^2$		
$\widetilde{B}_{s1}^{'}(6336.72)$	$2P_{s1/2}1^+$	$^\dagger B_s^*\pi^0$	$0.24\widetilde{g}_{SH}^2$	-	-
		$B_s^*\eta$	$2834.34\widetilde{g}_{TH}^2$	0.48	19.64
		$B^{*+}K^0$	$5792.74\widetilde{g}_{SH}^2$	0.99	40.14
		$B^{*-}K^+$	$5803.61\widetilde{g}_{SH}^2$	1	40.21
		Total	$14430.70\widetilde{g}_{SH}^2$		

These 2S and 2P wave bottom mesons can also decay to n=1 P-wave bottom mesons, but we have not considered them in our present work because of the small value of the coupling $\widetilde{g}_{HS}, \widetilde{g}_{HT}, \widetilde{g}_{SS}, \widetilde{g}_{ST}, \widetilde{g}_{TS}$ and $\widetilde{g}_{TT}$.

Now to have overall idea of bottom spectra, we have not only studied n = 2 bottom states, but have also analyzed the masses and strong decay rates of bottom states $B(1D)_{5/2}$ and $B(1F)_{5/2}$. To calculate the masses for $B(1D)_{5/2}$ states, we have used charm state $D_2(2740)$, $D_3^*(2760)$, $D_{s2}(2822)$ and $D_{s3}^*(2860)$ discussed in chapter 3 with masses as:

$$M(D_2(2740)) = 2737.00 \text{ MeV} \tag{5.35}$$

$$M(D_3^*(2760)) = 2775.50 \text{ MeV} \tag{5.36}$$

$$M(D_{s2}(2822)) = 2822.00 \text{ MeV} \tag{5.37}$$

$$M(D_{s3}^*(2860)) = 2860.50 \text{ MeV} \tag{5.38}$$

Using the flavor symmetry property of the heavy quarks $\lambda_F^{(b)} = \lambda_F^{(c)}$ and $\Delta_F^{(b)} = \Delta_F^{(c)}$ for Y field states, obtained $B(1D)_{5/2}$ bottom masses are listed in Table 5.7.

Table 5.6: Strong decay width of non-strange and strange n=2 P-wave with $S_l = 3/2$ bottom mesons $B(2^1P_1)$, $B(2^3P_2)$, $B_s(2^1P_1)$ and $B_s(2^3P_2)$. Ratio in 5^{th} column represents the $\widehat{\mathbf{\Gamma}} = \frac{\Gamma}{\Gamma(B_J^{(*)} \to B^{*+}\pi^-)}$ for the non-strange mesons and $\widehat{\mathbf{\Gamma}} = \frac{\Gamma}{\Gamma(B_{sJ}^{*} \to B^{*0}K^+)}$ for the strange mesons. Fraction gives the percentage of the partial decay width with respect to the total decay width. † represents the isospin violating processes.

State	nLs_lJ^P	Decay channel	Decay Width(MeV)	Ratio	Fraction
$\widetilde{B}_1(6336.30)$	$2P_{3/2}1^+$	$B^*\pi^+$	$7021.89\widetilde{g}_{TH}^2$	1	53.58
		$B^*\pi^0$	$3522.08\widetilde{g}_{TH}^2$	0.50	26.87
		$B^*\eta$	$512.74\widetilde{g}_{TH}^2$	0.07	3.91
		B_sK	$2046.74\widetilde{g}_{HH}^2$	0.29	15.61
		Total	$13103.50\widetilde{g}_{TH}^2$		
$\widetilde{B}_2^*(6354.56)$	$2P_{3/2}2^+$	$B^*\pi^+$	$4571.90\widetilde{g}_{TH}^2$	1	29.08
		$B^*\pi^0$	$2292.95\widetilde{g}_{TH}^2$	0.50	14.58
		$B^*\eta$	$345.57\widetilde{g}_{TH}^2$	0.07	2.19
		B_s^*K	$1392.05\widetilde{g}_{TH}^2$	0.30	8.85
		$B^0\pi^0$	$1849.52\widetilde{g}_{TH}^2$	0.40	11.76
		$B^+\pi^-$	$3694.17\widetilde{g}_{TH}^2$	0.80	23.49
		$B^0\eta$	$300.86\widetilde{g}_{TH}^2$	0.06	1.91
		B_sK	$1274.68\widetilde{g}_{TH}^2$	0.27	8.10
		Total	$15721.70\widetilde{g}_{TH}^2$		
$\widetilde{B}_{s1}(6429.02)$	$2P_{s3/2}1^+$	$^\dagger B_s^*\pi^0$	$0.35\widetilde{g}_{TH}^2$	-	-
		$B^{*+}K^0$	$6149.63\widetilde{g}_{TH}^2$	0.98	34.07
		$B^{*-}K^+$	$6212.01\widetilde{g}_{TH}^2$	1	34.41
		$B_s^*\eta$	$2098.43\widetilde{g}_{TH}^2$	0.33	11.62
		Total	$18047.90\widetilde{g}_{TH}^2$		
$\widetilde{B}_{s2}^*(6447.41)$	$2P_{s3/2}2^+$	$^\dagger B_s^*\pi^0$	$0.23\widetilde{g}_{TH}^2$	-	-
		$B^{*+}K^0$	$4053.03\widetilde{g}_{TH}^2$	0.99	23.08
		$B^{*-}K^+$	$4092.49\widetilde{g}_{TH}^2$	1	23.31
		$B_s^*\eta$	$1414.93\widetilde{g}_{TH}^2$	0.34	8.05
		B^+K^-	$3387.56\widetilde{g}_{TH}^2$	0.82	19.29
		B^0K^0	$3352.34\widetilde{g}_{TH}^2$	0.81	19.09
		$^\dagger B_s\pi^0$	$0.19\widetilde{g}_{TH}^2$	-	-
		$B_s\eta$	$1255.43\widetilde{g}_{TH}^2$	0.30	7.15
		Total	$17555.76\widetilde{g}_{TH}^2$		

The comparison of predicted masses with other theoretical data shows, the strange masses in present work are in agreement with the masses obtained by the potential model in Ref. [35]. Strange masses for bottom states $B_{2s}^{'}$ and B_{3s}^{*} deviates only by 0.04% from the masses in Ref. [35]. Masses for the non-strange bottom $B_{2}^{'}$ deviate by 0.19%, 0.43% and 1.7% when compared with the masses in Ref. [19], Ref. [35] and Ref. [31] respectively. A similar pattern is observed for non-strange bottom state B_{3}^{*} mass, where deviations are 0.27%, 0.37% and 1.8% with the masses in Ref. [19], Ref. [35] and Ref. [31] respectively.

Similarly, bottom states $(2^{+}, 3^{+})$ for the $1F_{5/2}$ doublet have been studied in [43]. The calculated masses $M(B_{2}^{*}) = 6518.29$ MeV, $M(B_{3}) = 6462.36$MeV, $M(B_{2s}^{*}) = 6550.45$ MeV and $M(B_{3s})$ =6556.06 MeV are again in good agreement with the mass predictions made in Ref. [19] and Ref. [31]. Masses calculated using heavy quark symmetry scheme are only 1.63% and 3.80% deviating from the results in Ref. [19] and Ref. [31] respectively.

We apply these calculated masses, to study the other properties like strong decay widths, branching ratios for $1D_{5/2}$ bottom states. The numerical value of the partial and total decay rates for bottom state $1D_{5/2}$ obtained using Eq.(2.55) are tabulated in Table 5.8. Table shows, $B^{*+}\pi^{-}$ and $B^{+}\pi^{-}$ appears as the dominant decay modes for bottom state $B_{2}^{'}$ and B_{3}^{*}. These decay modes contribute 62.61% and 31.73% to the total decay widths of $B_{2}^{'}$ and B_{3}^{*} state. And for the strange states $B_{2s}^{'}$ and B_{3s}^{*},

Table 5.7: Predicted masses for the non-strange and strange bottom state doublet $(2^{-}, 3^{-})_{5/2}$. All masses are in the units of MeV.

$J^{P}(n^{2s+1}L_{J})$	Our	Ref. [31]	Ref. [19]	Ref. [35]
$2^{-}(1^{1}D_{2})$	6091.40	5985	6103	6065
$3^{-}(1^{3}D_{3})$	6108.79	5993	6091	6085
$2^{-}(1^{1}D_{2s})$	6160.89	6095	6189	6157
$3^{-}(1^{3}D_{3s})$	6178.62	6103	6191	6172

B^*K^+ and B^+K^- decay modes emerge as the prominent modes for their experimental exploration in future. Using the coupling constant $g_{YH} = 0.61$ [7], the total decay width for these $S_l = 5/2$ D-wave bottom states are obtained as: $\Gamma(B_2^{'}) = 227.98$ MeV, $\Gamma(B_3^*) = 325.38$ MeV, $\Gamma(B_{s2}^{'}) = 184.18$ MeV and $\Gamma(B_{s3}^*) = 282.77$ MeV. The suppression factor ϵ^2 reduces the decay width values for $1D_{5/2}$ stranged bottom states to $\Gamma(B_{s2}^{'}) = 124.03$ MeV and $\Gamma(B_{s3}^*) = 196.97$ MeV. Apart from the mentioned partial decay widths, these bottom states also decays to P-wave bottom mesons. But these decays are not included in our calculations because of their small contribution.

Similarly OZI allowed two body strong decays for the $1F_{5/2}$ bottom doublet have also been calculated in Ref. [43]. Using the coupling value $g_Z = 0.15$ [7] obtained from the charm state $D_2^*(3000)$, the decay rates for bottom states $1\mathrm{F}(2^+, 3^+)$ comes out as $\Gamma(B_2^*) = 363.81$ MeV, $\Gamma(B_3) = 135.42$ MeV. State B_2^* appears to be broader as compared to its spin partner B_3.

Table 5.8: Strong decay width of non-strange and strange n=1 D-wave with $S_l = 5/2$ bottom mesons $B(1^1D_2)$, $B(1^3D_3)$, $B_s(1^1D_2)$ and $B_s(1^3D_3)$. Ratio in 5^{th} column represents the $\widehat{\mathbf{\Gamma}} = \frac{\Gamma}{\Gamma(B_J^{(*)} \to B^{*+}\pi^-)}$ for the non-strange mesons and $\widehat{\mathbf{\Gamma}} = \frac{\Gamma}{\Gamma(B_{sJ}^* \to B^{*0}K^+)}$ for the strange mesons. Fraction gives the percentage of the partial decay width with respect to the total decay width. † Decay widths for stranged bottom mesons are calculated without considering the effect of suppression factor [41] occurring through mixing of π^0 and η.

State	nLs_lJ^P	Decay channel	Decay Width (MeV)	Ratio	Fraction	Compared Value (MeV)
$B_2^{'}(6091.40)$	$1D_{5/2}2^-$	$B^*\pi^+$	$383.66g_{YH}^2$	1	62.61	
		$B^*\pi^0$	$193.33g_{YH}^2$	0.50	31.55	
		$B^*\eta$	$23.31g_{YH}^2$	0.06	3.80	
		B_sK	$12.38g_{YH}^2$	0.03	2.02	
		Total	$612.69g_{YH}^2$			213.40 [42]
$B_3^*(6108.79)$	$1D_{5/2}3^-$	$B^*\pi^+$	$254.77g_{YH}^2$	1	29.13	
		$B^*\pi^0$	$128.34g_{YH}^2$	0.50	14.67	
		$B^*\eta$	$18.02g_{YH}^2$	0.07	2.06	
		B_s^*K	$10.19g_{YH}^2$	0.03	1.16	
		$B^0\pi^0$	$139.48g_{YH}^2$	0.54	15.95	
		$B^+\pi^-$	$277.84g_{YH}^2$	1.09	31.73	
		$B^0\eta$	$27.22g_{YH}^2$	0.10	3.11	
		B_sK	$18.56g_{YH}^2$	0.07	2.12	
		Total	$874.45g_{YH}^2$			31.08 [42]
$B_{2s}^{'}(6160.89)$	$1D_{s5/2}2^-$	$B_s^*\pi^0$	$161.74g_{YH}^2$	0.96	32.66	
		$B^{*+}K^0$	$162.20g_{YH}^2$	0.97	32.76	
		$B^{*-}K^+$	$167.18g_{YH}^2$	1	33.76	
		$B_s^*\eta$	$3.95g_{YH}^2$	0.02	0.79	
		Total	$495.09g_{YH}^2$			194 [42]
$B_{3s}^*(6178.62)$	$1D_{s5/2}3^-$	$B_s^*\pi^0$	$108.22g_{YH}^2$	0.91	14.24	
		$B^{*+}K^0$	$114.38g_{YH}^2$	0.97	15.09	
		$B^{*-}K^+$	$117.98g_{YH}^2$	1	15.52	
		$B_s^*\eta$	$3.16g_{YH}^2$	0.02	0.41	
		B^+K^-	$146.10g_{YH}^2$	1.23	19.22	
		B^0K^0	$142.09g_{YH}^2$	1.20	18.69	
		$B_s\pi^0$	$122.37g_{YH}^2$	1.03	16.10	
		$B_s\eta$	$5.32g_{YH}^2$	0.04	0.70	
		Total	$759.95g_{YH}^2$			134.05 [42]

5.4 Conclusion

With so many newly available charm states, the data for the higher excited bottom states is limited as compared to the charm sector. In this work, we focus on predicting the masses and the strong decay widths of the experimentally missing radially excited bottom states B(2S), B(2P), $B_s(2S)$, $B_s(2P)$, $B(1D)_{5/2}$ and $B(1F)_{5/2}$ using heavy quark effective theory.

- We apply the heavy quark symmetry property to the experimentally available radially excited charm mesons observed by LHCb and evaluate the similar spectra for the bottom sector. The predicted mass of bottom state $\widetilde{B}_1^*$ in our work is only 0.33% deviating from the experimental measured mass of $B_J(5970)$ state. The Closeness in the experimentally observed mass for bottom state $\widetilde{B}_1^*$ and the mass obtained in our work shows the authenticity of this heavy quark symmetry.

- These masses are then studied by taking the QCD and $1/m_Q$ corrections in the form of $\delta\Delta_F$ and $\delta\lambda_F$. Masses obtained using these corrections are tabulated in Table 5.1. While studying these correction, we realize that $\delta\lambda_F$ shifts the bottom masses at most by 0.06% and has reduced the existing gap between the experimental and the observed mass of $\widetilde{B}_1^*$ state. While the correction $\delta\Delta_F$ results in proportionate reduction in the bottom masses by the amount of $|\delta\Delta_F|$.

- Evaluating the strange bottom masses in the similar manner, we discover that calculated masses are in good agreement with maximum 2.5% deviation from the other theoretical stranged bottom masses. Corrections results in deviating the S-wave masses by 0.22%. And the masses for P-wave get deviated by 0.77% and 0.58% respectively for $S_l = 1/2^+$ and $S_l = 3/2^+$. The calcu-

lated strange bottom masses in this work for n=2 are ~ 90 MeV higher than the masses of the non-strange bottom masses except for the low lying S-wave states. These kinds of corrections for n=2 bottom mesons are showing similar pattern of behavior but with a reduced effect, when compared with results for n=1 bottom states. This is something we expect when we study the properties of the heavier mesons for higher excited states.

- With these obtained masses, we further calculated the strong decay widths of these bottom states, which are collected in Table 5.4,5.5,5.6. The predicted decay widths are in the terms of strong coupling constants $\widetilde{g}_{HH}$ $\widetilde{g}_{SH}$ and $\widetilde{g}_{TH}$. To avoid these unknown couplings, we have also computed the branching ratios and fractions for the possible OZI allowed decay channels.

- While analysing the decay widths in the Table 5.4,5.5,5.6, we observe $B^*\pi^-$ (B^+K^-) mode to be the dominant decay mode both for $\widetilde{B}_1^*$ ($\widetilde{B}_{s1}^*$) and $\widetilde{B}_0$ ($\widetilde{B}_{s0}$) bottom states. Similarly, for the low lying P=wave bottom mesons $\widetilde{B}_0^*$ and $\widetilde{B}_1'$, $B^+\pi^-$ and $B*^+\pi^-$ emerge as the dominant decay modes with contribution of 42.15% and 42.83% to their total decay widths. For their strange partners, B^-K^+ and B^*K^+ comes as prominent decay channels for $\widetilde{B}_{s0}^*$ and $\widetilde{B}_{s1}'$ states respectively. Lastly, for the excited P-wave bottom mesons, $B^*\pi^+$ and B^*K^- are seen to be the best suitable decay modes for the study of the missing non-strange states ($\widetilde{B}_1, \widetilde{B}_2^*$) and strange states ($\widetilde{B}_{s1}, \widetilde{B}_{s2}^*$) respectively. With the obtained decay widths, we have further checked their sensitivity to the QCD and $1/m_Q$ corrected masses. It is found that these corrections shift the decay width values at most by 30 MeV ($\sim 12\%$).

Finally, to complete the bottom spectra, we have predicted the masses and the strong decay widths of the experimentally not yet observed n=1 D and F-wave states $(2^-, 3^-)$, $(2^+, 3^+)$ and n=2 S and P-wave bottom states $(0^-, 1^-)$, $(0^+, 1^+)$

and $(1^+, 2^+)$. These predicted bottom states has opened a window to investigate the higher excitations of bottom mesons and can be confronted with the future experimental data at the LHCb, DØ, CDF, Belle II, BES III..

Bibliography

[1] M. Tanabashi et al. [Particle Data Group Collaboration], Phys. Rev. D **98** 030001(2018).

[2] R. Aaij et al.,[LHCb Collaboration], JHEP **2013** 145.

[3] P. del Amo Sanchez et al.,[BaBar Collaboration], Phys. Rev. D **82**, 111101 (2010).

[4] R. Aaij et al.,[LHCb Collaboration], Phys. Rev. D **94**, 072001 (2016).

[5] B. Aubert, et al., [BaBar Collaboration], Phys. Rev. D **80** 092003 (2009).

[6] R. Aaij, et al., [LHCb Collaboration], Phys. Rev. Lett. **113** 162001 (2014).

[7] P.Gupta and A. Upadhyay, Phys. Rev. D **97**, 014015 (2018).

[8] S. Behrends et al. [CLEO Collaboration], Phys. Rev. Lett. **50**, 881 (1983).

[9] K.Han et al., Phys. Rev. Lett. **55**, 36 (1985).

[10] T. Aaltonen et al. [CDF Collaboration], Phys. Rev. Lett. **102** 102003 (2009).

[11] T. A. Aaltonen et al., [CDF Collaboration], Phys. Rev. D **90** 012013 (2014).

[12] J. Lee-Franzini et al., Phys. Rev. Lett. **65** 2947-2950 (1990).

[13] R. Aaij et al. [LHCb Collaboration],JHEP **2015** 024.

[14] T. A. Aaltonen et al. [CDF Collaboration], Phys. Rev. D **90**, 012013 (2014).

[15] S. Godfrey and N. Isgur, Phys. Rev. D **32**, 189 (1985).

[16] Hao Xu, Xiang Liu, Takayuki Matsuki, Phys. Rev. D **89**, 097502 (2014).

[17] L. Y. Xiao and X. H. Zhong, Phys. Rev. D **90**, 074029 (2014).

[18] T. Matsuki, T. Morii, and K. Sudoh, Eur. Phys. J. A **31**, 701 (2007).

[19] D. Ebert, R. N. Faustov, and V. O. Galkin, Eur. Phys. J. C **66**, 197 (2010).

[20] Y. Sun, Q.-T. Song et al., Phys. Rev. D **89**, 054026 (2014).

[21] P. Colangelo, F. De Fazio et al., Phys. Rev. D **86** 054024 (2012)

[22] A.Falk and T. Mehen, Phys. Rev. D **53**, 231 (1996).

[23] Zhi-Gang Wang, Eur. Phys. J. Plus **129** 186 (2014).

[24] Cheunh C.Y, Hwang C.W., J. High Energ. Phys. **2014** 177.

[25] Hai-Yang Cheng, Fu-Sheng Yu, Phys. Rev. D **89**, 114017 (2014).

[26] G. Amoros, M. Beneke and M. Neubert, Phys. Lett. B **401**, 81 (1997).

[27] A. Upadhayay et. al., Adv.High Energy Phys. **2014** 619783.

[28] Q. T. Song et al., Phys. Rev. D **92** 074011 (2015).

[29] Zhi-Gang Wang, Phys. Rev. D **88**, 114003 (2013).

[30] G. L. Yu, Z.-G. Wang et al., Chin. Phys. C 39, 063101 (2015).

[31] M. Di Pierro and E. Eichten, Phys. Rev. D **64**, 114004 (2001).

[32] T.A. Lahde, Nucl. Phys. A **674**, 141-167 (2000).

[33] Cheng H.Y., Yu F.S., Eur. Phys. J. C **77** 668 (2017).

[34] Stephen Godfrey, Kenn Moats, Phys. Rev. D **93**, 034035 (2016).

[35] Virendrasinh Kher et.al., Chin.Phys. C **41**, 073101 (2017).

[36] Pietro Colangelo, Fulvia De Fazio, Phys. Rev. D **81**, 094001 (2010).

[37] Q. T. Song et al., Phys. Rev. D **91**, 054031 (2015).

[38] B. Zhang, X. Liu, W.Z. Deng, S.L. Zhu, Eur. Phys. J. C **50**, 617 (2007).

[39] J. Segovia, D.R. Entem, F. Fernandez, Phys. Rev. D **91**, 094020 (2015).

[40] Gui-Liang Yu et. al., Chin.Phys. C **39**, 063101 (2015).

[41] T. Matsuki and K. Seo, Phys. Rev. D **85**, 014036 (2012).

[42] Stephen Godfrey, Kenn Moats, Phys. Rev. D **94** 054025(2016).

[43] Vipin, M.sc Thesis, Thapar Institute of Engineering and Technology, Patiala, India (2018).

Chapter 6

Summary and Future Outlook

With the discovery of heavier hadrons, either baryons or mesons, the excitation spectrum of heavy-light mesons have received considerable theoretical and experimental attention. Upcoming experimental information provide opportunities to study the low energy properties of these hadrons with various phenomenological models.

The work of the present thesis concerns two different aspects. One is to develop a formalism for studying the strong interactions of the heavy-light mesons with the pseudoscalar mesons for their decays, masses and couplings. Second is the analysis of all the experimentally known strange and non strange excited states of bottom and charm states for calculating the other unknown higher radially excited states for their masses, decays and splittings.

The framework of "Heavy Quark Effective Theory (HQET)" involves the approximations of theory at two different scale that incorporates the heavy quark symmetries and the chiral symmetries. In HQET, a $Q\overline{q}$ meson is approximated as a bound state of a heavy quark and other light degrees of freedom. HQET gives a precise method of limiting the heavy quark mass to infinity. In the $m_Q \to \infty$, gluon exchange between the heavy quark and the light degree of freedom is independent of the mass and spin of heavy quark, resulting in $SU(2N_f)$ flavor and spin symmetry. For light degrees of freedom, heavy quark seems like a static color source, which is similar to the hydrogen atom system. So hadron properties are mainly retrieved from the

nature of light degrees of freedom. This $SU(2N_f)$ symmetry plays a crucial role in understanding the properties of heavy hadrons.

For studying the heavy hadrons, HQET is more appropriate than any other available theories because the mass and the spin degeneracy of heavy hadrons appears to be the approximate internal symmetry of the effective Lagrangian. Besides the fact that HQET contains many unknown parameters, it is still being successfully applied in conjugation with the chiral perturbation theory to study the strong interactions of heavy hadrons. Heavy quark symmetry helps in reducing the parameters by imposing constraints on these constants. In this thesis, the D and B heavy-light mesons containing c and b as heavy quarks are focused for analyzing various low energy properties like decays, branching ratios, coupling constants and masses.

Motivated from the experimental success in the heavy-light meson sector, we analyzed all the experimentally available charm states. In specific, we examined charm mesons like $D_J^*(2460)$, $D_J(2560)$, $D_J^*(2680)$, $D_J(2740)$, $D_J^*(2760)$, $D_J(3000)$, $D_J^*(3000)$, $D_{sJ}(3040)$, $D_{s1}^*(2710)$, $D_{s1}^*(2860)$, $D_{s3}^*(2860)$ observed at BaBar, LHCb, CDF etc as our candidates for HQET analysis. In the recent decade, enormous experimental data have been received in heavy charm and bottom meson sector. Therefore, much refined theoretical approaches are required to understand the spectrum of these heavy-light quark dynamics within the meson through fundamental interactions.

Notating a particular J^P value to the charm mesons are very crucial in deciding a specific place in the spectroscopy. As we move towards higher energy levels, the splittings between the higher states become smaller than those of the lower states, so various possibilities of orbital or radial assignments arises for a single state. Hence, assigning a proper position to the newly observed excited states is very important, as various other properties like decay widths, splittings, coupling constants, branching ratios etc, are dependent on their J^P values.

To achieve our objectives, we have examined the experimentally available non-strange charm states $D_J^*(2460)$, $D_J(2560)$, $D_J^*(2680)$, $D_J(2740)$, $D_J^*(2760)$, $D_J(3000)$

and $D_J^*(3000)$ using hqet formulism and assigned their J^P's as $1P_{\frac{3}{2}}2^+$, $2S_{\frac{1}{2}}0^-$, $2S_{\frac{1}{2}}1^-$, $1D_{\frac{5}{2}}2^-$, $1D_{\frac{5}{2}}3^-$, $2P_{\frac{1}{2}}1^+$ and $2P_{\frac{1}{2}}0^+$ respectively by studying their various properties like masses, branching ratios, decay widths, parity.

On the similar pattern, we have reviewed the strong decay widths, branching ratios for the available stranged charm states $D_{sJ}(3040)$, $D_{s1}^*(2710)$ and $D_{s3}^*(2860)$ and specify their J^P's as $2P_{\frac{1}{2}}1^+$, $2S_{\frac{1}{2}}1^-$ and $1D_{\frac{5}{2}}3^-$ respectively. In our analysis, the mismatch of the theoretical and experimental values for branching ratio R = $\frac{Br(D_{sJ}^*(2860)\to D^*K)}{Br(D_{sJ}^*(2860)\to DK)}$ for strange charm state $D_{sJ}^*(2860)$ is justified by an assumption that, instead of $D_{s1}^*(2860)$ belonging to a pure state $1D_{\frac{3}{2}}1^-$, it is a mixture of $1D_{\frac{3}{2}}1^-$ and $2S_{\frac{1}{2}}1^-$. The associated analysis and corresponding decays widths calculations are presented in chapter 3.

In addition to these above charm states, we have analyzed $D_2^*(3000)$ state which was recently observed at LHCb in 2015 and have also assigned a suitable J^P to it. By studying its branching ratio BR=$\frac{\Gamma(D_2^*(3000)\to D^*\pi)}{\Gamma(D_2^*(3000)\to D\pi)}$, we concluded $D_2^*(3000)$ to be best belonging to $1F2^+$ position in the charm spectra.

By comparing the experimental decay widths of the above mentioned charm states for their assigned J^P's, we have fixed various effective strong coupling constants as $g_{TH} = 0.40 \pm 0.01$, $g_{XH} = 0.12 \pm 0.01$, $g_{ZH} = 0.15 \pm 0.02$, $\widetilde{g}_{HH} = 0.31 \pm 0.05$ and $\widetilde{g}_{SH} = 0.15 \pm 0.01$. Using these couplings, we have calculated the strong decay widths of experimentally missing charm states $D(1^1F_3)$, $D_S(1^1F_3)$, $D_S(1^3F_2)$, $D_S(2^1S_0)$, $D_S(2^3P_0)$ and $D_S(1^1D_2)$ and found them to be 55.40 MeV, 120.66 MeV, 178.79 MeV, 68.19 MeV, 225.94 MeV and 35.30 MeV respectively.

The symmetries like $D_{u,d}^* - D_{u,d} = D_s^* - D_s$ suggests that, the hyperfine splittings between the spin partners within the same doublet are same for both strange and non-strange charm states. Using these symmetries, we have also calculated the masses for unknown charm states $2S_{\frac{1}{2}}0^-$, $2P_{\frac{1}{2}}0^+$ and $1D_{\frac{5}{2}}2^-$ and their associated

decay widths. Masses obtained with this symmetry are showing deviations up to the order of 3.86% when compared to other theoretical approaches. This analysis have helped in understanding the charm spectra for $2S_{1/2}, 2P_{1/2}, 1D_{3/2}, 1D_{5/2}$ and $1F_{5/2}$ states.

In the bottom sector also, many new higher excited bottom states are observed by LHCb, CDF, $D\emptyset$ in 2013, 2014 and 2015. So, it become crucial to reanalyze the fundamental parameters of HQET in the bottom sector also. Chapter 4 involves the similar study for the available bottom states $B_1(5721)$, $B_2^*(5747)$, $B_{s1}(5830)$, $B_{2s}^*(5840)$, $B_J(5840)$ and $B_J(5970)$. By using the experimental masses and strong decay widths, we have specified that $B_J(5721)$ and $B_2^*(5747)$ along with their strange partners $B_{s1}(5830)$ and $B_{2s}^*(5840)$ belong to J^P's $1P_{3/2}1^+$ and $1P_{3/2}2^+$ respectively. The bottom state $B_J(5970)$ is seen by CDF and LHCb collaboration in 2009 and 2015 respectively, concluding it to be the member of radially excited S-wave doublet with J^P $2S1^-$.

In this chapter, we have assigned a relevant position to the recently observed bottom state $B_J(5840)$ that was seen in 2015 by LHCb. As LHCb observed this state in the $B^0\pi^+$ decay mode, so by analyzing its branching ratio $BR = R_1 = \frac{\Gamma(B_J(5840)\to B\pi)}{\Gamma(B_J(5840)\to B^*\pi)}$, we concluded $1D1^-$ to be best possible J^P for this state. However, the broad decay width for this state belonging to $2S0^-$ can not be fully ignored. So we hope in future, experimental information about the decay modes for $B_J(5840)$ broaden up, to clearly identify the exact J^P for this state.

By comparing the experimental strong decay widths for these above mentioned higher excited bottom states, coupling constants are calculated to be $g_{XH} = 0.41\pm0.02$, $g_{TH} = 0.50\pm0.01$, $g_{TH} = 0.37\pm0.01$ and $\widetilde{g}_{HH} = 0.15\pm0.01$. Two values of g_{TH} correspond to data obtained from bottom states $B_1(5721)$ and $B_2^*(5747)$. These obtained couplings allowed us to compute the strong decay widths of the experimentally missing bottom states $B(2^1S_0)$, $B_s(2^3S_1)$, $B_s(2^1S_0)$, $B(1^1D_2)$, $B_s(1^3D_1)$ and $B_s(1^1D_2)$. The calculated decay width 241.33 MeV for $B(1^1D_2)$ is in same range

as predicted by Q.-F. Lu with 3.87 % deviation. For its strange partners, total decay widths are calculated as $\Gamma(B^*_{s1}) = 522.09$ MeV and $\Gamma(B_{s2}) = 318.62$ MeV. We concluded B^*_{s1} to be the broader state as compared to its spin partner B_{s2}. For the radially excited bottom states 2S, decay rates are predicted as $\Gamma(B_0) = 38.85$ MeV, $\Gamma(B^*_{s1}) = 37.41$ MeV and $\Gamma(B_{s0}) = 48.56$ MeV. Predicted rates shows that, the strange partners follow the same pattern as the non-strange bottom states i.e. B^*_{s1} state is seen to be broader as compared to its spin partner B_{s0}.

To complete the understanding of bottom spectra, we have also predicted the masses and strong decay rates for experimentally missing 2S, 2P, $1D_{5/2}$ and $1F_{5/2}$ bottom states in chapter 5. The heavy quark symmetry implies that the spin averaged mass splittings between the higher states and the ground state i.e. Δ_F, and the mass splittings between the spin members of the same doublet i.e. λ_F are flavor independent i.e. $\Delta^{(b)}_F = \Delta^{(c)}_F$ and $\lambda^{(b)}_F = \lambda^{(c)}_F$. We have applied this symmetry on the experimentally available data for n=1 and n=2 charm mesons to predict the masses and decay widths of the corresponding bottom mesons. We have also analyzed these bottom masses by applying the QCD and $1/m_Q$ corrections to the leading order lagrangian that leads to the modification of flavor symmetry parameters as $\Delta^{(b)}_F = \Delta^{(c)}_F + \delta\Delta_F$ and $\lambda^{(b)}_F = \lambda^{(c)}_F \delta\lambda_F$.

The mass for the radially excited n=2 S-wave bottom state $\widetilde{B}^*_1$ is calculated as 5981.50 MeV, which is very close to its experimentally observed mass 5978 MeV and 5969.20 MeV for bottom state $B_J(5970)$ predicted by CDF and LHCb collaboration respectively. Results for other excited states are also in agreement with the available masses in literature. The bottom meson masses calculated by inheriting QCD corrections show deviations from initial masses by 1 or 2 MeV except for the $\widetilde{B}^*_1$ state, where the deviation is of 4 MeV. The other $1/m_Q$ correction in Δ parameter $\delta\Delta_F$ has resulted in proportionate reduction in the bottom masses. The effect of corrections to λ_F is small, so the resultant masses are close to the masses obtained

by applying corrections to the Δ_F parameter. Correction to Δ_F relation results in deviating the mass of n=2 S-wave bottom states by 0.22% . And the masses for n=2 P-wave get deviated by 0.77% and 0.58% respectively for $s_l = 1/2^+$ and $s_l = 3/2^+$. D-wave bottom states for n=1 ($B_2^{'}$, B_3^*) and ($B_{2s}^{'}$, B_{3s}^*) are comparable with available theoretical masses varying only by 1.8% and 0.04% respectively.

While analyzing the decay widths for radially excited n=2 S-wave, we have concluded $B^*\pi^-$ (B^+K^-) mode to be the dominant decay mode both for $\widetilde{B}_1^*$ ($\widetilde{B}_{s1}^*$) and $\widetilde{B}_0$ ($\widetilde{B}_{s0}$) bottom states. Similarly, for the low lying P=wave bottom mesons $\widetilde{B}_0^*$ and $\widetilde{B}_1^{'}$, $B^+\pi^-$ and $B*^+\pi^-$ emerge as the dominant decay modes with contribution of 42.15% and 42.83% to their total decay widths. For the excited P-wave bottom mesons, decay modes $B^*\pi^+$ and B^*K^- are seen to be best suitable for the experimental search of non-strange states ($\widetilde{B}_1, \widetilde{B}_2^*$) and strange states ($\widetilde{B}_{s1}, \widetilde{B}_{s2}^*$) respectively. QCD and $1/m_Q$ corrections shift the decay width values at most by 30 MeV ($\sim 12\%$).

With the analysis and various results of the strange and non strange bottom and charm mesons in hqet framework, we believe to provide a useful insight to the spectroscopy of the heavy light mesons. It is our hope and belief that our predictions of the unknown couplings, masses, decay rates can provide a useful insight to experimentalists for searching new states. We are still very far from the ultimate goal of understanding the QCD properties of heavy-light mesons. The study of heavy-light mesons in this thesis has provided a good stepping stone, but this present work can be extended in future to study the highly excited spectra of charm and bottom mesons. This extension can be done by constructing the effective lagrangian by including the higher order of $1/m_Q$ corrections. Moreover, one can also extend the work by looking into the strong decays decaying to ground state not only along with the light pseudo-scalar mesons $J^P = 0^-$, but also through vector mesons with $J^P = 1^-$. To get a clear approach, semileptonic weak and electromagnetic decays

can also be studied along with the strong decays. The same approach can also be extended for studying the baryons containing a single heavy quark.